

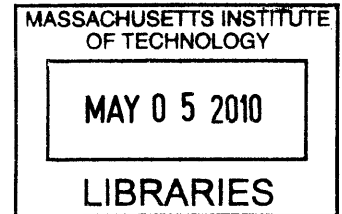
Variable Buoyancy System Metric

by

Harold Franklin Jensen III

B.S. Mechanical Engineering
Columbia University, 2006

B.S. Applied Physics
Pacific Lutheran University, 2004



Submitted to the in partial fulfillment of the requirements for the degree of
Master of Science in Mechanical Engineering

at the

ARCHIVES

MASSACHUSETTS INSTITUTE OF TECHNOLOGY

and the

WOODS HOLE OCEANOGRAPHIC INSTITUTION

June 2009

© 2009 Harold Franklin Jensen III. All rights reserved.

The author hereby grants to MIT and WHOI permission to reproduce and distribute publicly paper and electronic copies of this thesis document in whole or in part.

Author
Joint Program in Applied Ocean Science and Engineering
May 20, 2009

Certified by
Dana Yoerger
Thesis Supervisor
Senior Scientist, Woods Hole Oceanographic Institution

Accepted by
James C. Preisig
Chairman of Joint Committee for Applied Ocean Science and Engineering
Woods Hole Oceanographic Institution

Accepted by
David E. Hardt
Chairman of Graduate Studies for the Department of Mechanical Engineering
Massachusetts Institute of Technology

Variable Buoyancy System Metric

by

Harold Franklin Jensen III

Submitted to the Joint Program in Applied Ocean Science and Engineering
on June 1, 2009, in partial fulfillment of the
requirements for the degree of
Master of Science in Mechanical Engineering

Abstract

Over the past 20 years, underwater vehicle technology has undergone drastic improvements, and vehicles are quickly gaining popularity as a tool for numerous oceanographic tasks. Systems used on the vehicle to alter buoyancy, or variable buoyancy (VB) systems, have seen only minor improvements during the same time period. Though current VB systems are extremely robust, their lack of performance has become a hinderance to the advancement of vehicle capabilities.

This thesis first explores the current status of VB systems, then creates a model of each system to determine performance. Second, in order to quantitatively compare fundamentally different VB systems, two metrics, β_m and β_{vol} , are developed and applied to current systems. By determining the ratio of performance to size, these metrics give engineers a tool to aid VB system development. Finally, the fundamental challenges in developing more advanced VB systems are explored, and a couple of technologies are investigated for their potential use in new systems.

Thesis Supervisor: Dana Yoerger

Title: Senior Scientist, Woods Hole Oceanographic Institution

Acknowledgments

It is *exciting* to finally be writing these words of thanks! I've needed some added buoyancy from *many* people to stay afloat these past few years, and the following words do not convey the *extent* of my gratitude.

Foremost, it has been a privilege and honor *to* work with Dana Yoerger, and I am much in debt to his tutelage (never limited to just *engineering*). The same can be said for Al Bradley, and I have the utmost respect for his patience and willingness to teach. Both of these men share an enthusiasm for the pursuit of knowledge that is nothing short of contagious, and this thesis could not have been completed without them.

I would also *like* to thank the following engineers for the time they took to *pause* their tasks and answer more than just my original questions: Rod Catanach, Andy Billings, Matt Heintz, Phil Forte, Chip Breier, John Ahvery, Lane Abrahms, Robert Tavares, and Jake Maysmith. Additionally, I am extremely grateful to Leslie Regan, Joan Kravit, Marsha Gomes, and Judy Fenwick for all their help; you made *my* educational process so smooth, thank you!

Finally, a few measly words can't come close to acknowledging the support from my family; I am truly blessed. Mom, Dad, and Shalene; I missed not seeing you more often, but it was comforting knowing *you* always had my back. Erik, you're the best. Amigo, thank you for being the friend. Nick and Jamie, thanks for being rad. Nate, Jess, & Boyd, thanks for the good times. Amelia, you're cool too.

I will be forever grateful to WHOI for their educational and financial support. The access to amazing resources pushed me to grow both academically and personally, a debt *most* hard to repay.

THIS PAGE INTENTIONALLY LEFT BLANK

Contents

1	Introduction	15
1.1	Motivation	15
1.2	Thesis Goals	16
2	Buoyancy	17
2.1	Buoyancy Primer	17
2.2	Variable Buoyancy Benefits	19
3	Current VB Systems	21
3.1	Discharge VB System	21
3.2	Pumped Water VB System	22
3.3	One-way Tank Flood VB System	24
3.4	Pumped Oil VB System	24
3.5	Piston-Driven Oil VB System	25
4	Variable Buoyancy Metric	27
4.1	Metric Theory	27
4.2	Metric Application to Existing Systems	28
4.2.1	Discharge VB Systems	28
4.2.2	One-Way Tank Flood VB System: Titanium Sphere	30
4.2.3	Water Pumped VB System: Alvin HOV	33
4.2.4	Pumped Oil VB System: Spray Glider	41
4.2.5	Piston-driven Oil VB System: SOLO Float	43
4.3	Existing System Results	45
4.4	Existing System Conclusion	49
5	Future System Design	51
5.1	Chemical Energy Systems	53
5.1.1	Carbonate or Bicarbonate Reaction VB System	53
5.2	Mechanical Energy Systems	55
5.2.1	Compressed Gas VB System	55
6	Conclusion	63
7	Future Work	65

A Symbols and Abbreviations	67
B Gas Compression Modeling	69
B.1 Van der Waals Equation of State	69
B.2 Gas Solubility: Henry's Law	71
C Deep Submergence Battery Specifications	73
D Manuals	75
E Modeling Code (MATLAB)	77
E.1 Code: Alvin HOV Pumped-Water VB System Model	77
E.2 Code: Pre-compressed Gas Tank VB System	87
E.3 Code: Spray Glider Pumped Oil VB System	96
E.4 Code: SOLO Float Piston-Driven Oil VB System	100
E.5 Code: Discharge VB System	103
E.6 Code: Floodable Volume Model	105
E.7 Code: Roark's Stress on Thin-walled Spheres Model	107
E.8 Code: Modeling Constants	108

List of Figures

2-1	Archimedes Principle force diagram. F_G is the weight, or force of gravity on the object, F_H is the hydrostatic forces exerted from the fluid pressure, F_B is the sum of the hydrostatic forces, or net buoyant force, and B is the sum of all forces, or the net buoyancy.	18
3-1	Water Pump VB System Schematic	23
3-2	Pumped oil VB system schematic. The external bladder displacement increases from A to B , thereby increasing buoyancy.	24
3-3	Piston-driven oil VB system schematic. The external bladder displacement increases from A to B , thereby increasing buoyancy.	25
4-1	Mass discharge VB system: mass metric (β_m) vs depth. Steel, lead, and calcium bromide ($SG = 3.4$) increase buoyancy, whereas syntactic foam, alumina spheres, glass spheres and methanol ($SG = 0.8$) decrease buoyancy.	29
4-2	Mass discharge VB system: volume metric (β_{vol}) vs depth. Steel, lead, and calcium bromide ($SG = 3.4$) increase buoyancy, whereas syntactic foam, alumina spheres, glass spheres and methanol ($SG = 0.8$) decrease buoyancy.	30
4-3	Mass discharge VB system: volume metric (β_{vol}) vs depth. Steel, lead, and calcium bromide ($SG = 3.4$) increase buoyancy, whereas syntactic foam, alumina spheres, glass spheres and methanol ($SG = 0.8$) decrease buoyancy.	31
4-4	Floodable Sphere VB system: β_m vs depth. Titanium (Ti-Al6-V4) sphere.	32
4-5	Floodable Sphere VB system: β_{vol} vs depth. Titanium (Ti-Al6-V4) sphere.	33
4-6	Alvin HOV: β_m vs depth. Battery mass is not included.	36
4-7	Alvin HOV: β_{vol} vs depth. Battery mass is not included.	36
4-8	Alvin HOV: consumed energy vs depth.	37
4-9	Alvin HOV using lead acid battery system: β_m vs depth.	37
4-10	Alvin HOV using lead acid battery system: β_{vol} vs depth.	38
4-11	Alvin HOV: β_m vs depth. The current vehicle uses pressure-compensated lead acid rechargeable batteries. The next generation vehicle will use lithium ion rechargeable batteries in a titanium housing.	38

4-12	Alvin HOV: β_{vol} vs depth. The current vehicle uses pressure-compensated lead acid rechargeable batteries. The next generation vehicle will use lithium ion rechargeable batteries in a titanium housing.	39
4-13	Alvin HOV: β_m vs depth comparison of tank pre-charge and battery type for a 200 kg buoyancy addition.	39
4-14	Alvin HOV: β_{vol} vs depth comparison of tank pre-charge and battery type for a 200 kg buoyancy addition.	40
4-15	Alvin HOV: energy consumption vs depth comparison of tank pre-charge for 50 and 100 kg buoyancy addition.	41
4-16	Alvin HOV: effectiveness vs depth comparison of tank pre-charge for 50 and 100 kg buoyancy addition. Effectiveness of system components is approximately 52%, however the energy stored in the compressed gas reduces consumed battery power.	42
4-17	β_m and β_{vol} vs depth for the Spray Glider.	44
4-18	β_m and β_{vol} vs depth for the SOLO float.	44
4-19	β_m vs buoyancy cycles for VB systems on Spray Glider at 1,500 m and SOLO float at 1,800 m).	46
4-20	Alvin HOV pumped water VB system: β_m vs buoyancy cycles at 6,500 m (13 MPa pre-charge).	46
4-21	Alvin HOV pumped water VB system: β_m vs buoyancy cycles at 1,800 m (13 MPa pre-charge).	48
4-22	Alvin HOV pumped water VB system: β_m vs buoyancy cycles at 1,800 m (13 MPa pre-charge).	48
5-1	Gas molar density vs depth (pressure).	54
5-2	Gas specific gravity (SG) vs depth (pressure).	54
5-3	Molar density and aqueous concentration of CO ₂ gas vs depth. Aqueous concentration in units of moles per L of <i>seawater</i> , and CO ₂ gas density in moles per L of <i>gas</i> . The density spike at 350 m is the transition from gas to liquid.	55
5-4	Pre-compressed gas tank VB system schematic.	56
5-5	Total added buoyancy vs depth for a compressed gas VB system using tank #4 (120 L, 70 MPa).	58
5-6	β_m vs depth for a compressed gas VB system using tank #4 (120 L, 70 MPa).	59
5-7	β_{vol} vs depth for a compressed gas VB system using tank #4 (120 L, 70 MPa).	59
5-8	β_m vs depth for a compressed gas VB system using helium gas.	60
5-9	β_{vol} vs depth for a compressed gas VB system using helium gas.	60
6-1	β_m vs depth for systems explored in this thesis.	64
6-2	β_{vol} vs depth for systems explored in this thesis	64
B-1	Gas volumetric molar density vs depth	70
B-2	Gas mass density vs depth	70

B-3	Molar density and aqueous concentration of CO ₂ gas vs depth. Aqueous concentration in units of moles per L of <i>seawater</i> , and CO ₂ gas density in moles per L of <i>gas</i> . The density spike at 350 m is the transition from gas to liquid.	71
D-1	Specs for carbon fiber gas tank used in pre-compressed VB system design.	75
D-2	Autoclave valve for Compressed Gas VB system	76

THIS PAGE INTENTIONALLY LEFT BLANK

List of Tables

3.1	Example valve plan for pre-charged pumped water VB system shown in Figure 3-1.	23
4.1	The Alvin HOV VB system specifications. Three power system configurations shown: without batteries, with lead acid batteries (current battery system), and with lithium ion batteries (Alvin II). Performance values given for a depth of 6500 m.	35
4.2	Specifications and metric results for Spray Glider and SOLO Float.	43
4.3	Ratio of the one-way buoyancy range (B^+) to system mass and volume (battery is excluded).	49
5.1	Specifications for deep submergence battery systems. Syntactic foam was added to each system (w/float) to achieve neutral buoyancy ($SG = 0.61$, 11,500 m). E is total energy, m is mass, V is volumetric displacement, and B system buoyancy. [Dana Yoerger & Dan Gomez-Ibanez, WHOI, 2009]	52
5.2	Pre-compressed gas tank VB system specifications and performance. B and SG are the static buoyancy and specific gravity of the system at the surface. B^+ is the amount of added buoyancy the system can create. B^+ , β_m , and β_{vol} are all stated for 3,000 m. LT are Lincoln Composites Tuffshell [®] carbon fiber gas tanks [13]. *The 100 MPa tank is not yet available.	57
5.3	Specific gravity (SG) vs depth for 3 types of buoyant materials and the compressed gas VB system (using tanks #2, 4, & 5). For buoyant material specifications, see: [1], [20], & [23].	61
5.4	Specifications and performance for compressed gas VB systems. B is the static buoyancy of the system and B^+ is the added buoyancy (kg) at the subscripted depth (mass and displacement are for the entire system). See Appendix D for tank and valve manuals.	62
B.1	Gas constants used for van der Waals equation of state.	69

C.1 *A variation of Table 5.1 using alumina spheres for buoyancy ($SG = 0.35$, rated to 11,000 m) rather than syntactic foam.* Specifications for deep submergence battery systems. Syntactic foam was added to each system (w/float) to achieve neutral buoyancy ($SG = 0.61$, 11,500 m). E is total energy, m is mass, V is volumetric displacement, and B system buoyancy. [Dana Yoerger & Dan Gomez-Ibanez, WHOI, 2009] 73

Chapter 1

Introduction

In the past 20 years, impressive technological advances have been made in nearly all areas of underwater vehicle technology. With such advancement, underwater vehicles have become a valuable and productive tool used for a variety of reasons. Fisheries Management, Port Safety and Security, Law Enforcement, Oil and Mineral Exploration, Military, and Ocean Science are a few of the main sectors that have either already begun or plan incorporating underwater vehicles into their fleets[24].

Of the three main vehicle types: human occupied submersibles (HOVs), remotely operated submersibles (ROVs), and autonomous underwater vehicles (AUVs): it is AUVs that have been at the forefront of advancement. Utilizing new technologies in sensors, acoustics, computing, lighting, imagery, and batteries, the AUV has become a technologically advanced and useful ocean exploration and instrumentation platform [7]. With a range of vehicle size and capabilities, AUVs are being developed to perform routine tasks that may be dangerous, expensive, or inaccessible to other types of platforms. Their ability to cover large areas of the ocean environment at any depth [2] gives them a distinct advantage, as they can overcome sound attenuation, surface noise, and tracer dilution problems hindering surface level instrumentation [4].

1.1 Motivation

Despite the recent innovations, AUVs are still in a developmental stage, and need further advancements to improve reliability and capability. The need for greater range, advancement in sensor capabilities and data processing are commonly expressed as requirements for better integration of the vehicles into the various ocean communities [4]. The commonality between these shortcomings is lack of onboard energy, which is currently the most limiting resource in AUV design [3], [4].

The amount of energy available to a vehicle has a direct affect on its capabilities. Much has been done to advance the hydrodynamic efficiency and battery technology of the current vehicle fleet to increase the amount of energy available onboard. However, more advancement is needed, as an increase in energy would not only allow for greater range, but also more powerful sensors, higher resolution data, and better

maneuverability. Adjusting the buoyancy on a vehicle is one method that may be able to save substantial energy, but has not seen advancement in many years, and may be the weakest part of current vehicles.

Though not openly apparent, variable buoyancy is an important part of advancing underwater vehicle capabilities. In many modern AUVs, propulsion can use up to half the energy onboard [11]. Choosing to reduce risk and complication, many vehicles drive to and from depth, and operate positively buoyant at depth [2], [11], [6]. This requires a constant downward thrust to counter the buoyant force. This energy is immediately saved if a more capable buoyancy system were developed that could efficiently alter the buoyancy of the vehicle throughout the dive.

There are numerous other benefits from an advanced VB system. To maintain a slightly positive buoyancy at working depth, survey vehicles require a pre-dive buoyancy and trim adjustment to match the mission environment [11], [6]. This procedure could be eliminated for a vehicle with a self-regulating system; reducing ship time, man power, and guesswork. It would also enhance vehicle control and efficiency in areas of changing density. This then allows for surveys at multiple depths, prevents early dive termination should drastically different density be encountered [22], and reduce risk for difficult missions under polar ice [6]. Having a neutrally buoyant vehicle will also add maneuverability, allowing vehicles to easily hover or reverse directions. Using less propulsion will reduce the noise of already quiet vehicles [7], thereby reducing disturbance to biology, sediment, and acoustic measurements. Lastly, an advanced VB system can potentially increase the payload capacity for sample retrieval, a direct benefit to scientific results, as well as total operating cost.

Underwater vehicles have long had a variety of different variable buoyancy systems. These systems, though effective, are large and energy intensive; impractical for the newer generation of light and small AUVs and ROVs. Thus, new technology needs to be adapted to create new VB systems, and allow further development of underwater vehicles.

1.2 Thesis Goals

The first goal of this thesis is to thoroughly understand and explain the current status of variable buoyancy technology as it pertains to underwater vehicles (particularly deep submergence vehicles). Most of the common systems are explored, and their strengths and weaknesses addressed. The second goal is to develop a metric to quantitatively compare the various systems. Such a metric allows comparison of variable buoyancy systems that are different in the mechanisms they use to alter buoyancy. Lastly, the future development of VB systems is explored by identifying technology with potential for VB application. Where possible, the metric is applied to future systems. Therefore, this thesis sets out to give the reader a thorough understanding of current VB technology and an insight towards promising future developments.

Chapter 2

Buoyancy

2.1 Buoyancy Primer

“A body immersed in a fluid will experience an upward force due to hydrostatic pressure equal and opposite to the weight of the fluid displaced by the body [8].”

The above quotation elegantly explains Archimedes Principle, defining the buoyant force exerted on submerged bodies. Illustrated in Figure 2-1(A), the hydrostatic pressure of a fluid exerts a force (F_H) normal to every surface on the submerged body. The lateral forces on the object cancel because they are equal in magnitude, but opposite in direction. The bottom surface of the object experiences a greater pressure than the top surface, and thus a net vertical force is exerted on the body. This net force is called the buoyant force (F_B), shown in Figure 2-1(B), and is equal to the weight of the displaced fluid, regardless of body shape (see Equation 2.1).

The upward buoyant force exerted on a submerged body can be found if the volumetric displacement (∇_{body}) and density of the fluid (ρ_{fluid}) are known:

$$F_B = \nabla_{body} \cdot \rho_{fluid} \cdot g \quad (2.1)$$

This is the mathematic definition of Archimedes Principle: the buoyant force is equal to the weight of the fluid displaced. The total force is cumulative, and thus for a complicated body, total force is a summation of the buoyant forces on each part:

$$F_B = F_{B,1} + F_{B,2} + \dots F_{B,n} = \sum_n F_{B,n} \quad (2.2)$$

In addition to the buoyant force, the submerged body is also subject to the downward force of gravity (F_G). The net force on the body, or the sum of these two forces, is known as the *buoyancy* B of the submerged body:

$$B = F_B + F_G \quad (2.3)$$

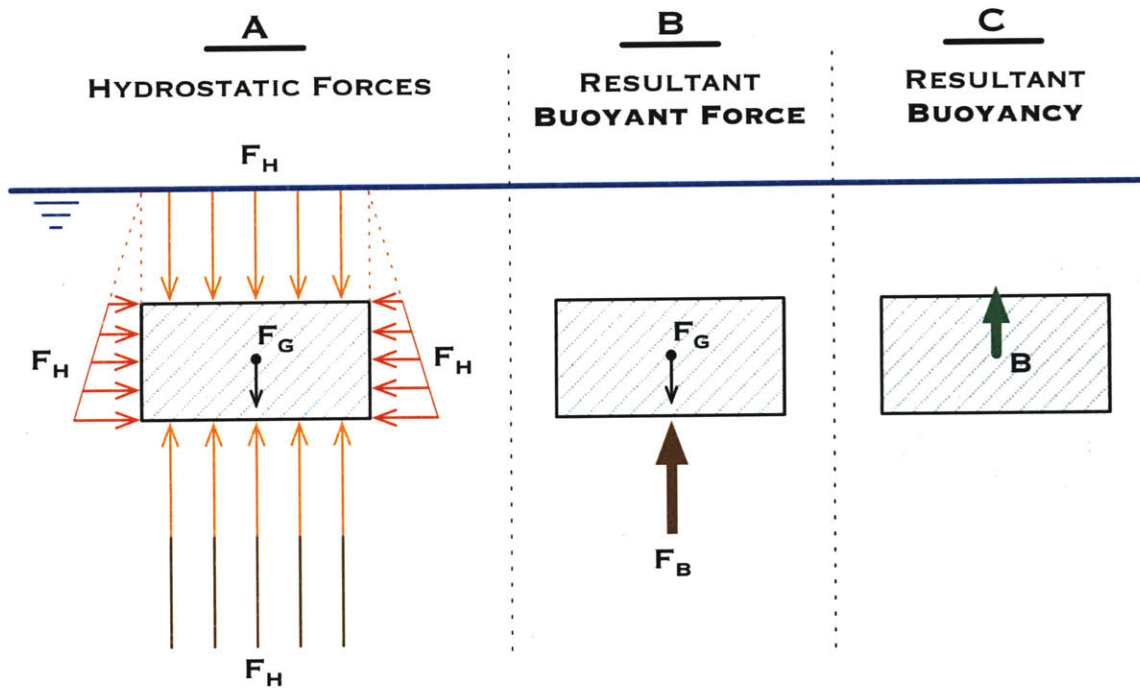


Figure 2-1: Archimedes Principle force diagram. F_G is the weight, or force of gravity on the object, F_H is the hydrostatic forces exerted from the fluid pressure, F_B is the sum of the hydrostatic forces, or net buoyant force, and B is the sum of all forces, or the net buoyancy.

Shown in Figure 2-1(C), the resultant buoyancy (B) of the body will be upward, or positive, if the buoyant force is greater than the gravitational force: $F_B > F_G$. In this condition, the body is said to be “positively buoyant,” and will rise in the fluid or float at the surface. In reverse, if the buoyant force is less than the weight, $F_B < F_G$, the body will be “negatively buoyant” and sink. Lastly, if the two forces are equivalent, $F_B = F_G$, the body is “neutrally buoyant” and will remain suspended in the fluid¹.

To be technically correct, the buoyancy of a submerged object is expressed in units of force, and as such, is measured in newtons (N). Different however, the standard practice in underwater vehicle and sensor design is to express buoyancy in units of mass (kg). This is equivalent to dividing the force of buoyancy by the gravitational acceleration constant ($g = 9.80665 \text{ m/s}^2$).

$$B_{mass} = \frac{B_{force}}{g} = \nabla \cdot \rho_{water} - m_{body} \quad (2.4)$$

Equation 2.4 is the difference between the mass of the submerged object and the mass of the water displaced. When using this equation, one must remember that each part of the submerged body has both a mass and a displacement. If an object

¹Note the difference between *buoyancy* and *buoyant force*. The Buoyant force is the net hydrostatic force upward on a submerged object. Buoyancy is the net force on the submerged object, and can be upward or downward.

has a positive buoyancy of 10 kg, simply adding a 10 kg object will *not* bring the vehicle to neutral buoyancy. The added object will also displace water, increasing the buoyant force. Therefore, the net change in buoyancy will be the difference between the displacement and mass of the added object, which will be less than 10 kg for this example.

2.2 Variable Buoyancy Benefits

The ability to change buoyancy is a highly desirable and, in many instances, necessary capability for underwater vehicles. Improving capability in buoyancy control may have one or all of the following benefits: lower operating cost and energy consumption; increased mission duration and range; increased payload capacity; simplified pre-dive maintenance; improved maneuvering and vehicle control; and reduced noise emissions. Currently, there are a variety of methods used to alter vehicle buoyancy, however no system has been standardized, leaving each as a custom engineered solution.

Many of the features added by a VB system give the vehicle distinct capabilities no other system can replicate. Simple VB systems are often designed to fulfill a single design specification, however, if advanced VB systems are developed, they could potentially give the vehicle most, if not all, of the characteristics and capabilities discussed in this section.

The major motivation for advancing VB technology is the need for increased maneuverability and control. A VB system with a wide range to both increase and decrease buoyancy gives the vehicle a number of useful capabilities. Firstly, the ability to lower buoyancy enough to sink to and park on the ocean floor has numerous applications. For example, a time series measurement can be accomplished as follows: after taking a series of measurements, the vehicle parks on the ocean floor in a low energy sleep state, wakes after a set time, repeats the measurements, then returns to the parked position. Sensitive instruments needing a motionless sample platform, such as a gravimeter [9], can have the vehicle park at each survey location to obtain measurements. Additionally, after mission completion, a vehicle could park and wait for the ship to return for retrieval, perhaps avoiding dangerous weather, or adding flexibility to the science schedule.

The ability to match vehicle buoyancy to the ambient conditions is a major advantage for controlling vehicle depth. Operating at multiple depths, or in locations where density rapidly changes (under sea ice or in an estuary), a vehicle with a VB system could quickly adjust buoyancy to maintain depth control. A VB system also enhances the stability, and thus positioning control, of the vehicle. When neutrally buoyant a vehicle can more easily hover, which is beneficial for a range of applications requiring the vehicle to move slowly or hold a fixed position. Robotic arm manipulation is one such application that a stable platform gives the operator better manipulator control, thus reducing task time and increasing dexterity. Maintaining constant depth without heavy thruster use also reduces disturbance in sensitive environments, where a burst of thrust could disturb the ecology or disturb a silty bottom, creating an opaque cloud of silt.

Increased payload capacity is an additional capability of an advanced VB system. Current vehicles either use vertical thrust or discard material (often steel) to offset the added mass of collected samples. This can be on the order of hundreds on pounds per dive (The Jason ROV (WHOI) has collected up to 180 kg per dive, 130 kg of which were offset by discharging steel weight [Matt Heintz, WHOI Engineer, 2009]). By instead offsetting the added mass with added buoyancy, the payload capacity is increased, discharge material is saved, thruster energy is reduced, and vehicle maneuverability is maintained throughout the dive.

Energy savings is an additional benefit of advanced VB systems. Vehicles today are typically ballasted pre-dive to be positively buoyant, and thus must use thrusters to keep the vehicle at the desired depth [11], [6]. A VB system capable of actively maintaining neutral buoyancy would reduce the need for thruster depth control. Decreasing thruster use also diminishes noise and vibration generated by the propulsion system, which may yield better sensor measurements. Additionally, a VB system capable of trimming the vehicle allows pitch adjustment to the most hydrodynamically efficient position, also saving valuable energy.

Large operating costs is one of the major drawbacks to using underwater vehicles. Aside from the smallest vehicles, a large ship is required to transport, deploy, run (ROV), and retrieve the vehicle. Ship time is expensive, and reducing this cost is very important for further development. Though larger vehicles will always require a deployment vessel, a smartly designed VB system can better optimize both ship and science time in multiple ways. A speedy descent and ascent from mission depth is a direct time savings. Many vehicles either propel themselves to and from depth, or carry expendable descent and ascent weights. A capable VB system would save this propulsion energy and reduce discharged material, thus saving time, money, and possibly reducing vehicle weight and freeing up payload capacity. If the system allows for a vehicle to park and wait on the ocean floor after mission completion, the ship has more freedom for other tasks when the vehicle is gone. Lastly, a well designed system reduces the turnaround time needed between dives by removing the need to adjust the vehicle's net buoyancy to match the predicted conditions of the next dive.

Safety enhancements are also possible from a well designed VB system. In the event a vehicle becomes trapped or stuck on the ocean floor, adding or decreasing buoyancy may help to free the vehicle. Also, emergency ascent time can be shortened, and once on the surface, having the ability to create a large freeboard allows for easier, quicker, and safer vehicle retrieval.

There are currently VB systems that are quite capable, and can enhance the vehicle in a number of the ways mentioned. However, they are prohibitively large and energy intensive for all but the largest of vehicles. This leaves a need for a capable system in a smaller package, and thus the time is ripe for an advancement in technology.

Chapter 3

Current VB Systems

There are three main types of VB systems (known to the author) used in underwater vehicles: mass discharge, pumped water, and oil displacement systems. Other than equipment upgrades and minor variations, there has been no major recent advancements in the technology. The systems are reliable however, and have proven their durability through the tests of time.

There are two fundamental mechanisms by which a vehicle can alter its buoyancy. As shown in Equation 2.3, buoyancy (B) is the sum of a vehicle's weight (F_G) and the buoyant force exerted by displacing water (F_B), so either of these can be adjusted to alter vehicle buoyancy. For example; an increase in B is accomplished by either decreasing F_G (reducing vehicle weight), increasing (F_B) (increasing displacement), or both. The method each system uses to adjust buoyancy is explained in the following chapter.

3.1 Discharge VB System

The most simple way to adjust the buoyancy of a vehicle is to discharge material. The system is effective for vehicles in need of either an increase or decrease in buoyancy, the result of which depends on the density of the released material. From Equation 2.2, the total buoyancy of a vehicle is the sum of buoyancy for each part. Thus, discharging a mass more dense than water will remove the negative buoyancy of that mass, thereby increasing the net buoyancy of the vehicle.

This is a common system used to speed ascent and descent, and increase payload capacity. Most vehicles are ballasted to be positively buoyant at working depth, and must therefore use propulsion to get to and from mission depth. To quicken descent, many vehicles add lead or steel 'descent weights' to reduce vehicle buoyancy. Once at the desired depth, the weight is released, returning the vehicle to the desired buoyancy. Oppositely, when a vehicle is ready to return to the surface, an "ascent weight" is commonly dropped, increasing buoyancy so the vehicle floats to the surface. There may also be an "emergency weight" that can be dropped in addition to the ascent weight if the vehicle malfunctions or becomes stuck.

ROVs are often used to retrieve samples and instrumentation from the ocean floor.

As items are collected, the buoyancy of the vehicle decreases. It is not uncommon for vehicles to retrieve hundreds of kilograms of samples, which would put a great strain on the propulsion system if the buoyancy were left unadjusted. To regain lost buoyancy, a vehicle will discharge mass, typically steel plates.

Alternatively, it is sometimes necessary for a vehicle to reduce buoyancy. This is accomplished by discharging materials less dense than water. This may be necessary for a vehicle that is depositing instrumentation of the seafloor, and needs to remain near neutral buoyancy after the heavy instrumentation is placed. At other times, a vehicle may need to match a density change in an environment to keep from using thruster power to maintain depth. Ceramic spheres, syntactic foam, and fluids less dense than water are materials that may be used for discharge.

This system is very effective at accomplishing a quick one-way buoyancy change. Perfected through experience, the release mechanisms are simple and reliable, respond instantly, and use negligible energy. There are major drawbacks however, as the system only allows set increments of buoyancy change, and adds considerable weight and/or volume to the vehicle. Additionally, the material discharged is lost to the ocean environment, increasing cost and leaving waste behind (albeit a relatively small source of waste).

3.2 Pumped Water VB System

A pumped water VB system is a highly flexible method for controlling vehicle buoyancy, and can accommodate a wide range of design parameters. Fixed in volume, the system changes buoyancy by adding or removing weight (i.e. water). Shown schematically in Figure 3-1, the system has three major components; a pressure tank, pump, and a system of valves. When empty, the tank is positively buoyant, whereas filled with water, it is negatively buoyant. Thus, vehicle buoyancy is controlled by the water level in the tank.

In the most simple form, air in the tank is originally at atmospheric pressure, and vehicle buoyancy decreases when water is allowed to fill the tank. To increase buoyancy, water is pumped out. In this scenario, the tank must be strong enough to withstand the hydrostatic forces when empty (maximum pressure differential). In a more complicated scenario, air inside the tank is pressurized prior to diving. This reduces the pressure difference between the tank and the water, thus reducing the required tank strength. In this case, the system must not only be able to pump water out of the tank, but when tank pressure is greater than ambient water pressure, it must be able to pump water into the tank to decrease buoyancy. This is accomplished with a more complicated valve structure.

In addition to reducing the required tank strength, a precharge can reduce the energy used by the pump. This is explained in further detail in Section 4.2.3.

A common modification of this system is to use compressed air, rather than a pump, to force the water out of the tank. Used by Naval submarines for many years, the system requires a large source of gas (typically air) compressed to a pressure higher than ambient water conditions. Water is forced out of the tank when the high

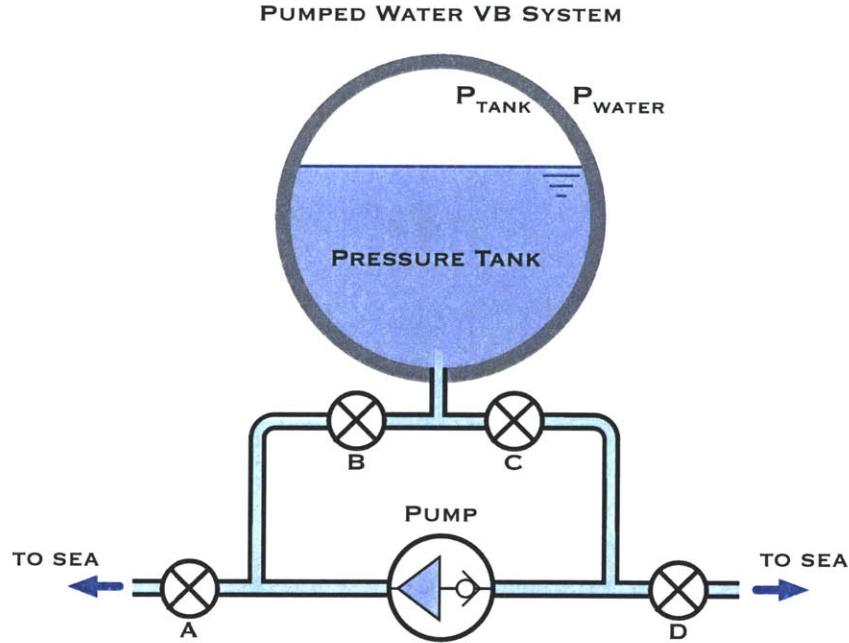


Figure 3-1: Water Pump VB System Schematic

Table 3.1: Example valve plan for pre-charged pumped water VB system shown in Figure 3-1.

Pressure	Flow	Valves Open
$P_{water} < P_{tank}$	Pump in	D & B
$P_{water} < P_{tank}$	Flow out	A & B or C & D
$P_{water} > P_{tank}$	Pump out	C & A
$P_{water} > P_{tank}$	Flow in	A & B or C & D

pressure air tanks are opened to the top of the ballast tanks. Previously limited to shallow depths, recent advancements in carbon fiber tanks make it possible to extend the depth of the system (see Section 5.2.1 for a detail analysis of such a system).

Flexibility in design is a major benefit of a pumped water VB system. It can be custom engineered to meet specifications for a variety of needs. Tanks can be repeatedly flooded and emptied, and can be as large as needed. The system is limited by the power available however, and the energy requirement increases with depth. The rate of buoyancy change is also very slow, limited by pump power. Pre-charging the pressure in the tank can offset these drawbacks, reducing energy consumed and tank strength required.

3.3 One-way Tank Flood VB System

A one-way tank flood VB system is simply an empty tank that can be flooded to increase vehicle weight, thus reducing buoyancy. A simple, yet effective system, it has nearly the same results as releasing a buoyant ceramic sphere. This system does not discharge material however, and can be drained for use on subsequent dives.

3.4 Pumped Oil VB System

The pumped oil VB system is commonly used to achieve repeatable, two-way buoyancy changes. Similar to the pumped water system, it changes buoyancy by pumping a liquid in and out of a pressure housing. Different however, the pumped oil system has a fixed mass, and thus buoyancy is controlled by adjusting the displacement of the vehicle. To increase buoyancy, oil is pumped from inside a pressure housing to an external flexible bladder. As the bladder expands, it displaces water, increasing the buoyant force (F_B) on the system. The mass of the system remains unchanged, and the buoyancy increase equals the added F_B . When a decrease in buoyancy is needed, a valve is opened and water pressure forces the oil back into the internal reservoir. The two states of the system are shown schematically in Figure 3-2; in part A buoyancy is low, and in part B the buoyancy is high.

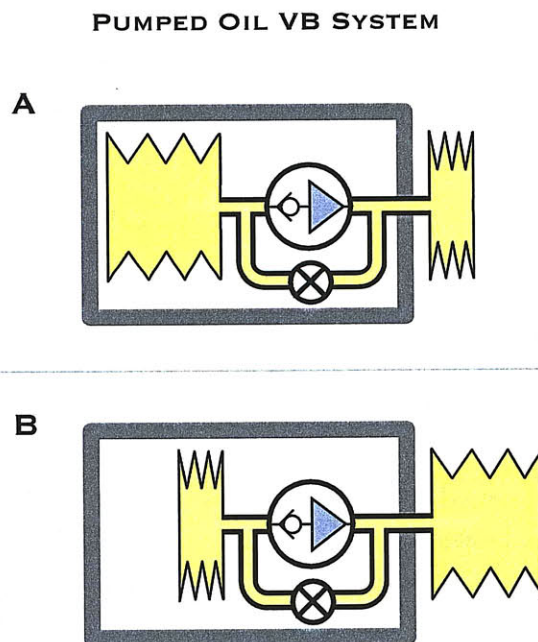


Figure 3-2: Pumped oil VB system schematic. The external bladder displacement increases from A to B, thereby increasing buoyancy.

Repeatability and reliability are the primary benefits of this system. Since no material is discharged, the number of buoyancy adjustment cycles are limited only by the power available. By using oil, rather than seawater, the risk of pump malfunctions

is reduced (such as clogging or biofouling). For these reasons, the system is often selected for vehicles requiring small buoyancy changes or long deployments. These attributes can be disadvantageous for other vehicles however. Since the oil must be contained within a pressure housing and there must be room for bladder expansion, the system may be too large for vehicles requiring large one-way buoyancy changes. Also, the rate of buoyancy change is dependent on pump speed, and pump power consumption increases with pressure. Thus, the system is not a common selection for deep submergence vehicles.

3.5 Piston-Driven Oil VB System

The piston-driven oil VB system is identical to the oil pumped system described above (Section 3.4), except the oil is forced into the external reservoir by a piston rather than a pump. As shown in Figure 3-3, the location of the piston controls the flow of oil. To increase buoyancy, the piston is moved rightward to reduce the volume of the cylinder, forcing oil into the external reservoir. To decrease buoyancy, the piston reverses direction, drawing oil back into the cylinder, and decreasing the displacement of the vehicle. The piston is typically controlled by a motor and screw mechanism.

PISTON DRIVEN OIL VB SYSTEM

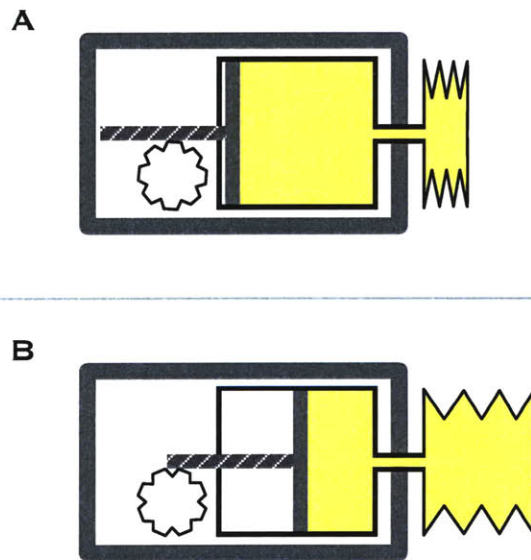


Figure 3-3: Piston-driven oil VB system schematic. The external bladder displacement increases from **A** to **B**, thereby increasing buoyancy.

The strengths and weaknesses of this system are similar to those of the pumped oil system. The non-incremental, two-way, repeatable buoyancy change is also limited by battery power and space. In addition to the internal oil bladder, the entire piston and motor mechanism must also be completely contained in a pressure housing. This may increase the total volume of the system versus a pumped oil system of equal

capabilities. Different from the pump system, the simple piston mechanism reduces risk involved with a pump, such as particles or gas bubbles causing pump malfunction.

Chapter 4

Variable Buoyancy Metric

One goal of this thesis is to develop a method to simplify the VB system design process. The creation of a tool to allow a quantitative comparison of fundamentally different types of systems will not only indicate the best system for a particular vehicle, but also reveal the strengths and weaknesses of each system.

4.1 Metric Theory

Most importantly, a metric for variable buoyancy systems must be useful by comparing the variables most important to designers. Though different variables are important for different vehicles, the size and performance are typically of primary consideration. Performance of a system is defined in this thesis as the total change in buoyancy a system can create. It is an absolute measurement, meaning a system capable of adding and removing 10 kg of buoyancy has a total buoyancy change of 20 kg. It will be represented by the symbol B^\pm . The size of a system is a straightforward measurement of mass or volume.

The mass and volume of a VB system are often unrelated, and thus two metrics are required to accurately understand the performance of a system. Each is a ratio of the performance to the size of the VB system. The first, a mass ratio, is the total change in buoyancy created divided by the mass of the VB system. Called the VB mass metric (β_m), it is represent by the following equation:

$$\beta_m = \frac{\text{Total Buoyancy Change (kg)}}{\text{Mass of the VB System (kg)}} = \frac{B^\pm}{m_{\text{VB}}} \quad (4.1)$$

The second metric is a volume ratio: the total change in buoyancy created, divided by the volume of the VB system. Different from the VB mass metric (β_m), the numerator of the VB volume metric (β_{vol}) has units of volume, and thus represents the volume of water displaced that would be equivalent to the buoyancy change in mass, at the given depth.

$$\beta_{\text{vol}} = \frac{\text{Total Buoyancy Change in units of water volume}}{\text{VB System Surface Volume}} = \frac{\nabla^\pm}{\nabla_{\text{VB}}} \quad (4.2)$$

To further explain, the buoyancy change in units of water volume is not always equivalent to the actual volume of displaced water created by the VB system. For example, a VB system discharging a steel weight changes the volumetric displacement of the vehicle much less than the change in mass of the vehicle. Thus, the change of buoyancy in units of water volume, ∇^\pm , is represented as:

$$\nabla^\pm = \frac{B^\pm}{\rho_{\text{SW}}} \quad (4.3)$$

for ρ_{SW} is the density of ambient seawater at the given depth¹. Equation 4.2 becomes:

$$\beta_{\text{vol}} = \frac{\nabla^\pm}{\nabla_{\text{VB}}} = \frac{B^\pm}{\rho_{\text{SW}} \cdot \nabla_{\text{VB}}} \quad (4.4)$$

These metrics, β_m and β_{vol} , successfully incorporate the important variables of VB system design, size and performance. Careful consideration must be paid to the numerator of the metrics because the performance is not the *one-way* buoyancy added, but the absolute or *two-way* buoyancy created. Energy consumption is indirectly incorporated by including the power source (typically batteries) into the system mass and volume. Also important to the design process, the reliability, complexity, environmental impact, safety, and maintenance needs are design variables not easily compared quantitatively, and must instead be analytically discussed for each system investigated. Lastly, an additional metric can be developed to include the cost of a system. Using either lifetime or trip cost, it can be compared to B^\pm to quickly demonstrate the price per kg of buoyancy added. Cost was not researched in this thesis, however, and is left for future work.

4.2 Metric Application to Existing Systems

The mass and volume VB metrics, developed in the previous section, are applied to five common types of VB systems. A model for each system was first created to determine performance versus depth. For each model, density insitu was calculated using average² salinity and temperature values of 34.75 PSU and 2°C respectively, with a surface temperature of 17°C. Compression of system components was not factored into the models.

4.2.1 Discharge VB Systems

As detailed in Section 3.1, discharge VB systems are commonly used to create both positive and negative buoyancy changes. For the materials commonly discharged, a

¹Seawater density calculated at depth from the UNESCO 1983 (EOS 80) polynomial used in the MATLAB function `sw_dens.m` [Phil Morgan, 1992]. Obtained from course 12.808 in Fall of 2007, taught by Jim Price.

²Average salinity and temperature were taken from data given by Jim Price in course 12.808, Fall 2007. The values are not critical however, as the salinity range of the ocean averages, and the narrow temperature range of 0 to 4°C for water deeper than 2000 m changes the density by less than 3%.

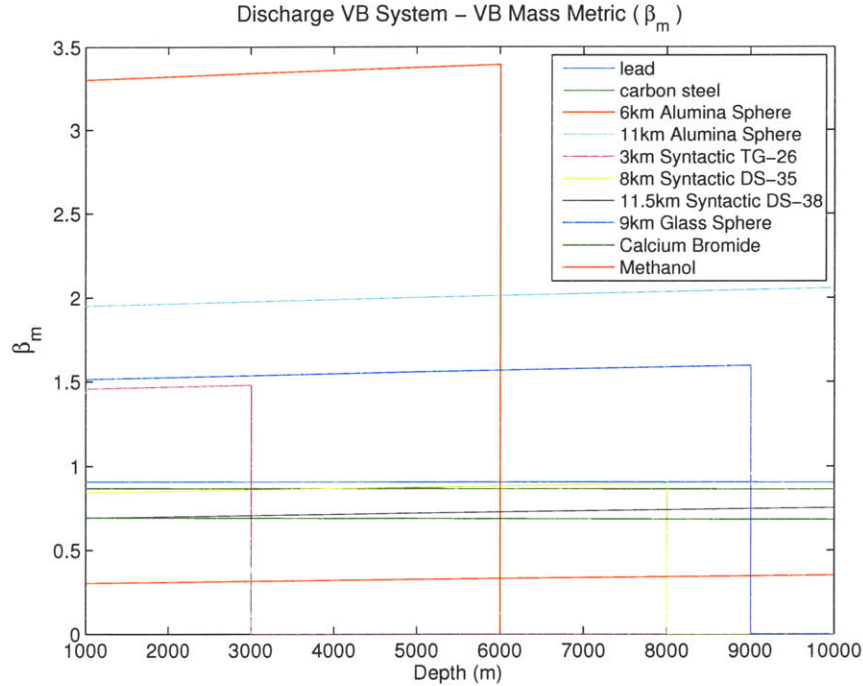


Figure 4-1: Mass discharge VB system: mass metric (β_m) vs depth. Steel, lead, and calcium bromide ($SG = 3.4$) increase buoyancy, whereas syntactic foam, alumina spheres, glass spheres and methanol ($SG = 0.8$) decrease buoyancy.

model was developed to determine the buoyancy created vs depth. Only the material discharged is factored into the model, and it is assumed that the auxiliary equipment, including battery power, is negligible. Also, system volume is the actual volume of the system, without regard to packing geometry. Some materials are limited to spherical shapes and sizes, and cannot be scaled to fit any arbitrary volume. See Appendix E.5 for MATLAB model code.

The results for the mass metric (β_m) are shown in Figure 4-1. All the solid and liquid materials, as well as the high-strength syntactic foam rated deeper than 7 km, had a metric value less than unity; $\beta_m < 1$. Simply, this means the system weighs more than the buoyancy it creates. Having a value greater than unity ($\beta_m > 1$), the ceramic spheres and syntactic foam weigh less than the buoyancy change they create. Of the materials tested, the highest values were achieved by the Alumina SeaSpheres, manufactured by Deep Sea Power & Light [20]. When released, the spheres decrease vehicle buoyancy by an amount greater than 3x their weight. The lowest values of β_m were achieved by the liquid materials because their density is closer to that of water.

The VB volume metric (β_{vol}) yields slightly different results. Seen in Figure 4-2, materials with a density greater than water exhibit $\beta_{vol} > 1$. Thus, they occupy a smaller volume than the volume of water equal to the buoyancy change they create ($\nabla^\pm > \nabla_{VB}$). Oppositely, all the materials less dense than water have a $\beta_{vol} < 1$. This result is a fundamental application of the density ratio to water, as materials less dense than water cannot displace more water than their own volume. In Figure 4-

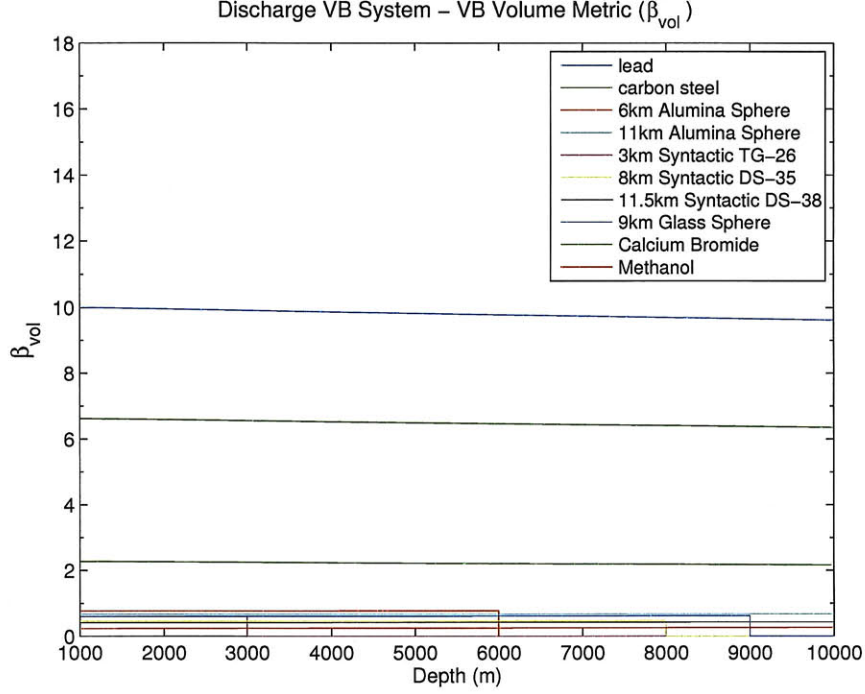


Figure 4-2: Mass discharge VB system: volume metric (β_{vol}) vs depth. Steel, lead, and calcium bromide ($SG = 3.4$) increase buoyancy, whereas syntactic foam, alumina spheres, glass spheres and methanol ($SG = 0.8$) decrease buoyancy.

3, the axis is magnified to display results for the values of $\beta_{vol} < 1$. Similar to the mass metric results, the ceramic spheres outperform the syntactic foams.

4.2.2 One-Way Tank Flood VB System: Titanium Sphere

Flooding a volume is a simple one-way VB system used to create a decrease in buoyancy. This system model uses a spherical pressure tank, a geometry chosen for its superior strength to weight ratio. The titanium alloy Ti-Al6-V4 was also chosen for its good strength to weight ratio³. The model assumes air can be released and the entire tank volume can be flooded. See Appendix E.6 for model code.

The air in the sphere is at a pressure of 1 atmosphere, and the sphere must be strong enough to withstand the ambient pressure. Sphere size was determined using Roark's formula [18] for a spherical vessel under uniform external pressure with a safety factor of 1.25⁴. The maximum stress at the outer edge of the sphere is expressed as:

$$\sigma_{max} = \frac{\sigma_{cy}}{SF} = \frac{-3qa^3}{2(a^3 - b^3)} \quad (4.5)$$

³Ti-Al6-V4: $\rho_{sphere} = 4430 \text{ kg/m}^3$, compression yield strength, $\sigma_{cy} = 970 \text{ MPa}$ [18].

⁴ABS Standard: 13.1 Hydrostatic Test: After out-of-roundness measurements have been taken, all externally-pressurized pressure hulls are to be externally hydrostatically proof tested in the presence of the Surveyor to a pressure equivalent to a depth of 1.25 times the design depth for two cycles.

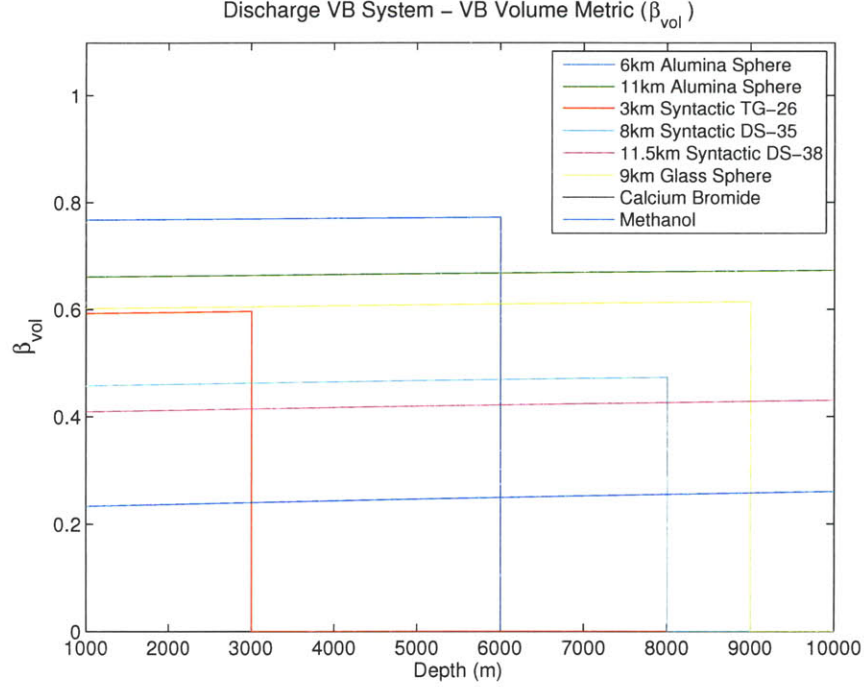


Figure 4-3: Mass discharge VB system: volume metric (β_{vol}) vs depth. Steel, lead, and calcium bromide ($SG = 3.4$) increase buoyancy, whereas syntactic foam, alumina spheres, glass spheres and methanol ($SG = 0.8$) decrease buoyancy.

for σ_{max} is the maximum stress (equivalent in the longitudinal and circumferential directions from symmetry), SF is the safety factor, σ_{CY} is the compression yield strength of the sphere, q the maximum external pressure, a the outer radius of the sphere, and b the inner radius of the sphere. Substituted into the mass metric, Equation 4.1 becomes:

$$\beta_m = \frac{\frac{4}{3}\pi b^3}{\frac{4}{3}\pi(a^3 - b^3)\rho_{sphere}} \quad (4.6)$$

Solving for b and substituting from Equation 4.5, β_m becomes:

$$\beta_m = \frac{1}{\rho_{sphere}} \left(\frac{2}{3} \frac{\sigma_{cy}}{q \cdot SF} - 1 \right) \quad (4.7)$$

Thus, the mass metric is independent of the sphere volume. Similarly, the VB volume metric is not dependent on the size of the sphere, and simplifies to:

$$\beta_{vol} = 1 - \frac{3q \cdot SF}{2 \sigma_{cy}} \quad (4.8)$$

The depth rating for a spherical tank has a large impact on the metric performance for a floodable VB system. For an increase in depth rating, the mass added to strengthen a sphere to withstand greater pressure is substantial compared to the buoyancy generated. Shown in Figure 4-4, a system rated to 4,000 m has a 2.5x

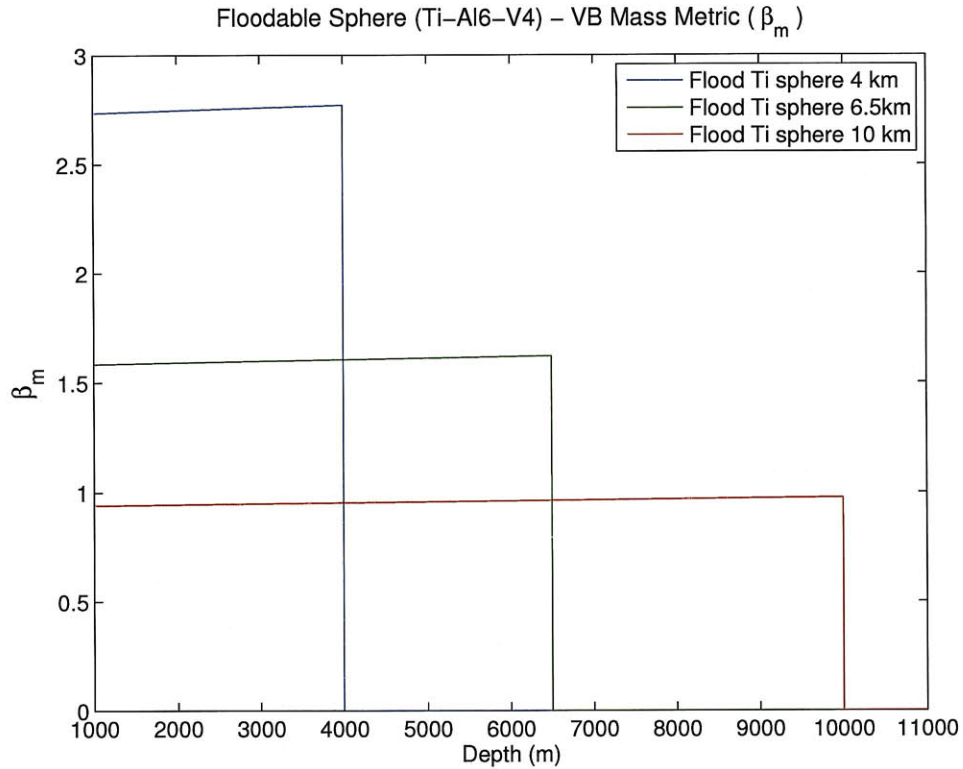


Figure 4-4: Floodable Sphere VB system: β_m vs depth. Titanium (Ti-Al6-V4) sphere.

greater β_m than a system rated to 10,000 m. The results for β_{vol} are much closer because the volume added to increase strength is less compared to the buoyancy generated. Shown in Figure 4-5, there is approximately a 15% difference between the 4,000 m and 10,000 m sphere.

This system is nearly identical in concept to releasing a ceramic sphere, because in both cases a volume of air is replaced by water. The ceramic spheres are lighter in weight and thus have higher metric values, however a floodable volume has two additional benefits. First, the system is reusable, unlike the discharged ceramic spheres that are lost and must be replaced. Second, the amount of water flooded into the volume can be regulated, and it is possible to create any amount of buoyancy change within a sphere's limits. Discharging a ceramic sphere has a preset buoyancy change.

It is possible to increase the metric performance of the system by pre-pressurizing the air inside the tank prior to dive. This reduces the pressure difference the tank experiences, and thus reduces the required strength. The metric result is simply an increase of depth rating to that of a tank with the corresponding pressure difference. For example: a tank rated for 6,500 m could be extended to 10,000 m if pre-pressurized to a pressure equivalent to the difference, or 3500 m in this case (35 MPa). Thus, a 10,000 m system would go from $\beta_m = 0.95$ to $\beta_m = 1.55$, the value for a 6,500 m system. The Alvin submersible currently uses this technique on all its buoyancy spheres, pre-pressurizing them to 13 MPa (1910 psi) in order to increase their depth rating.

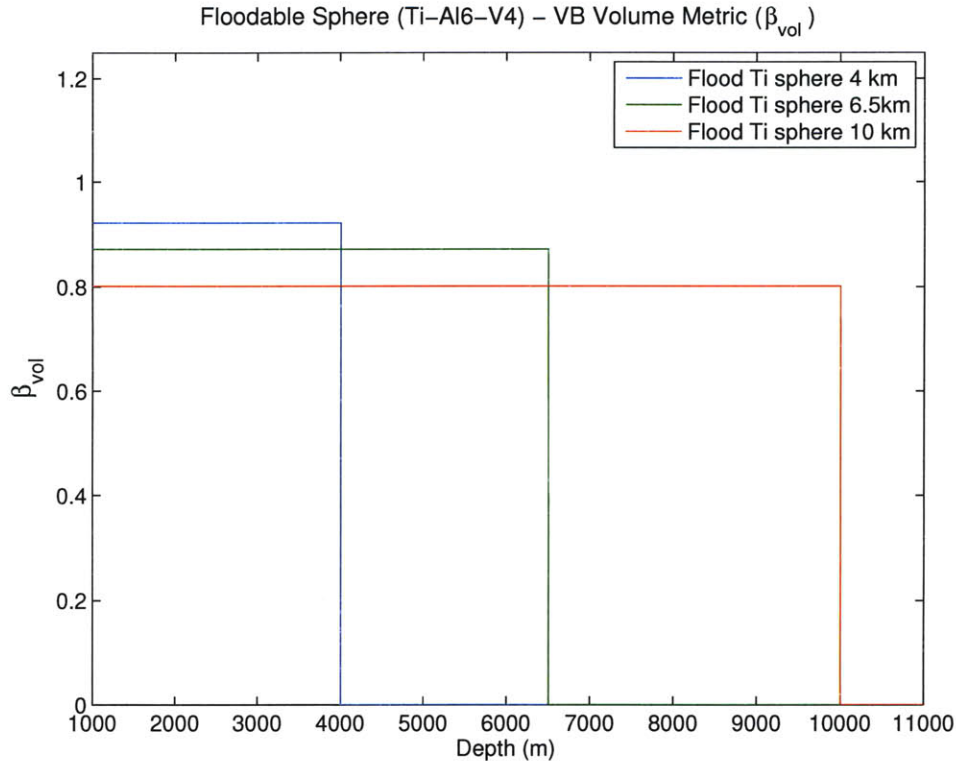


Figure 4-5: Floodable Sphere VB system: β_{vol} vs depth. Titanium (Ti-Al6-V4) sphere.

4.2.3 Water Pumped VB System: Alvin HOV

The HOV Alvin is a deep submergence submersible operated by the Wood Hole Oceanographic Institution. An icon in ocean exploration, the vehicle has made over 4,400 dives since it began operation in 1964. Modified and updated numerous times over the years, the current vehicle is rated to a depth of 4,500 m, weighs over 17,000 kg, and carries 3 people. The vehicle has a pumped water VB system rated to 6,500 m, a complex yet robust system that has been part of the vehicle since it replaced the original pumped oil VB system in 1970 [Barrie Walden, WHOI]. Slightly different than the system described in Section 3.2, the pumped water system on Alvin uses six titanium spheres as pressure tanks. Two lower tanks are used to fill with water, and four upper tanks are used to store the compressed air displaced from the two lower tanks when filled with water. To increase the depth rating of the spheres, the air is pre-pressurized with 13 MPa (1910 psi, or 1300 m depth in seawater). As explained later, pre-pressurization also increases the efficiency of the system. The system is also capable of pumping both to and from the tanks, and uses a dedicated hydraulic system to operate the moderately complicated valve system.

A detailed model of Alvin’s VB system was created to quantify performance versus depth (see Appendix E.8 for code). The mass and volume of all system components are included, except the syntactic foam packed around the spheres, which are not part of the system (the VB system is slightly buoyant, and does not need added

flotation). Since the total buoyancy created (B^\pm) by the system is limited only by the power available, the model was run in 3 different configurations. The first without including the battery mass and volume in the metric, the second using the lead acid batteries currently used in Alvin, and a third using the lithium ion batteries and titanium housing design for the next generation Alvin II. Additionally, each of the three configurations were run at 4 different amounts of *added* buoyancy generated per dive: $B^+ = 25, 50, 100, \text{ and } 200$ (maximum) kg. Lastly, system performance for an increase in the initial tank pre-charge was determined. For this configuration, all the system components (piping, valves, etc.) were unaltered, and assumed to be capable of the increased pressure.

The power requirements for the system were determined from actual system efficiencies and pump specifications given by WHOI engineers. Assuming the pump flow rate to be constant, the work done by the pump (W_{pump}) is determined by:

$$W_{pump} = P_D \dot{V} \quad (4.9)$$

for $P_D = P_{water} - P_{tank}$, or the difference between the tank and ambient water pressure, and \dot{V} is the volumetric flow rate through the pump. Knowing the pump's displacement per revolution (V_{rev}) and rotation rate (ω), the equation becomes:

$$W_{pump} = P_D(V_{rev} \cdot \omega) \quad (4.10)$$

The power input to the system is then determined from the efficiencies of the system components. In this case, the work done is:

$$W_{input} = W_{pump}(\eta_{mc} \cdot \eta_m \cdot \eta_p) \quad (4.11)$$

where η_{mc} , η_m , and η_p are the efficiencies of the motor controller, motor, and pump respectively. From the desired buoyancy change, the pumping time (t_{pump}) is found from:

$$t_{pump} = \frac{B^+}{\rho_{insitu}}(V_{rev} \cdot \omega) \quad (4.12)$$

where B^+ is the desired buoyancy addition, ρ_{insitu} is the water density at the given depth. From this, the amount of battery used for the VB system can be found:

$$E_{input} = W_{input} t_{pump} \quad (4.13)$$

Knowing the overall battery capacity, the fraction of the batteries used for VB can be found, and the corresponding mass and volume added to the overall VB system.

In this system, the round trip energy required for the buoyancy change was calculated starting from an empty tank. For example: for an increase of 100 kg of buoyancy when $P_D > 0$, the model assumes the tanks are allowed to freely flood 100 kg of water into the tank, which is then pumped out against the pressure. Oppositely, for $P_D < 0$, 100 kg of water is first pumped into the tank, then allowed to freely flow out. As water fills the tank, P_D is not constant because the air volume inside the tank

Table 4.1: The Alvin HOV VB system specifications. Three power system configurations shown: without batteries, with lead acid batteries (current battery system), and with lithium ion batteries (Alvin II). Performance values given for a depth of 6500 m.

	No Battery	Lead Acid	Lithium Ion
Depth (m)	6500	6500	6500
Mass (kg)	724	1140	837
Volume (L)	776	959	834
Static B (kg)	71	-156	18
B⁺ (added kg)	200	200	200
Energy Used (kWh)	5.19	5.19	5.19
Battery Mass (kg)	0.00	415	113
Efficiency	0.52	0.52	0.52
β_m	0.55	0.35	0.48
β_{vol}	0.50	0.41	0.47

is reduced. To accommodate this change, the power consumption is calculated using the average pressure head during the pump cycle. The mass and pressure change of the air is calculated using van der Waal’s equation of state (see Appendix B.1). Since the air in the tanks do not escape, its mass is added to the system mass.

The results of the model for a buoyancy addition of 200 kg at 6,500 m are shown in Table 4.1. The addition of 200 kg is the maximum one-way buoyancy change when the lower two spheres are filled with water. Since this is a two-way system, the total buoyancy change for the metric calculations is twice the amount of buoyancy added: $B^\pm = 2B^+$. A plot of the β_m and β_{vol} versus depth are shown in Figures 4-6 & 4-7. The results are constant versus depth because the battery mass and volume is not incorporated into this configuration. Also, since the mass and volume of the VB system are fixed, the metric results increase linearly with B^+ .

Incorporating the mass and volume of the battery used by the VB system can have a substantial effect of the metric results. The current lead acid battery system on Alvin has a capacity of 30 kWh [Lane Abrams, WHOI], and as Figure 4-8 depicts, the VB system can consume over 15% of the battery in order to create 200 kg of added buoyancy at full depth. In a more representative depiction of Alvin’s VB system performance, Figures 4-9 and 4-10 incorporate the mass and volume of the battery into the metrics. The peaks in the figures occur at the depth where the pressure head (P_D) is minimum. At this point, the ambient water pressure nearly matches the tank pre-charge, and a very small amount of battery power is needed to pump the water. As pressure becomes greater than the pre-charge, both β_m and β_{vol} decline because more battery power is needed to pump against the increased pressure head. This decline in the metrics increases for larger buoyancy changes, as the ratio of battery mass to system mass increases. At the maximum, 6,500 m and 200 kg of added buoyancy, the battery constitutes over one-third of the total VB system mass. Additionally, β_m experiences a greater decline from the peak than β_{vol} because the

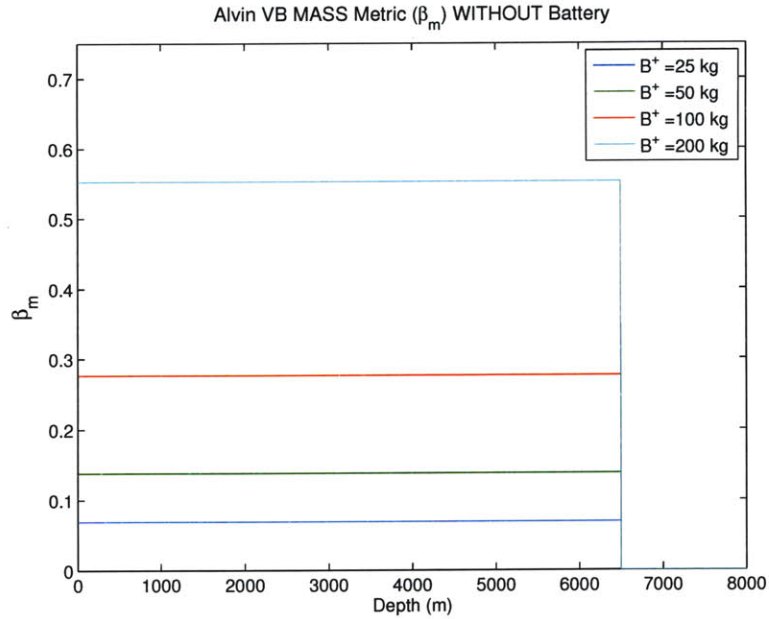


Figure 4-6: Alvin HOV: β_m vs depth. Battery mass is not included.

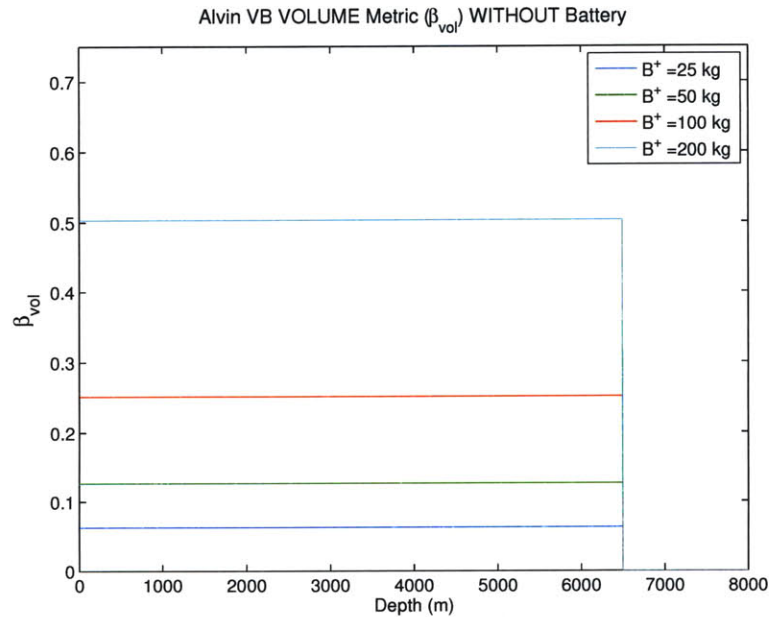


Figure 4-7: Alvin HOV: β_{vol} vs depth. Battery mass is not included.

lead acid battery is very dense ($SG = 2.2$), and adds more mass than volume to the system.

The next generation Alvin vehicle will replace the lead acid batteries with lithium ion batteries in a titanium pressure housing (see Table 5.1 for specs). This new battery system has a much greater energy density, and as seen in Figures 4-11 and 4-12, reduces the decline in the metric. At 6,500 m, the battery weight is reduced by

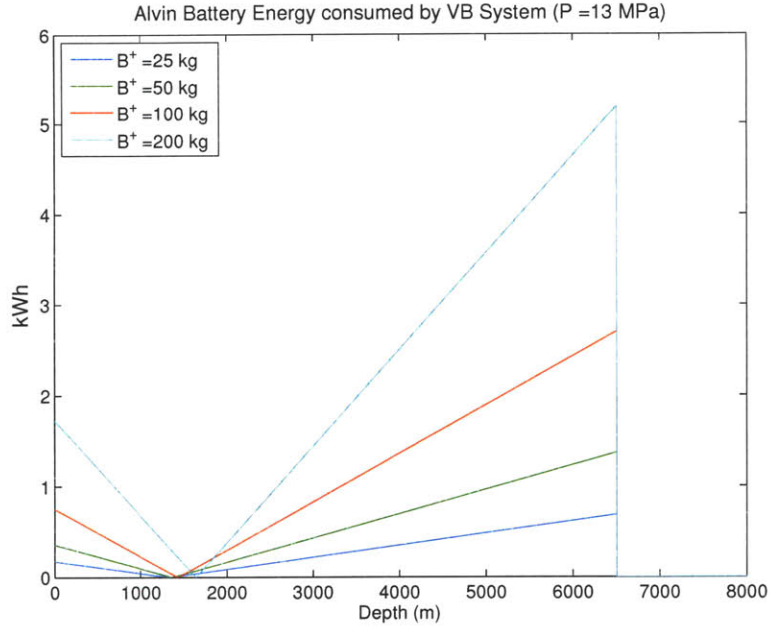


Figure 4-8: Alvin HOV: consumed energy vs depth.

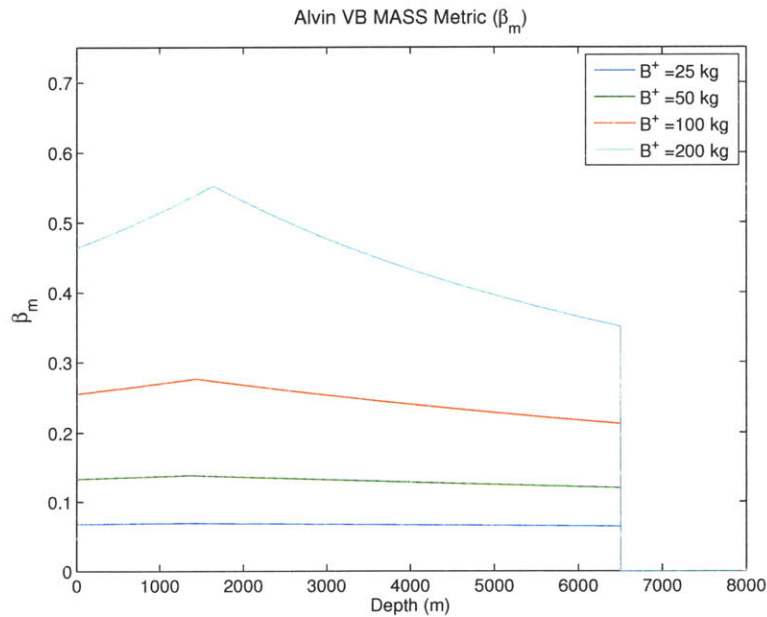


Figure 4-9: Alvin HOV using lead acid battery system: β_m vs depth.

over 70%, which increases β_m by 37%, and β_{vol} by 14%.

To investigate the effect of a pre-charge on the metric results, the model was run at twice the initial tank pressure. Figure 4-13 and 4-14 compare the metric results between the original 13 MPa (1910 psi) and a 26 MPa (1820 psi) pre-charge when 200 kg of buoyancy is added, both for lead acid and lithium ion batteries. As seen in the figures, a higher initial pre-charge shifts the metric results right. This occurs because

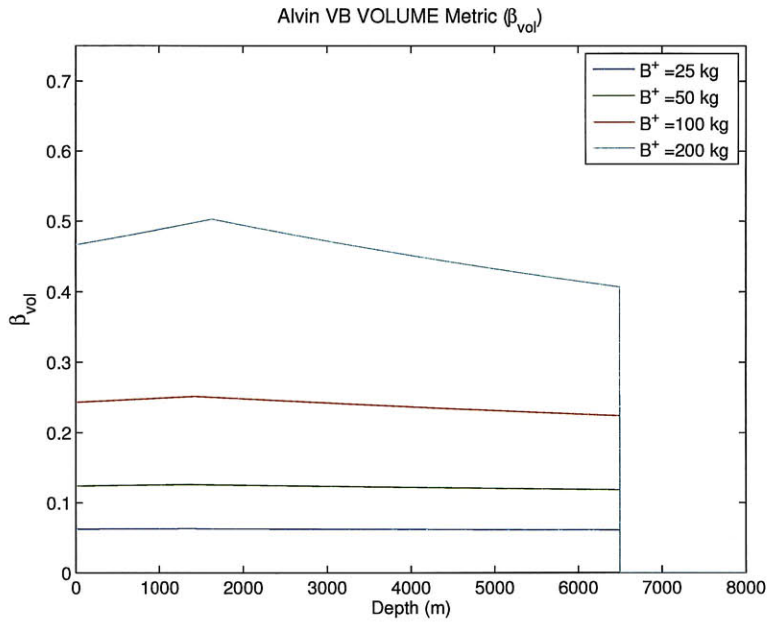


Figure 4-10: Alvin HOV using lead acid battery system: β_{vol} vs depth.

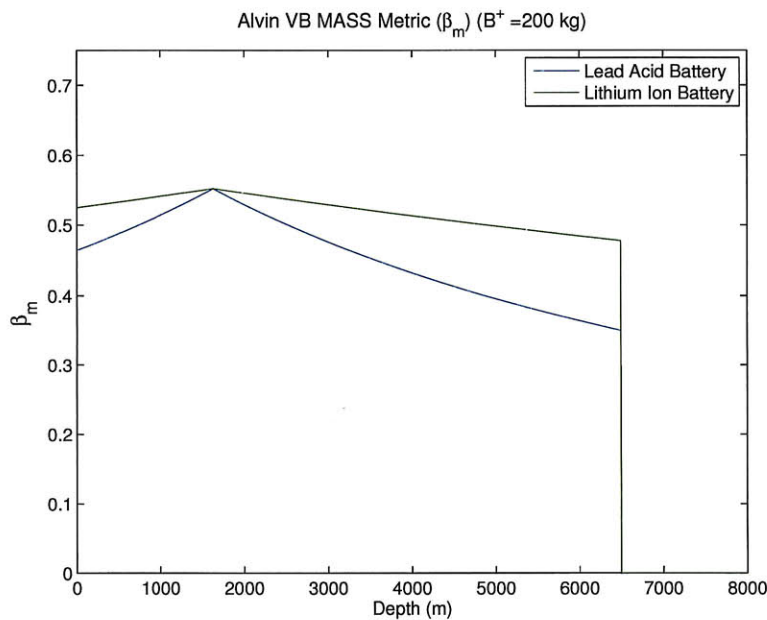


Figure 4-11: Alvin HOV: β_m vs depth. The current vehicle uses pressure-compensated lead acid rechargeable batteries. The next generation vehicle will use lithium ion rechargeable batteries in a titanium housing.

the ambient water pressure must be greater to match the increased tank pressure at the maximum metric values, thus increasing the depth of peak.

To better conceptualize the effect of a pre-charge, energy consumption for two different values for B^+ are plotted vs. pre-charge in Figure 4-15. Similar to the

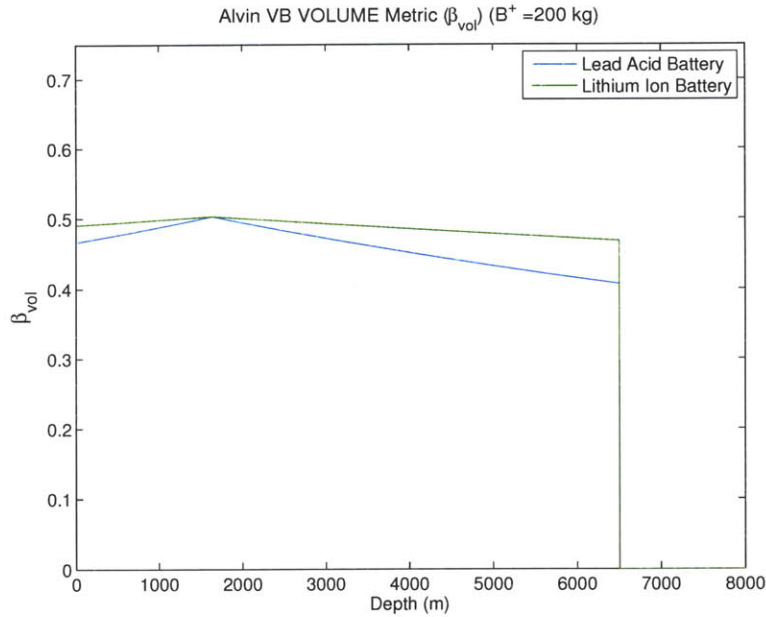


Figure 4-12: Alvin HOV: β_{vol} vs depth. The current vehicle uses pressure-compensated lead acid rechargeable batteries. The next generation vehicle will use lithium ion rechargeable batteries in a titanium housing.

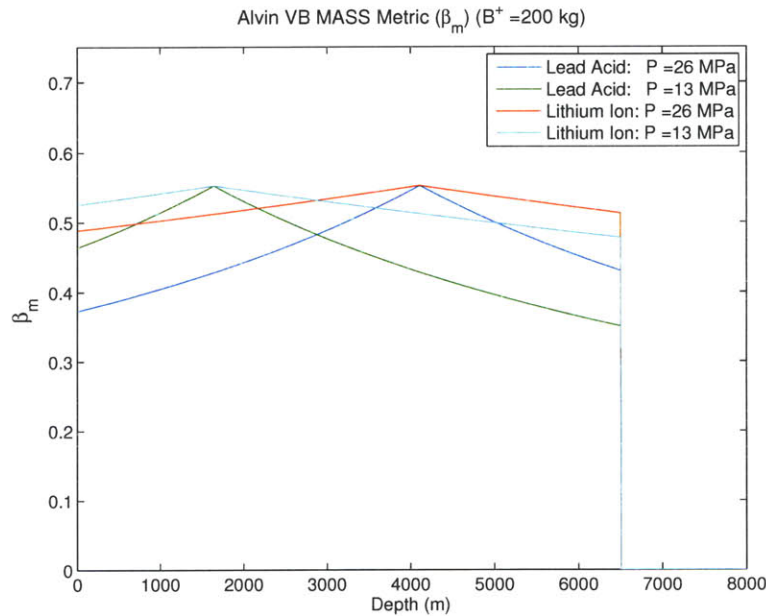


Figure 4-13: Alvin HOV: β_m vs depth comparison of tank pre-charge and battery type for a 200 kg buoyancy addition.

metric results, the energy consumption minimum is shifted to greater depths. The energy savings for the greater pre-charge is approximately 50% at 6,500 m, however at shallower depths (< 2,000 m) the energy input is 3x greater. Also of interest, the

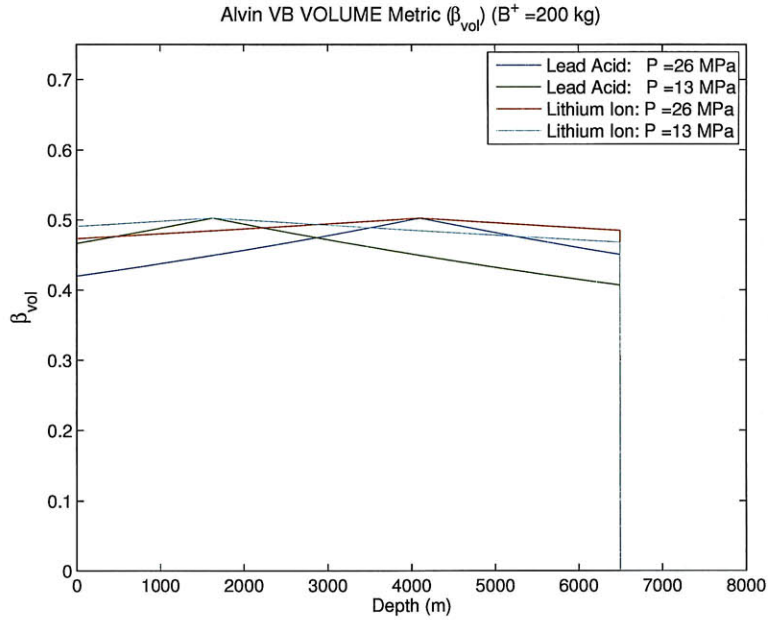


Figure 4-14: Alvin HOV: β_{vol} vs depth comparison of tank pre-charge and battery type for a 200 kg buoyancy addition.

energy minimum for a 26 MPa pre-charge is 1,000 m deeper for a B^+ of 200 kg versus 50 kg. This occurs because at a given depth, the *average* tank pressure during the buoyancy addition is greater for a larger buoyancy shift than a smaller shift. Since the energy minimum occurs when the ambient water pressure equals the *average* pressure, the larger buoyancy shift requires a greater depth to minimize energy consumption. This effect is more pronounced as pre-charge is increased, but can also be observed for the lower pre-charge in Figure 4-8.

The net efficiency of the system components (pump, motor, and motor controller) is 52%. Inclusion of the pressure work done by the pre-charge greatly affects the overall effectiveness however. Figure 4-16 plots the actual effectiveness of the system vs pre-charge and buoyancy change. The plot clearly demonstrates that pre-charging the pressure tank saves a substantial amount of energy. At the currently used 13 MPa pre-charge, the system is more than 100% effective from 1,000 to 3,000 m. To clarify, this effectiveness is the ratio of total work done to work input when pumping *against* the pressure difference. Thus, effectiveness is at a maximum when the average tank pressure during a buoyancy change is equivalent to the ambient pressure, as very little energy is needed to pump against the minimal pressure difference. As depth increases or decreases from that point, effectiveness decreases. Thus, storing energy as compressed air can be very advantageous, as it not only reduces the size (strength) of the pressure tanks, but also adds to the overall effectiveness of the system.

In service since the early 1970's, Alvin's pumped water VB system has proven itself a reliable system for repeatable buoyancy creation. Using six pre-charged spheres gives the system an extremely large range of buoyancy change, greatly reduces energy consumption, and adds a safety mechanism for depths less than pre-charge depth. To

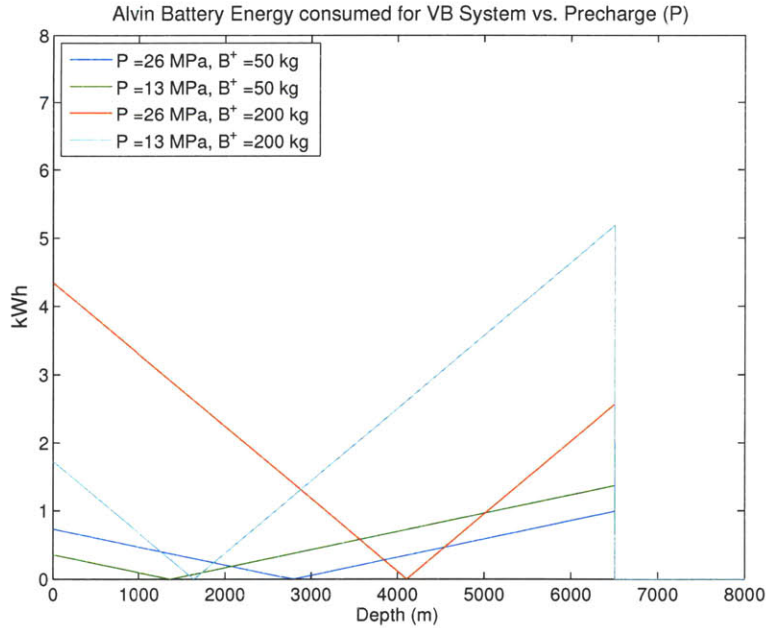


Figure 4-15: Alvin HOV: energy consumption vs depth comparison of tank pre-charge for 50 and 100 kg buoyancy addition.

maintain the pre-charge without going above the system pressure rating, four spheres are needed for pressurized air storage only⁵. Though they add safety and reduce energy consumption, they do so at a cost, as they comprise over 83% of the system mass (603 of 724 kg including air and without batteries) and 60% of the volume of the system (470 of 780 L). Additionally, no material is discharged, leaving only a battery recharge to prepare the system for the next dive. As a drawback, the response time of the system when pumping against a pressure is limited to the speed of the pump, currently 21.5 minutes per 100 kg of buoyancy added. For small changes the slow response time may be acceptable, but it could be a detriment when a quickly adjusting system is needed.

4.2.4 Pumped Oil VB System: Spray Glider

The Spray Glider is an AUV that was developed at Scripps Institute of Oceanography, and is now owned by Bluefin Robotics⁶. The vehicle is 2 meters long, 20 cm in diameter, weighs 51.8 kg, and displaces 51 L [16]. Using a pumped oil VB system (see Section 3.4), the glider controls its buoyancy to propel itself thousands of kilometers in a single deployment. The pumped oil VB system, as described in Section 3.4, has a constant mass and controls vehicle buoyancy by pumping oil from a reservoir

⁵Alvin currently is designed for a maximum tank pressure of 21 MPa (3,000 psi), which occurs at the maximum buoyancy change of 200 kg when the lower two sphere are full of water. Increasing the pre-charge pressure would increase the maximum tank pressure at full capacity, and thus the system would need to be updated to handle higher pressures.

⁶Bluefin Robotics Corporation, 237 Putnam Ave, Cambridge, MA 02139. Phone: 617.715.7000

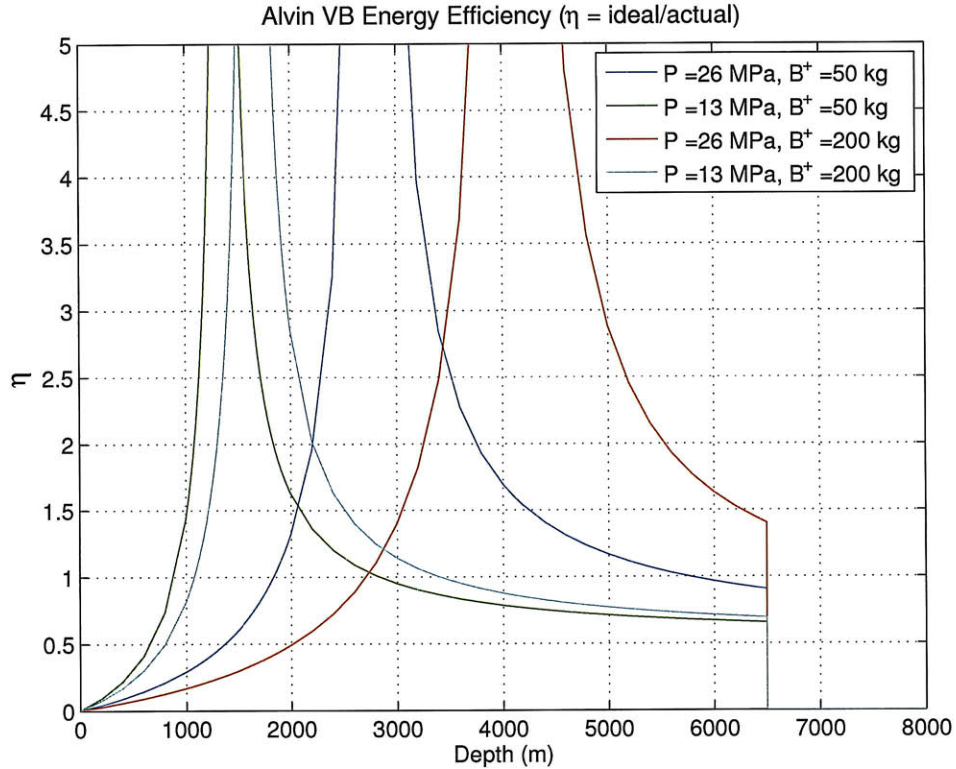


Figure 4-16: Alvin HOV: effectiveness vs depth comparison of tank pre-charge for 50 and 100 kg buoyancy addition. Effectiveness of system components is approximately 52%, however the energy stored in the compressed gas reduces consumed battery power.

in a pressure housing, to an external bladder. As the expanding bladder increases the volume of the vehicle, the buoyant force becomes greater, and the vehicle floats upward. Once the vehicle reaches the surface, the oil in the bladder is pumped back into the internal reservoir and the vehicle becomes negatively buoyant and sinks. Once at the desired depth, the process is repeated and the vehicle returns to the surface. No material is discharged during the cycle, limiting the one-way buoyancy change to the size of the bladder, and the overall buoyancy change to power available. Since the volume of the bladder is sized according to vehicle specifications, the limiting factor becomes the available power [19].

The Spray Glider is very small in comparison to nearly all other AUVs and, as such, does not require a large range of buoyancy change. The exterior oil bladders hold a maximum of 0.7 L of oil, giving the vehicle 0.724 kg of added buoyancy at the maximum depth of 1500 m. In one complete 10 hour dive cycle, the vehicle uses 12.3 Wh of power for all vehicle operations [Jake Mayfield, Bluefin Robotics Corp., 2009]⁷. The oil pump consumes 4.3 Wh, thus using 35% of the 4,500 Wh available from the lithium primary batteries onboard. Including the fractional mass and volume of the

⁷This power includes all navigational needs, and CTD sampling on the ascent for a trip to 1350 m in .

Table 4.2: Specifications and metric results for Spray Glider and SOLO Float.

	Spray Glider	SOLO float
Depth Rating (m)	1500	1800
VB System Mass (kg)	15.2	20.1
VB System Volume (L)	18.4	22.3
VB Batteries Mass (kg)	3.9	1.2
VB System SG	0.83	0.90
B⁺ (kg/cycle)	0.72	0.29
Total Cycles (Max depth)	350	200
VB System efficiency	0.62	0.71
β_m	33.3	5.8
β_{vol}	26.6	5.0

batteries and battery housing, the VB system constitutes 30% of the vehicle’s mass (15.2 of 51.8 kg), and 36% of the vehicle’s displacement (18.4 of 50.5 L). Within the VB system, the batteries represent 25% of the mass (3.9 of 15.2 kg) and 42% of the volume (7.8 of 18.4 L). These values are shown in Table 4.2.

The impressive metric results for the Spray Glider are shown in Figure 4-17. From the given component energy consumption, the vehicle has enough energy for 365 cycles. To leave room for error, the model uses 350 cycles, resulting in a total added buoyancy of $B^+ = 253$ kg. For a 10 hour dive cycle, the metric results for this two-way system are $\beta_m = 33$ and $\beta_{vol} = 26$. The metric results are constant versus depth because only the pump power consumption at full depth is known. If the glider operates at depths less than 1,500 m, the pump will use less power, thereby increasing the metric results because more cycles are possible for the same available power.

The error in these results is relatively large, approximately ± 7 for β_m , and ± 3 for β_{vol} . Linearly related to the total cycles completed, the metric results are ultimately dependent on power consumption. Mainly a function of dive depth, power consumption can also depend on sensor load, cycle time, and environmental conditions. When total power consumption is high, the number of dive cycles will be low, and metric results will be lower. Even at the low end however, the system performs extremely well compared to other VB systems. As a disadvantage, this system is limited in depth and maximum one-way buoyancy change. To determine the results for deeper and larger systems, a new model would need to be created.

4.2.5 Piston-driven Oil VB System: SOLO Float

To model the performance of a piston-driven oil displacement VB system, the SOLO float is investigated. Similar to a glider, the SOLO float is used by WHOI to measure a temperature and salinity profile. Using a variable buoyancy system, the SOLO float repeatedly sinks to a preset depth, then returns to the surface, taking sensor measurements along the way. Lacking a propulsion system for horizontal movements, the device drifts with current, and is thus classified as a float rather than an AUV.

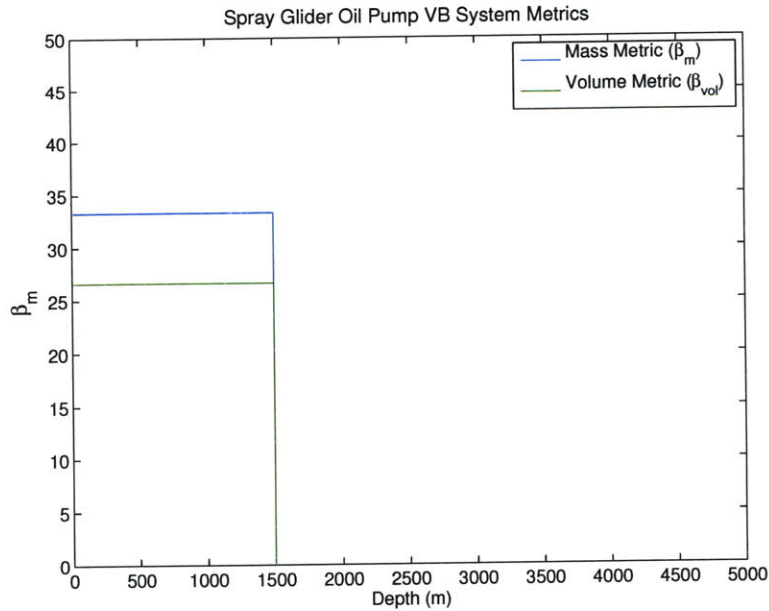


Figure 4-17: β_m and β_{vol} vs depth for the Spray Glider.

Similar in size to the Spray Glider, the SOLO float is 1.8 m long, 16.5 cm in diameter, 36 kg, displaces 35 L, and is rated to 1800 m [John Ahern, WHOI].

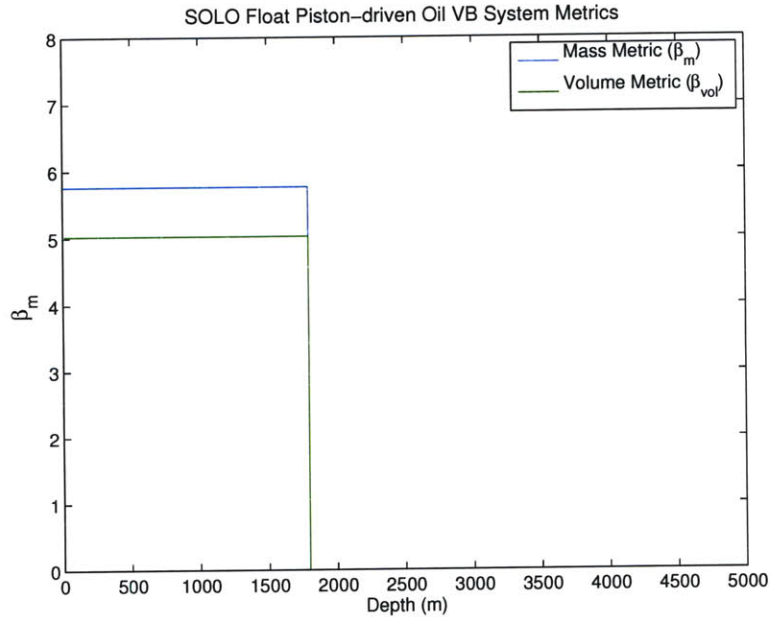


Figure 4-18: β_m and β_{vol} vs depth for the SOLO float.

The SOLO float uses a piston-driven oil VB system as described in Section 3.5. Nearly identical to the pumped oil VB system, this system uses a piston to transfer oil to an external bladder rather than a pump. As designed, the vehicle displaces only 280 cm³, or 0.29 kg, of seawater per cycle. With SOLO floats currently recording

over 200 cycles in a deployment, the float can generate a total buoyancy of $B^+ > 58$ kg. Compared to the total vehicle size, the VB system constitutes 55% of the mass (20.1 of 36 kg) and 63% of the volume (22.3 of 35 L). Additionally, a second stage VB system activates when the vehicle reaches the top 10 m of water, pumping air from inside the pressure housing to an external bladder. This system creates 800 cm³ of additional buoyancy (0.82 kg), giving the float extra freeboard at the surface for a better link to the ARGO satellite system. Used only in the upper 10 m of water, this separate system uses only 2.4% of the total cycle energy, and will not be considered as part of the VB system.

The electrical and physical specifications of the SOLO float are well known, and the model created yields consistent agreement with field performance. In a single cycle, the float consumes 6.0 Wh of energy, of which the VB system consumes 33%, or 2.0 Wh per cycle. Having 1400 Wh of lithium primary batteries onboard, the vehicle can theoretically complete 233 cycles. To be conservative, only 200 cycles are used in the model. Also, only the fractional mass of the battery used by the VB system was used in calculating β_m . The entire battery volume was used in β_{vol} however, as no discount was given for power used elsewhere in the system because the batteries are contained in the VB pressure housing. The metric results, shown in Figure 4-18, are constant through depth because the piston power consumption is assumed constant (future refinement would take motor efficiency versus depth into the model). With $\beta_m = 5.8$ and $\beta_{vol} = 5.0$, the system proves to be an efficient method for creating buoyancy. Of a more impressive result however, the efficiency of the piston system at converting electrical power to displacement work is 72%. This is based on the motor power consumption given, the depth of which was not specified. Thus, until more data can be obtained, the value should only be used as a general comparison.

The piston-driven oil displacement VB system is a very good fit for the needs of the SOLO floats. Offering simple and reliable performance, the piston system removes the inherent difficulties of the oil pumped system (mainly gas bubble buildup [19]). Though the metric results of the pumped oil system on the Spray Glider are 6-7x better, this is primarily due to a lack of onboard battery power. Having a 15% better electrical to pressure work conversion efficiency, this system would reach comparable, if not better, metric results if equal battery power were given to each. The one-way displacement capability of this system is very small, and reduces the system to small vehicles. Additionally, the entire piston stroke must be contained within a pressure housing, which may reduce the effectiveness if scaled up in size. Overall, the simplicity and high efficiency are attractive features, and it is left to future work to determine the performance of the system scaled for larger vehicles and at greater depths.

4.3 Existing System Results

A simple metric comparison of the liquid displacement VB systems (pumped water, pumped oil, and piston-driven oil) leads one to believe the Spray and SOLO systems are much better than Alvin's. The metrics for Alvin are always less than unity,

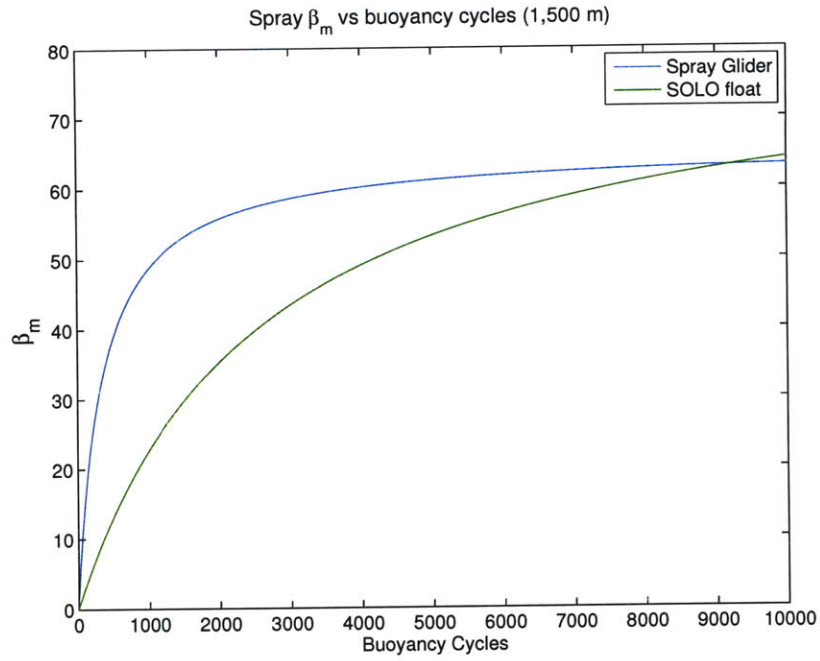


Figure 4-19: β_m vs buoyancy cycles for VB systems on Spray Glider at 1,500 m and SOLO float at 1,800 m).

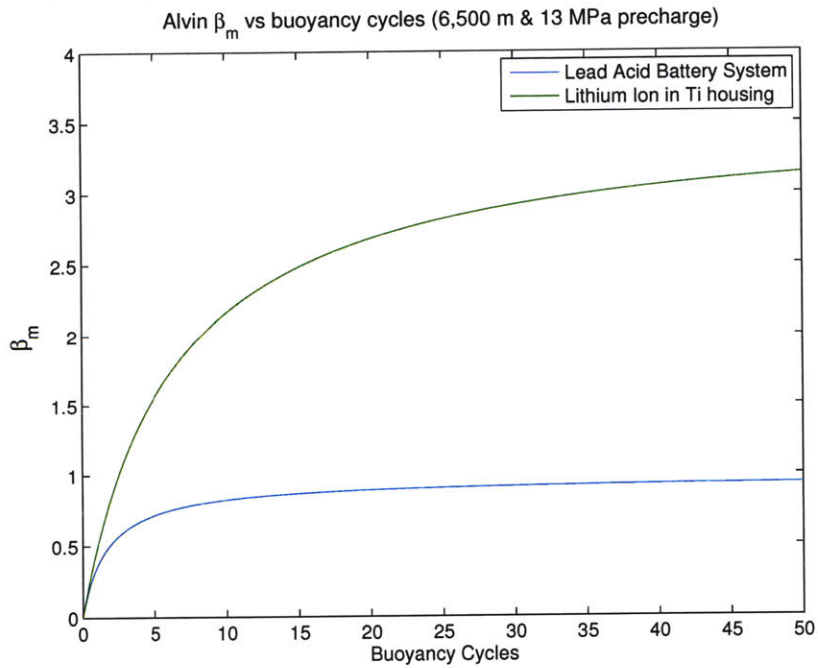


Figure 4-20: Alvin HOV pumped water VB system: β_m vs buoyancy cycles at 6,500 m (13 MPa pre-charge).

whereas SOLO metrics are between 5 and 6, and Spray between 25 and 35. Since the efficiency of the systems are with 30%, there must be something wrong with the metrics?

A more detailed look into the system shows that for systems limited by battery power, the number of cycles the system is designed for has a major effect on the metric results. The VB system on both Spray and SOLO are designed to have a small one-way range but a large total change in buoyancy. To generate the many cycles, a large amount of battery power, compared to the total system size, is required. Using lithium primary batteries (the most energy dense battery commercially available), the spray system system is capable of generating approximately 65 kg of buoyancy for every 1 kg of battery added at 1,500 m. The SOLO system has an even better efficiency, and yields approximately 75 kg of buoyancy per kg of battery at 1,800 m. Thus, β_m and β_{vol} will increase when additional battery power is added to the system, and will increase until the system size is dominated by the battery. At this point, the metric will reach a maximum, the value of which depends only on the power density of the battery system and the efficiency of the system at converting electrical power to displacement. This result can be seen in Figure 4-19. Therefore, the SOLO VB system has a lower metric value than Spray because it had small proportion of battery power to system size. Thus, if more battery is added to SOLO, β_m and β_{vol} will increase, and eventually surpass the Spray because it has a better efficiency, and thus a higher theoretical maximum.

The pumped water VB system on the Alvin HOV has a large one-way buoyancy range, but was only modeled for a single cycle. Thus, size of the system is large in comparison to the battery size, and thus the metric results have not begun to approach the system maximum. When plotted versus multiple cycles (Figure 4-20), β_m quickly increases. For the lead acid battery system, it takes approximately 5 cycles to begin to reach the maximum value of $\beta_m \approx 0.96$. When using the more energy dense lithium ion batteries, the since maximum increases to $\beta_m \approx 3.6$, however it takes over 40 cycles to approach this value.

The maximum metric value for Alvin is considerably less than the SOLO and Spray system for three reasons. First, the power density of the batteries used by Spray and SOLO are at least 6x greater than either of the two Alvin battery systems. Second, the overall efficiency is better. Most importantly however, the greater depth of the Alvin system requires a larger energy input per kg of buoyancy change. For accurate comparison, it is important that the depths are equivalent because the system size and efficiency is greatly affected by pressure. In Figure 4-21, the Alvin system is plotted at 1,800 m. At this depth, the system maximum is $\beta_m \approx 28$ for the lead acid battery system, and $\beta_m \approx 105$ for the lithium ion system. In addition to the reduced energy need, the tank pre-charge is nearly equivalent to the ambient pressure at this depth and so the system effectiveness is very high (see Figure 4-16).

This amount of total buoyancy is not practical for the Alvin system, as it needs a large range in buoyancy rather than repeated cycles. To instead compare the one-way buoyancy change capability of a system, a ratio of the one-way buoyancy range to the size of the system, excluding the battery, is shown in Table 4.3. This figure represents the size of a system relative to the one-way buoyancy range. As seen in the table,

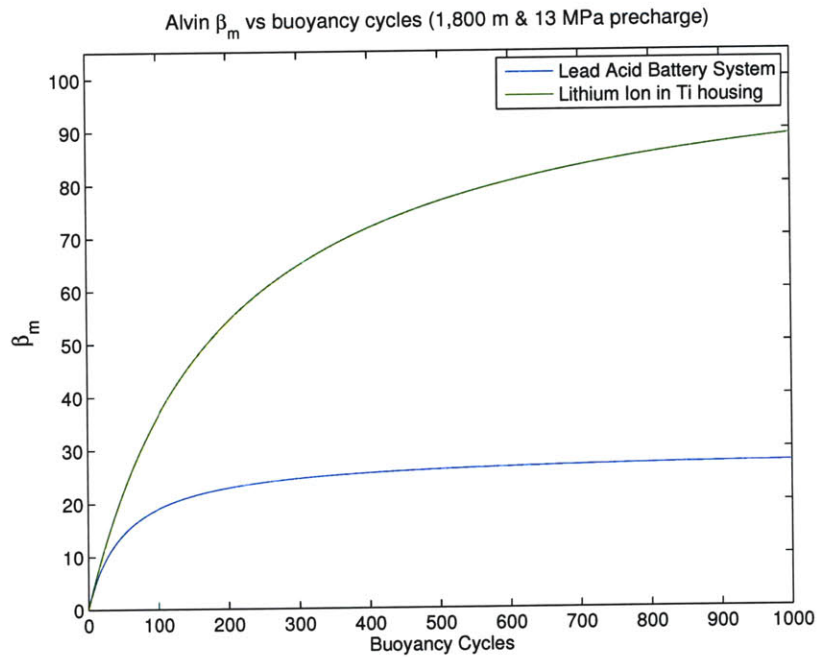


Figure 4-21: Alvin HOV pumped water VB system: β_m vs buoyancy cycles at 1,800 m (13 MPa pre-charge).

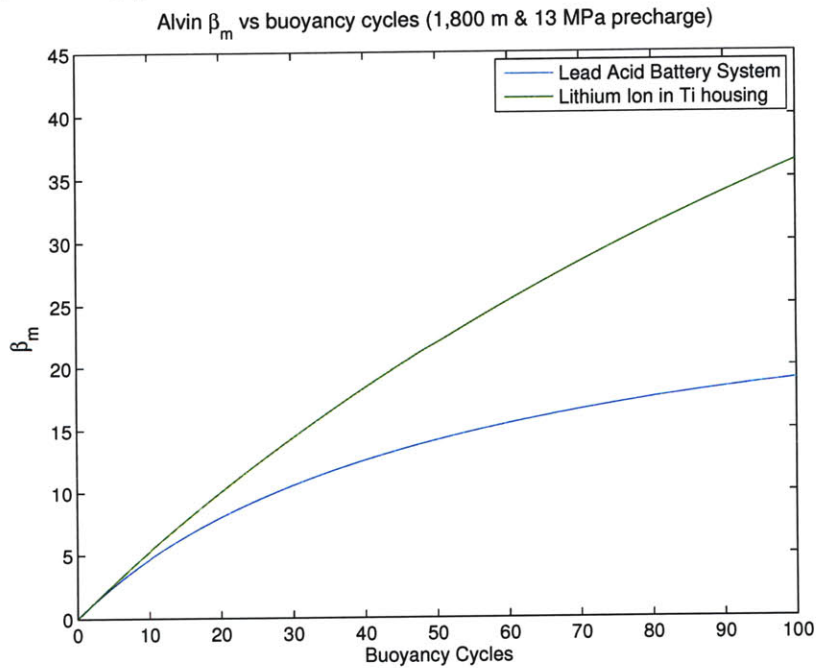


Figure 4-22: Alvin HOV pumped water VB system: β_m vs buoyancy cycles at 1,800 m (13 MPa pre-charge).

Alvin’s pumped water system is much better than the Spray and SOLO system, which are not only designed for cyclic buoyancy creation, but have to incorporate the oil used in the system into the system size.

	B^+/m	B^+/V
Spray	0.04	0.07
Solo	0.02	0.01
Alvin	0.28	0.25
Steel Discharge	0.86	6.6

Table 4.3: Ratio of the one-way buoyancy range (B^+) to system mass and volume (battery is excluded).

4.4 Existing System Conclusion

Most variable buoyancy systems are custom engineered for a precise application, and each system is very different from the next. Therefore, more than just the metrics results much be considered when comparing systems. Based completely on β_m and β_{vol} , the pumped oil system on the Spray Glider is clearly the best system of those investigated. Many capabilities are not reflected by these two values however, and for practical design purposes, a number of other factors need consideration to determine the best system for the desired requirements.

The speed and one-way range of buoyancy change are two important characteristics that do not directly affect β_m and β_{vol} . The mass discharge system has a practically instantaneous buoyancy change, whereas a fluid transfer system can change only as fast as the pump or piston transferring the fluid allows. This is indirectly reflected by the metric results. Since the mass of a pump or piston increases with power, a faster system has a greater mass, and thus a lower metric result than a similar system with a smaller pump. Similarly, the one-way buoyancy range is also indirectly included in the size of the system, as a vehicle requiring a large buoyancy range will typically have a larger pressure tank or bladder.

The geometry of the system and buoyancy increments are practical features that need assessment on a case by case basis. For example, ceramic spheres have better metric results than syntactic foam, however the metrics do not reflect the geometric packing density of the system. Syntactic foam can be formed to nearly any shape, whereas ceramic spheres are limited to the density of packed spheres. Depending on the space available, the syntactic foam may be a better choice when the overall design is considered. Additionally, the buoyancy change increments are not reflected in the metric comparison. A mass discharge system can only change buoyancy by the pre-set size of material to be discharged. Liquid mass discharge has a lower metric result, but can be released in a variable amount, and therefore may be a better system for some applications.

Lastly, the cost of a system is another important practical consideration in VB design. Some systems are expensive to build but have low operating costs, whereas other systems may be inexpensive to build, but have high operating costs. A cost metric is needed to compare systems, and must incorporate the lifetime costs of a system vs the buoyancy performance of a system.

Chapter 5

Future System Design

Variable buoyancy systems have seen little technological innovation in the last two decades, and have become a weak link to further advancement of underwater vehicles. Though there have been numerous obstacles, the main difficulties in VB system design stem from energy storage. Without ways to store enough energy in the high-pressure ocean environment, VB systems are often too large and do not generate enough buoyancy.

There are only two fundamental methods by which to alter vehicle buoyancy: changing either mass or displacement of the vehicle. Discharging material is limited to the amount a vehicle can carry. Thus, if a VB system needs to create a large amount of one-way or total buoyancy, the design must focus on altering the displacement of the vehicle. Work, or energy, is required to create added displacement because the water occupying a space must be ‘moved.’ Thus, the challenge of advancing VB technology can simply be seen as the development of a more efficient energy storage and transfer device. Herein lies the difficulty, as the amount of work needed to create buoyancy increases with depth, and can quickly become a substantial portion of the onboard energy.

From the definition of work, it can quickly be shown the minimum energy required to create displacement is:

$$E = PV \tag{5.1}$$

where P is the pressure at depth z and V the volume created. Substituting $P = \rho zg$, and solving for energy per kilogram of buoyancy created (J/kg), the equation becomes:

$$E = zg \tag{5.2}$$

Thus, for every meter of depth, the ideal minimum energy required to displace water is 9.807 kJ/kg_{B+}·km, or equivalently, 2.72 Wh/kg_{B+}·km. Thus, to generate 100 kg of buoyancy at 3,000 m, it requires a minimum of 0.82 kWh of energy.

This becomes problematic when using battery power as the source of energy. Two state-of-the-art rechargeable lithium ion battery systems are compared in Table 5.1. The Alvin II battery system uses a titanium pressure housing (rated to 6,500 m), whereas the smaller Sentry system uses an alumina ceramic housing (rated to 11,000 m, made of 96% AL₂O₃) [21]. Both systems are negatively buoyant, and thus require

flotation to be neutrally buoyant. The 2nd and 4th column of Table 5.1 use syntactic foam as flotation (rated to 11,500 m, $SG = 0.61$). The system housed in titanium has a greater size per energy ratio, requiring 37 kg and 36 L be added to the vehicle for each kWh of energy, whereas the system housed in ceramic requires approximately 40% less: 22 kg and 21 L per kWh. Applied to the minimum energy requirements, the vehicle would need 0.10 kg/kg_{B+}·km and 0.099 L/kg_{B+}·km for the titanium housing, and 0.06 kg/kg_{B+}·km and 0.06 L/kg_{B+}·km for the ceramic housing. Thus, for 100 kg of buoyancy generated at 3,000 m, the minimum battery requirement of 0.82 kWh would add 30 kg and 20 L of titanium house lithium ion battery to the vehicle, or 18 kg and 18 L for a ceramic housed lithium ion battery.

The actual energy required to generate buoyancy depends on the efficiency of the system use to create the displacement. Current efficiencies range from approximately 50 - 70%. For a system that is 50% efficient, generating 100 kg of buoyancy at 3,000 m requires 1.64 kWh of energy and 61 kg of lithium ion battery system in a titanium housing, or 36 kg in a ceramic housing. For vehicles with only onboard power, this can quickly become a substantial portion of the available battery power, thus reducing the value of a VB system. Using ceramic spheres as flotation rather than syntactic foam can reduce the size of the system by 27% for a titanium housing and 18% for a ceramic housing (see Appendix Table C.1), however, the power requirements remain unchanged.

	Alvin II	Alvin II w/float	Sentry	Sentry w/float
E (kWh)	37.5	37.5	12.8	12.8
m (kg)	816.5	1383.2	199.2	278.4
V (L)	420.0	1349.0	141.6	271.6
B (kg)	-385.8	0.0	-54.0	0.0
m/E (kg/kWh)	21.8	36.9	15.6	21.8
V/E (L/kWh)	11.2	36.0	11.1	21.2
B/E (kg/kWh)	-10.3	0.0	-4.2	0.0

Table 5.1: Specifications for deep submergence battery systems. Syntactic foam was added to each system (w/float) to achieve neutral buoyancy ($SG = 0.61$, 11,500 m). E is total energy, m is mass, V is volumetric displacement, and B system buoyancy. [Dana Yoerger & Dan Gomez-Ibanez, WHOI, 2009]

Battery technology has advanced a great deal in the past 20 years, however it still fails to have enough energy to generate the needed buoyancy for all but the largest vehicles. Finding alternative methods will be the keystone to the development of new VB systems. Chemically stored energy has extremely high density, and should be a major focus for VB system development. Using mechanically stored energy is another possibility, however of the various methods (flywheels, pumped hydro, springs, and compressed gas), only compressed gas appears to have potential. Nuclear energy has been utilized by Naval submarines for many years, however this technology has size and safety issues limiting its use to extremely large and government controlled vessels. Lastly, quickly evolving nanotechnology is thought to hold new developments

for energy storage, which may be applicable to advancing VB systems.

5.1 Chemical Energy Systems

Using chemically stored energy has very promising characteristics for application to advanced VB systems. There are numerous compounds that have very high energy densities and, if they can be used to create buoyancy, could give underwater vehicles the much needed compact VB system capable of efficient buoyancy creation.

The promise of chemical energy can be demonstrated with the following simple example. The well known explosive trinitrotoluene (TNT) has an energy density of approximately 0.65 kWh/kg, or 1.54 kg/kWh [14]. As shown in Equation 5.2, the ideal energy needed for creating displacement is 2.72 Wh/kg_{B+}·km. Using TNT, it would only require 4.2 g/kg_{B+}·km. Therefore, only 1.3 kg of TNT would be required to generate 100 kg of buoyancy at 3,000 m, whereas the Sentry battery system would require 18 kg (Lithium ion battery in ceramic housing, see Table 5.1). Though using an explosive sounds extremely unsafe, there may be ways to control similar reactions for integration into a VB system.

5.1.1 Carbonate or Bicarbonate Reaction VB System

It was hypothesized that a carbonate or bicarbonate chemical may be used to generate gas for a VB system. Both compounds play a vital role in the pH balance of the ocean, and much is known about their behavior. The idea was a carbonate or bicarbonate compound could be mixed with another compound, ideally water, to produce CO₂ gas. To determine the feasibility of this system, the solubility and density of CO₂ was first studied.

Plotting the density of CO₂, using van der Waals equation of state for a real gas, clearly demonstrated that CO₂ does not compress well (see Appendix B.1 for detailed van der Waals equation). In Figure 5-1, the molar density of the most common and best performing gases are shown. In the ideal scenario, a gas would have a linear behavior. However, the plot shows that at a pressure of approximately 20 MPa (2,000 m), the gases all begin to deviate from the ideal, curving negatively. This reduces efficiency at higher pressure, because the ratio of $\delta n/\delta P$ is increasing (for n is the moles per unit volume, and P the pressure). CO₂ performs much worse, having a very shallow slope at only 1,000 m depth. The specific gravity of the gases is plotted in Figure 5-2. CO₂ is shown to be nearly 6x more dense than neon, oxygen, and nitrogen, and over 15 times more dense than helium and hydrogen. Figure 5-3 demonstrates that CO₂ becomes a liquid at approximately 350 m in depth. Additionally, the solubility of CO₂ in seawater was plotted in moles of CO₂ per L of seawater (see Appendix B.2 for Henry's Law concentration equations) [17]. Having nearly equal concentrations of CO₂ below 400 m, and then again at approximately 3,000 m. The system would therefore require many moles of CO₂ to account for absorption into the water, which reduces the efficiency and increases the difficulty of system design.

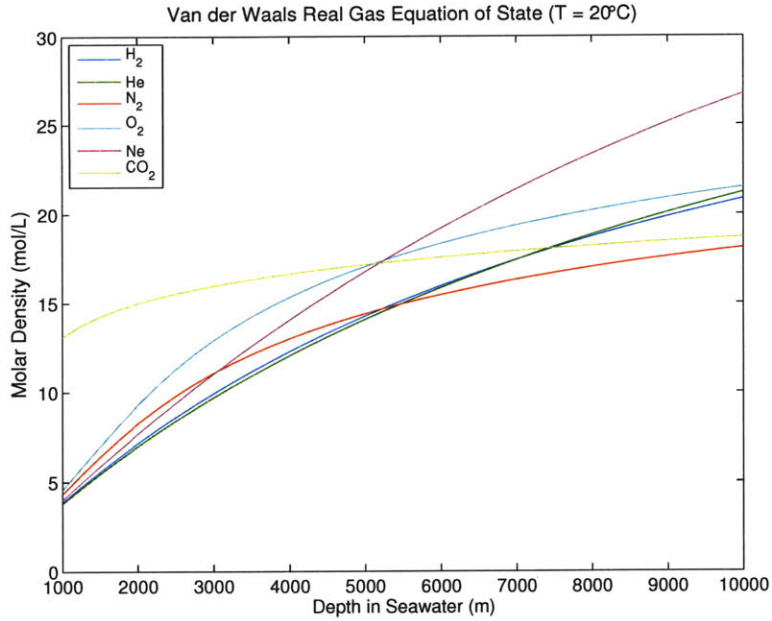


Figure 5-1: Gas molar density vs depth (pressure).

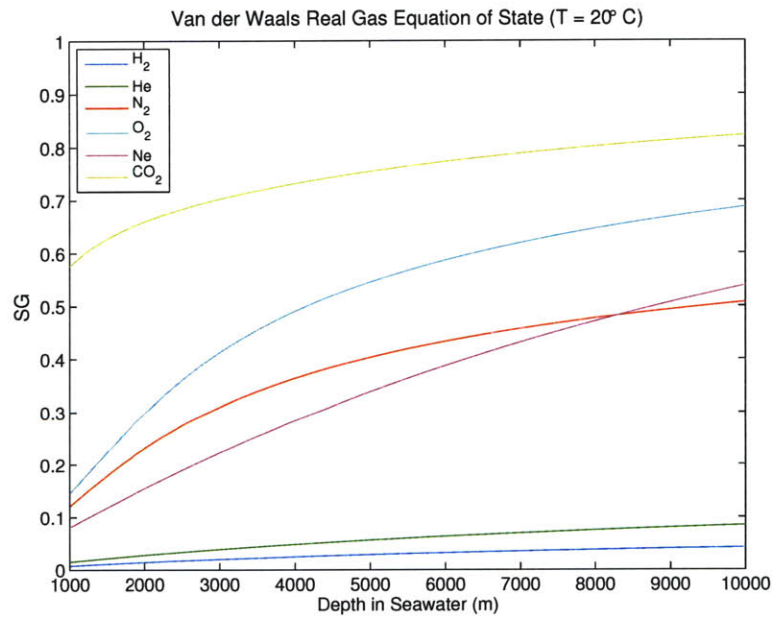


Figure 5-2: Gas specific gravity (SG) vs depth (pressure).

From these findings, it was concluded that CO₂ would not be a reasonable candidate for use as a gas in a displacement VB system. Though easy to generate, it has poor compression characteristics, and thus carbonate and bicarbonate reactions are not investigated further in this thesis.

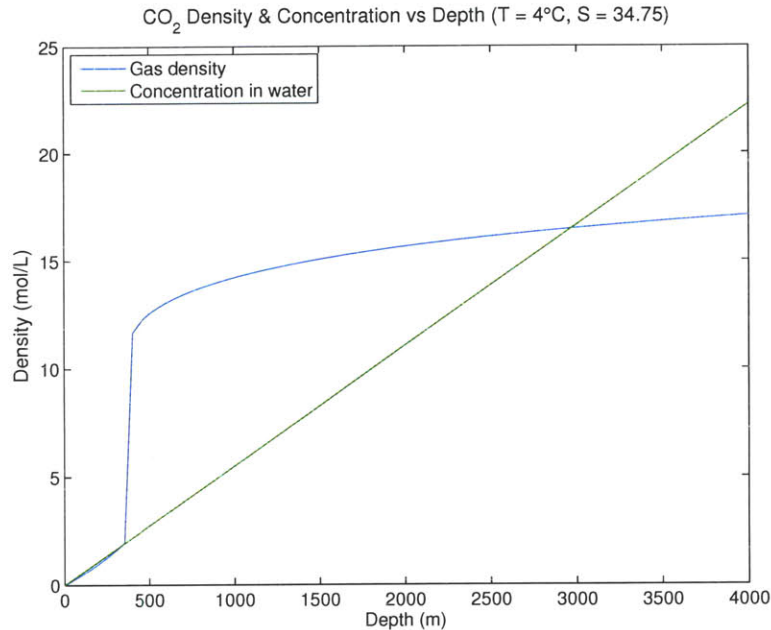


Figure 5-3: Molar density and aqueous concentration of CO₂ gas vs depth. Aqueous concentration in units of moles per L of *seawater*, and CO₂ gas density in moles per L of *gas*. The density spike at 350 m is the transition from gas to liquid.

5.2 Mechanical Energy Systems

5.2.1 Compressed Gas VB System

The compressed gas VB system is the most common type of VB system. Used by Naval submarines, scuba divers, and many other underwater vehicles; compressed gas systems store gas at a pressure greater than ambient conditions, and create buoyancy by forcing water out of a ballast tank or inflating a bladder. However, the relatively low pressure ratings of steel and aluminum tanks have restricted the system to operation in less than approximately 1,000 m of water. However, new high-pressure tanks made of carbon-fiber may be the most promising near-term technology for creating a more capable VB system.

In order to create hydrogen fueled automobiles with a range comparable to traditional gasoline vehicles, hydrogen must be stored at higher pressures. This has pushed the industry to advance the capabilities of high-pressure gas storage tanks from 35 MPa to 80 MPa (5,000 to 11,600 psi) [26] since 1999. To investigate the feasibility of incorporating these new high-pressure carbon-fiber gas storage tanks into VB systems, a model was created to determine the capabilities of this a system.

Nearly identical to the simple system SCUBA divers use to adjust buoyancy, a compressed gas VB system has few parts and uses minimal energy for operation. Shown in Figure 5-4, the system controls buoyancy by altering the volume of a bladder¹. Buoyancy is increased by allowing pressurized gas to flow into the bladder,

¹Many shallow underwater vehicles use ballast tanks rather than a bladder. However, the

increasing vehicle displacement and subsequently, increasing the buoyant force. To reduce buoyancy, the bladder is allowed to purge gas to the ocean, reducing the displacement of the bladder and thus the vehicle buoyancy.

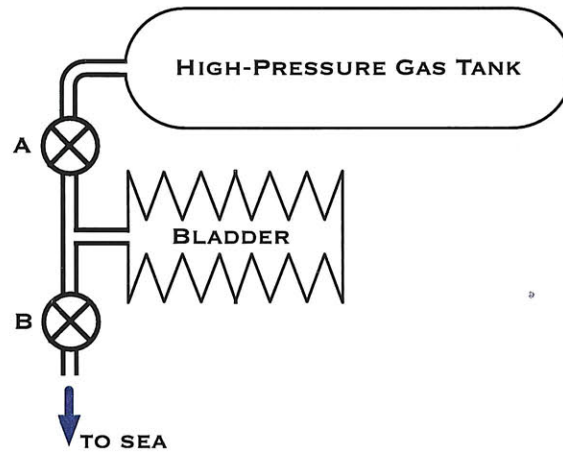


Figure 5-4: Pre-compressed gas tank VB system schematic.

System Specifications

A model was developed in order to determine the characteristics and capabilities of the above described compressed gas VB system (see Appendix E.2 for code). Specifications for model components were taken from items currently available off-the-shell (see Appendix D for specification manuals). Three different tank pressure ratings were tested: 35, 50, and 70 MPa, all manufactured by Lincoln Composites². Ranging from 30 to 120 L in volume, the tanks and valves comprise the major weight and volume of the system, and thus exact specifications for the auxiliary parts (tubing, attachment mechanisms, battery power, protective casings) were estimated to weigh 2 kg and be made of 316 stainless steel [5]. The weight of the gas is included into the model, however apparatus compression is not.

The model also determines the performance for 100 MPa (15,000 psi) storage tanks, which are the next generation of storage tanks. Though not yet commercially available, ASME has already begun developing the code and standards for tanks of this rating [15]. Compressing gas higher than 100 MPa shows diminishing returns of added hydrogen storage versus added wall mass[25], and thus 100 MPa tanks will likely be the highest pressure tank manufactured in the near future. Since the specifications for this theoretical 100 MPa tank are unknown, the mass was estimated to be a 25% increase over the 70 MPa tanks with density held constant.

amount of gas absorbed into water increases with depth, and depending on the type of gas used, may reduce the performance of the system.

²The Tuffshell© H₂ Fuel Tanks were design and manufactured by Lincoln Composites Inc, 6801 Cornhusker Highway, Lincoln, NE 68507, (402) 464-6611, www.lincolncomposites.com

	∇ (L)	m (kg)	B (kg)	SG	B^+ (kg)	β_m	β_{vol}
1: LT 35 MPa	60.06	26.94	34.79	0.44	3.40	0.25	0.11
2: LT 50 MPa	124.38	58.00	69.84	0.46	37.45	1.29	0.58
3: LT 70 MPa	46.67	30.54	17.42	0.65	22.74	1.49	0.94
4: LT 70 MPa	172.66	95.23	82.22	0.54	87.13	1.83	0.97
5: 100 MPa*	200.14	118.04	87.65	0.58	132.10	2.24	1.27

Table 5.2: Pre-compressed gas tank VB system specifications and performance. B and SG are the static buoyancy and specific gravity of the system at the surface. B^+ is the amount of added buoyancy the system can create. B^+ , β_m , and β_{vol} are all stated for 3,000 m. LT are Lincoln Composites Tuffshell[©] carbon fiber gas tanks [13]. *The 100 MPa tank is not yet available.

Results

To get an intuitive feeling for the performance of the compressed gas VB system, the total positive buoyancy vs depth is plotted (Figure 5-5). At a depth of 3,000m, a 120 L tank storing gas at 70 MPa is capable of displacing approximately 100 kg of seawater (for hydrogen, helium, or neon gas). The performance difference between gas types is apparent, as nitrogen and oxygen produce approximately half the added buoyancy at 3,000 m. CO₂ is also plotted to demonstrate its poor compression characteristics. Argon and Fluorine were also tested in the model, but because they only slightly outperformed the more common oxygen and nitrogen, they are excluded the results.

In a compressed gas VB system, the type of gas used for compression heavily influences the performance of the system. Shown in Figure B-1 of the appendix, the molar density for each gas increasingly deviates from linearity as depth increases. Neon exhibits the most linear behavior, and has the highest molar density of the selected gases above 5,000 m. This significantly increases the performance of pressurized tank systems because more molecules of gas can be stored in the tank. Carbon dioxide, oxygen, and nitrogen all show a decreasing curvature as pressure increases, resulting in inefficient pressurization, leading to poor system performance (see Appendix B.1 for gas pressurization behavior modelled from van der Waals equation of state) .

For this two-way system, the VB mass (β_m) and volume (β_{vol}) metrics for the selected gases using Tank #4 are shown in Figures 5-6 & 5-7. For β_m , hydrogen and helium out perform all other gases, including neon, because they both have extremely light molecular weights. They both maintain $\beta_m > 1$ for depths less than 4,000 m, whereas for oxygen and nitrogen, $\beta_m > 1$ only to 2,500 m. For β_{vol} , the results are less distinguished. Neon outperformed all other gases because of its superior compression characteristics.

The metric comparison for the different tanks³ is shown in Figures 5-8 & 5-9. As seen in Figure 5-8, β_m increases as tank pressure rating increases. At depths less than 2,000 m however, β_m is nearly equivalent for the 50, 70, and 100 MPa tanks. This occurs because the added mass to strengthen the tank wall offsets the added

³Tank #3 (70 MPa, 30 L) was omitted from the plot because it performs nearly identical to the larger volume Tank #4 (70 MPa, 120 L) for β_{vol} , and slightly lower values of β_m .

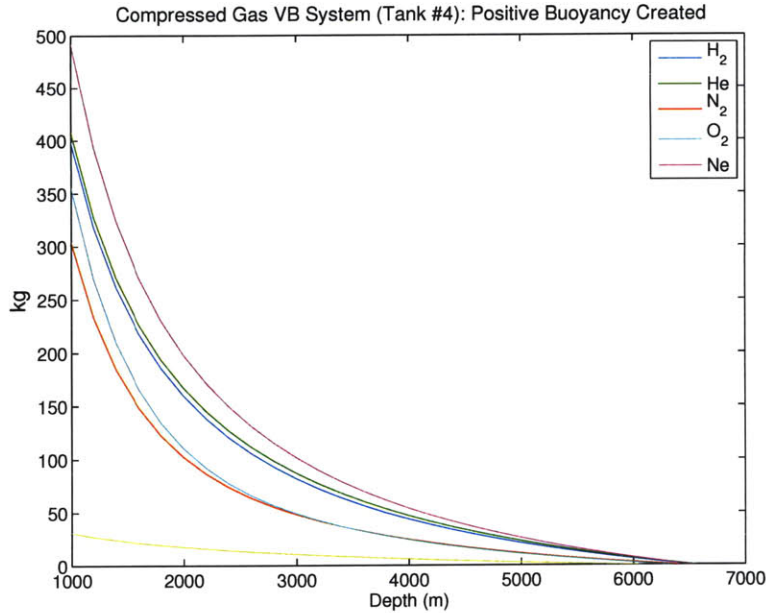


Figure 5-5: Total added buoyancy vs depth for a compressed gas VB system using tank #4 (120 L, 70 MPa).

performance, although B^+ still increases as tank rating increases. The results for β_{vol} are shown in Figure 5-9. For this metric, there is a larger difference in performance as tank rating increases. Thus, the volume added to the system for strengthening the tank walls is less than the additional displacement created.

Conclusion

Using a compressed gas VB system, hydrogen, helium, and neon clearly outperform all other gases in terms of both β_m and β_{vol} . Neon created approximately 10-20% more buoyancy than hydrogen and helium from 1,000 - 5,000 m. The much larger atomic weight of neon was a disadvantage in terms of β_m however, where hydrogen and helium were approximately 20% higher.

Safety, availability, and cost were not thoroughly investigated, though they are very important for the design and application of a compressed gas VB system. Helium and neon are much more stable, and thus safer than hydrogen. A quick cost analysis found neon to be 15x more expensive than helium⁴. Therefore, in terms of performance, safety, and cost, it was concluded that helium is the best gas to use for a compressed gas VB system.

Utilizing the newest generation of high pressure gas tanks, compressed gas VB systems may be an attractive solution for new VB development. Though performance decreases with depth, a system using 70 MPa tanks provide a great deal of added buoyancy to depths of 4,000 m. When a 100 MPa tank is developed, it will add even

⁴Cost estimate for He and Ne from: American Gas Group, 6055 Brent Drive, Toledo, Ohio 43611. Phone: 419.729.7732

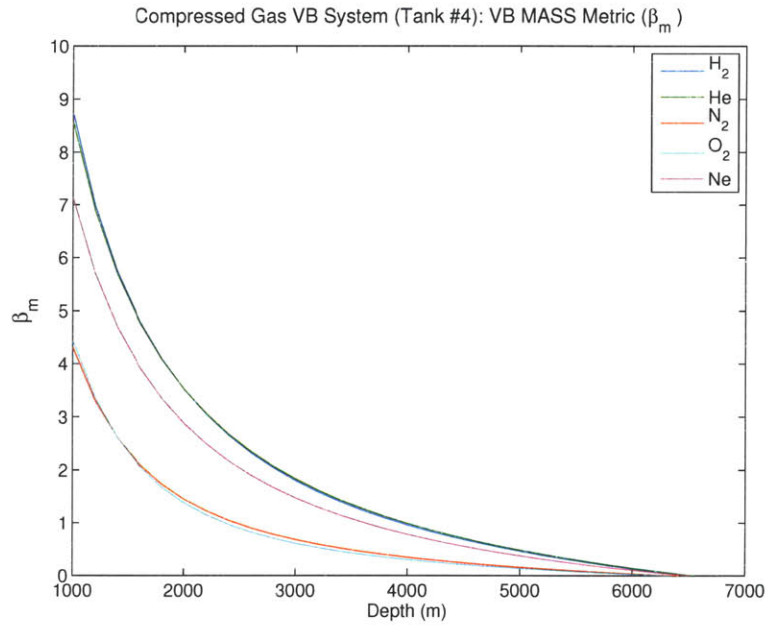


Figure 5-6: β_m vs depth for a compressed gas VB system using tank #4 (120 L, 70 MPa).

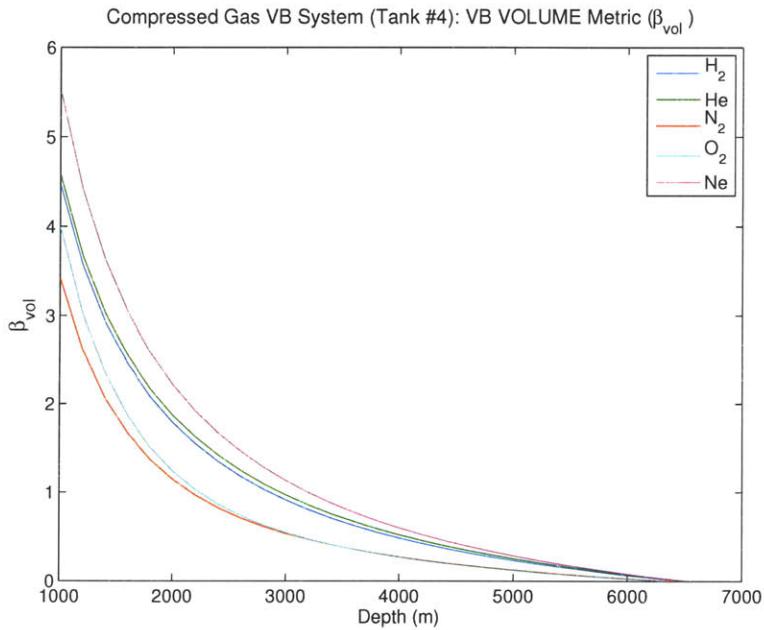


Figure 5-7: β_{vol} vs depth for a compressed gas VB system using tank #4 (120 L, 70 MPa).

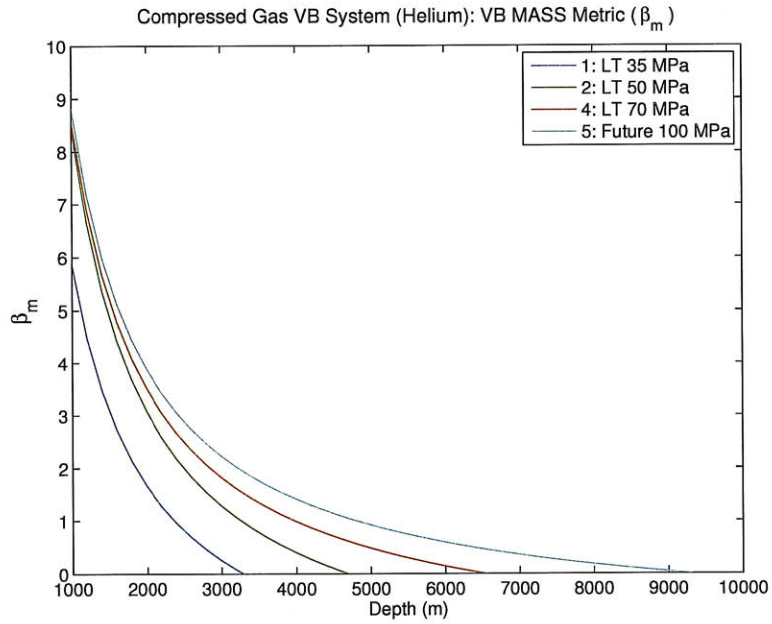


Figure 5-8: β_m vs depth for a compressed gas VB system using helium gas.

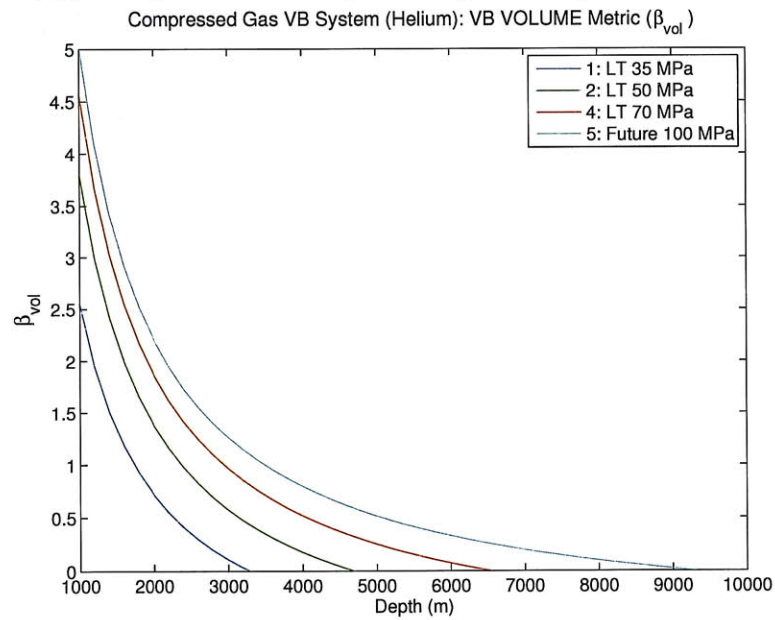


Figure 5-9: β_{vol} vs depth for a compressed gas VB system using helium gas.

more available buoyancy to greater depths, further strengthening the performance of the system.

In addition to providing a substantial amount of buoyancy, other system features of a compressed gas VB system may prove to be more important. Unlike other systems, a compressed gas system adds a considerable amount of static buoyancy. This is very advantageous, as most underwater vehicles are negatively buoyant and require substantial amounts of additional flotation. Thus, it may be possible to combine the VB and flotation system. As seen in Table 5.3, the entire compressed gas VB system has a specific gravity slightly better than syntactic foam.

	5 km	7 km	10 km
Alumina SeaSphere	0.24	0.35	0.35
Glass Sphere	0.48	0.48	0.41
Syntactic Foam	0.48	0.56	0.61
Gas Tank (2,4,5)	0.46	0.54	0.58

Table 5.3: Specific gravity (SG) vs depth for 3 types of buoyant materials and the compressed gas VB system (using tanks #2, 4, & 5). For buoyant material specifications, see: [1], [20], & [23].

The ability to quickly change buoyancy is another minor, but important feature. Current pumped systems are limited to a pump flow rate that decreases with depth, and can take many minutes to reach the desired buoyancy⁵. A compressed gas VB system can transfer gas very quickly, however, and one of the major design issues for this system will be to control, or slow, the flow of high pressure gas from the storage tank to the bladder in order to keep from potential freezing issues. Though not as fast as releasing a mass, this system has the potential to decrease response time substantially, possibly within a minute.

The capability to trim the vehicle and have a great deal of reserve buoyancy at the surface is another added benefit other VB systems cannot achieve. Having multiple bladders throughout the vehicle, the location of buoyancy change can be controlled to adjust vehicle pitch and roll. This would increase maneuverability, allowing the vehicle to adjust positions for improved sensor measurements, sample collection, and hydrodynamic alignment. Additionally, a vehicle that is highly buoyant at the surface is easier and safer to handle on deployment and retrieval. The compressed gas system has a great deal of added buoyancy capabilities at depths less than 1,000 m, allowing for as much freeboard as needed. For example, if a system using tank #4 used all the available buoyancy at 3,000 m, it would still have enough pressurized gas to generate 18,000 kg (27,000 L) of buoyancy at a depth of 5 m (at 70 MPa, the 120 L tanks holds 46,000 L of helium at STP). This added reserve can also be used to increase the speed of ascent.

As a final benefit, the compressed gas VB system uses a negligible amount of power. The energy needed to displace the water is stored in the pressurized gas.

⁵Alvin can take up to 40 minutes for a full buoyancy change.

Since the tank is charged at the surface, the only energy required from the onboard power source is the small amount used to operate the valves.

To give the vehicle designer a better idea of the size and capabilities of the system, further specifications are given in Table 5.4 gives more specifications. For example, when using tank 4, the system would occupy 173 L, weigh 95 kg, be 82 kg buoyant, and provide 87 kg of added buoyancy at 3,000 m, or 7 kg at 6,000 m.

Tank	m (kg)	∇ (L)	B (kg)	$B^+_{3 \text{ km}}$	$B^+_{4 \text{ km}}$	$B^+_{5 \text{ km}}$	$B^+_{6 \text{ km}}$
2: 50 MPa	58.0	124.4	69.8	37.5	11.5	0.0	0.0
3: 70 MPa	30.5	46.7	17.4	22.7	12.3	6.0	1.8
4: 70 MPa	95.2	172.7	82.2	87.1	47.0	22.9	6.7
5: 100 MPa*	118.0	200.1	87.7	132.1	83.5	54.3	34.8

Table 5.4: Specifications and performance for compressed gas VB systems. B is the static buoyancy of the system and B^+ is the added buoyancy (kg) at the subscripted depth (mass and displacement are for the entire system). See Appendix D for tank and valve manuals.

The model created for the compressed gas VB system generates the theoretical performance of the system, but is not a detailed system design. Minor components were estimated in size, and thus results are approximate. System compressibility was not taken into consideration, which may slightly affect the performance and static buoyancy of the system. Intended for use in the transportation industry, the tanks are designed with strict safety and durability requirements [10], intended for a 20 year life, and to withstand a temperature range of -40°C to 85°C [15]. The negative pressure rating of the tanks have not yet been researched. This is important to the practical design of the system because once a tank has been depleted, the tank pressure is equal to the ambient water pressure. Thus, an increase in depth will put a negative pressure on the tank. This may be a safety hazard, and is left to future research.

Chapter 6

Conclusion

Research of buoyancy systems employed by current underwater vehicles show there is much to gain from an advancement in VB technology. Vehicle capability, energy efficiency, safety, and ease of use are a few of the benefits of a more capable VB system. There are inherent difficulties in dealing with the harsh deep ocean environment however, and development of a new system is tied to creating better ways to store and transfer energy at depth.

The developed metrics (β_m & β_{vol}) quantitatively compare the performance versus mass and volume of a VB system. These two metrics do not completely compare one system against another however, because the number of cycles a system is designed for has a large influence on the results. To compare the overall system effectiveness, it is best to compare the metric maximum for many cycles. Analytical characteristics of a system is not incorporated into the metrics (safety, complexity, reliability, etc.), and must be compared on a system-by-system basis. Thus, the metrics give a larger understanding of a VB system's performance, but for use as a design tool, the systems must be compared at equal cycles and depth ratings.

The metric results for many of the systems are shown in Figures 6-1 & 6-2. For multiple cycles, the oil displacement systems are the best of those investigated, however a smartly designed pumped water system using the proper pre-charge may likely be a better solution. Compressed gas systems using carbon fiber pressure tanks may be the next system development, as they have favorable metric results with a number of additional features. However, the high energy density of chemical VB systems give them the most potential to be the compact and capable system needed for advancing underwater vehicle technology.

As underwater vehicles become more complex, so too does the requirements for a buoyancy system. Using the developed metrics, designers can determine the best system for the capabilities needed. This may not be a single system however, as the complex needs may best be fulfilled using multiple systems, each matched to the particular need.

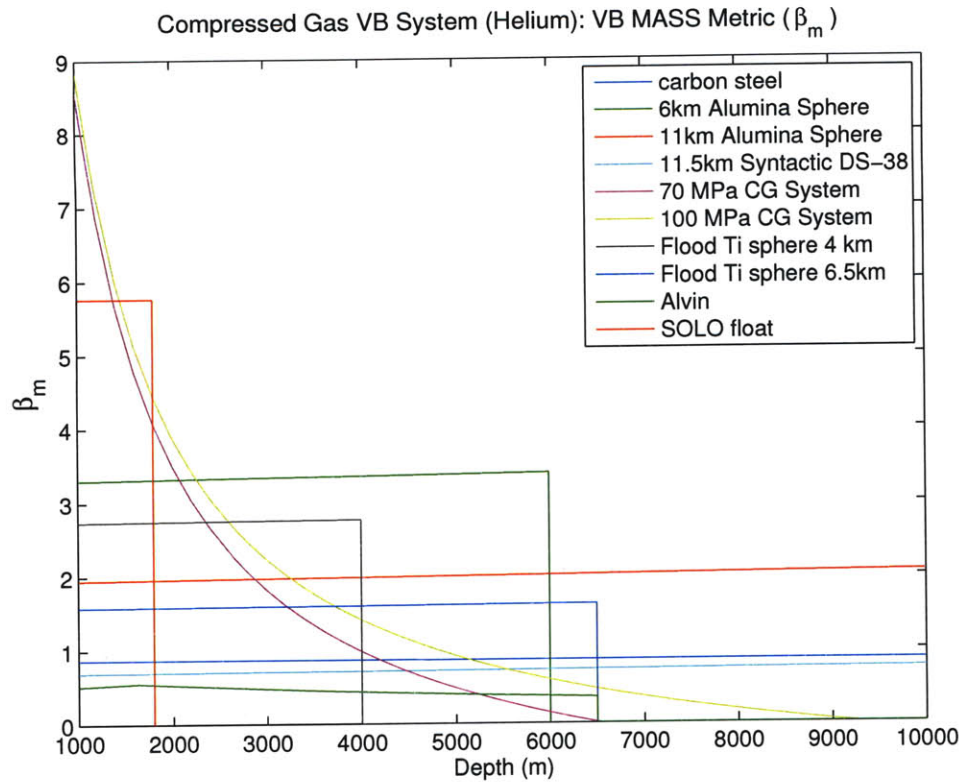


Figure 6-1: β_m vs depth for systems explored in this thesis.

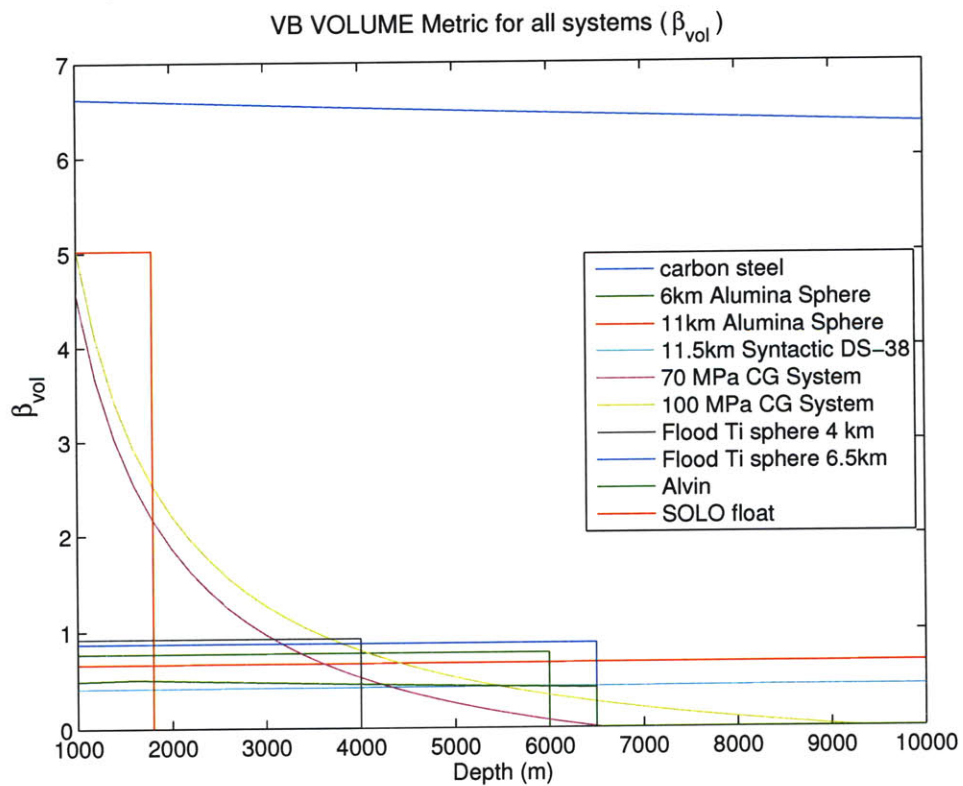


Figure 6-2: β_{vol} vs depth for systems explored in this thesis

Chapter 7

Future Work

This thesis is not the culmination of a research project, but a report documenting the first step towards developing a more capable variable buoyancy system. Though successful in creating a metric for comparison, further refinement is needed to deliver a more complete tool for engineers. At this point, there are three areas the author feels are the logical progression of future work. The first is to model current VB system in greater detail, incorporating material compression, and more accurately modeling the energy consumption and efficiencies versus depth. Second, more VB systems need to be added. The pumped oil and piston-driven oil systems performed well to 2,000 m, but a model of these systems with an increased depth rating is needed. Lastly, and most importantly, further research is needed to match new technology to the development of new VB systems. A system using chemical reactions to release energy appear to be most promising, but further investigation towards nanotechnology is also suggested.

The cost of a vehicle is nearly always the bottom line, and thus a cost metric may one-day be very useful. However, the capability of a system is paramount at this point in the research, and cost will thus be left to the system designer.

THIS PAGE INTENTIONALLY LEFT BLANK

Appendix A

Symbols and Abbreviations

F_H	hydrostatic force exerted on a submerged object
F_G	downward gravitational force on an object, or weight
F_B	net buoyant force exerted on a submerged object; the sum of the hydrostatic forces: $\sum F_H$
B	net buoyancy of a submerged body, equal to the weight of displaced water. Units in force, or mass if divided by g (mass = force/ g).
g	gravitational acceleration: 9.80665 m/s^2
∇	the volumetric displacement of a submerged body
Δ	the displacement of a submerge object, measured in force. Used in naval architecture for the displacement of a ship in English long tons, equivalent to the buoyant force on the ship[8] . Equal to the weight of a floating ship, however not equal to the weight of a submerged object.
ρ	density
m	mass
W	work
t	time
E	energy
V	volume
B^\pm	absolute total buoyancy created by a VB system in units of mass
∇^\pm	absolute total buoyancy created by a VB system in units of volume
β_m	VB mass metric
β_{vol}	VB volume metric
B^+	buoyancy addition (or subtraction) from a VB system
P_D	pressure difference between the tank and ambient water
SG	specific gravity with respect to <i>freshwater</i> : $\rho/\rho_{freshwater}$
AUV	autonomous underwater vehicle
HOV	human occupied vehicle
ROV	remotely operated vehicle
VB	variable buoyancy
WHOI	Woods Hole Oceanographic Institution

THIS PAGE INTENTIONALLY LEFT BLANK

Appendix B

Gas Compression Modeling

B.1 Van der Waals Equation of State

In Section 5.2.1, the Compressed Gas VB System is explored as a potential VB system, and in Section 5.1.1 bicarbonate reactions are explored. At high pressure the well known ideal gas equation, $PV = nRT$, fails to correctly model gas compression, and the van der Waals equation of state for a real gas must be used [12]:

$$\left(P + \frac{n^2a}{V^2}\right)(V - nb) = nRT \quad (\text{B.1})$$

where P is pressure (bar), T is temperature (K), V is volume (L), R the gas constant, and n is moles of gas. The two van der Waals constants, a and b are gas specific, independent of temperature. The values used in this thesis were obtained from the 89th Edition of the CRC Handbook [12], shown below in Table B.1.

Table B.1: Gas constants used for van der Waals equation of state.

	mol. wt	a (bar L ² /mol ²)	b (L/mol)
Hydrogen	2.016	0.2452	0.0265
Helium	4.003	0.0346	0.0238
Nitrogen	28.013	1.3700	0.0387
Oxygen	31.999	1.3820	0.0319
Neon	20.180	0.2080	0.0167
Carbon Dioxide	44.010	3.6580	0.0429

A plot of molar density (mol/L) is shown below in Figure B-1. Clearly visible, the negative curvature in the plots show the deviation from the linear ideal gas law. Incorporating the density of the gas yields a much different result which can be seen in the plot of mass density (kg/L) in Figure B-2. In both plots, the x-axis units are in depth of seawater. Used as units for pressure, the depth is dependent on the temperature and salinity of the water, which is different at any given ocean location. Thus the reader is asked to not hold accountability to the accuracy of the results.

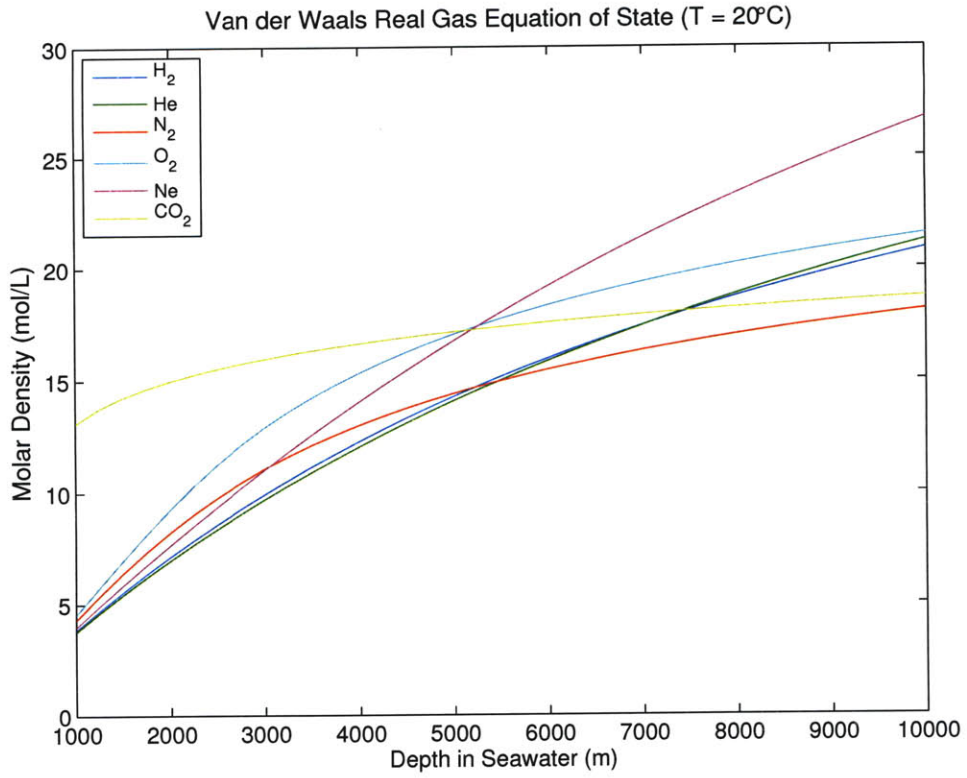


Figure B-1: Gas volumetric molar density vs depth

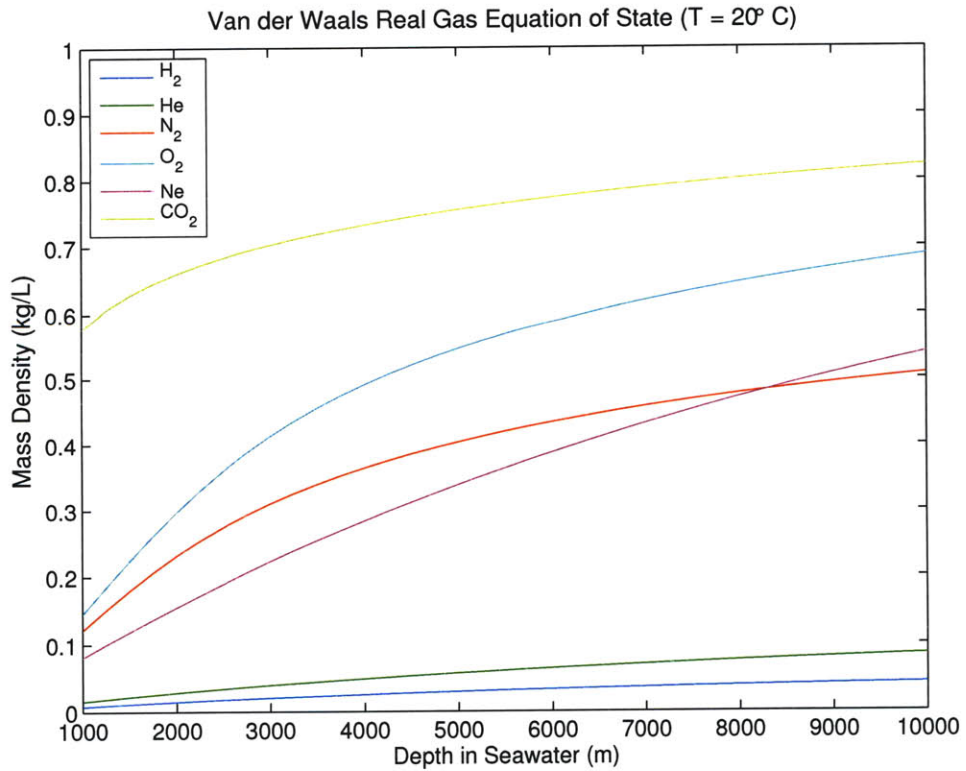


Figure B-2: Gas mass density vs depth

B.2 Gas Solubility: Henry's Law

In Section 5.1.1, the solubility of CO₂ gas was studied. The plots were generated using Henry's Gas Law:

$$[G] = H_G \cdot pp_G \quad (\text{B.2})$$

where G is the gas concentration (mol/kg seawater), pp_G the partial pressure of the gas (atm), and H_G is Henry's constant (mol/atm·kg seawater). For CO₂ solubility in seawater, H_G was found using [17]:

$$\ln(H_{CO_2}) = \frac{9345.17}{T} - 167.8108 + 23.3585(\ln T) + S(0.023517 - 2.3656 \times 10^{-4}T + 4.7036 \times 10^{-7}T^2) \quad (\text{B.3})$$

where T is in Kelvin and S is in psu. The results are plotted in Figure 5-3 and in Figure B-3 below.

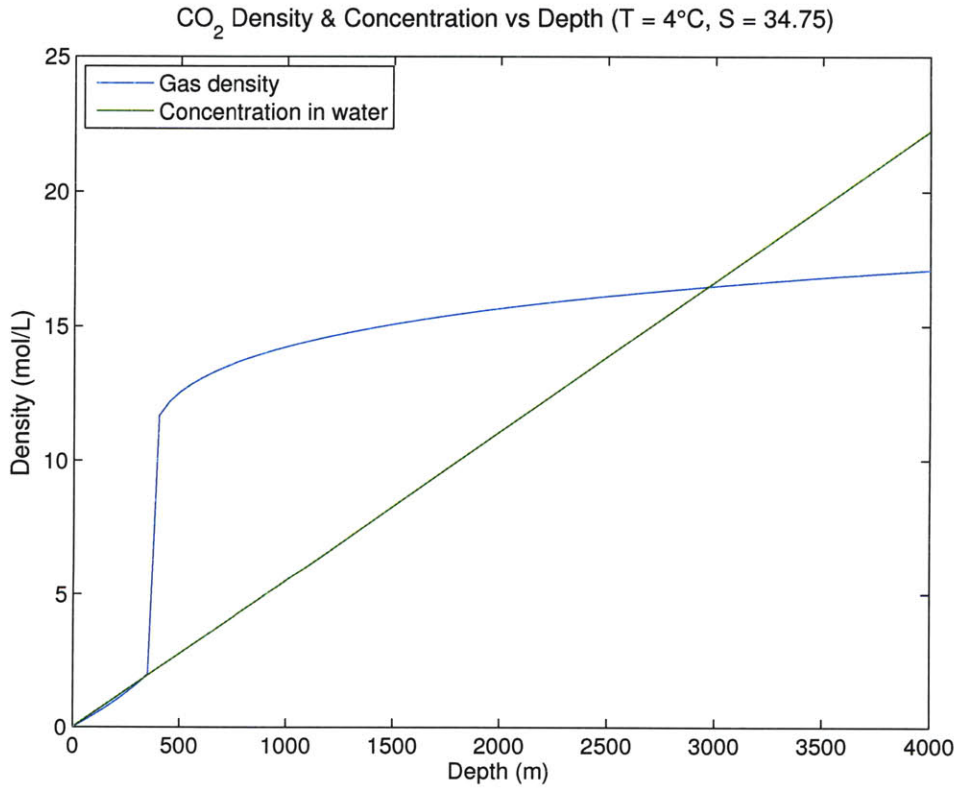


Figure B-3: Molar density and aqueous concentration of CO₂ gas vs depth. Aqueous concentration in units of moles per L of *seawater*, and CO₂ gas density in moles per L of *gas*. The density spike at 350 m is the transition from gas to liquid.

THIS PAGE INTENTIONALLY LEFT BLANK

Appendix C

Deep Submergence Battery Specifications

	Alvin II	Alvin II w/float	Sentry	Sentry w/float
E (kWh)	37.5	37.5	12.8	12.8
m (kg)	816	1016	199	227
V (L)	420	991	141	221
B (kg)	-385	0.0	-54	-0.0
m/E (kg/kWh)	21.8	27.1	15.6	17.7
V/E (L/kWh)	11.2	26.4	11.1	17.3
B/E (kg/kWh)	-10.3	0.0	-4.2	0.0

Table C.1: A variation of Table 5.1 using alumina spheres for buoyancy ($SG = 0.35$, rated to 11,000 m) rather than syntactic foam. Specifications for deep submergence battery systems. Syntactic foam was added to each system (w/float) to achieve neutral buoyancy ($SG = 0.61$, 11,500 m). E is total energy, m is mass, V is volumetric displacement, and B system buoyancy. [Dana Yoerger & Dan Gomez-Ibanez, WHOI, 2009]

THIS PAGE INTENTIONALLY LEFT BLANK

Appendix D

Manuals

Figure D-1: Specs for carbon fiber gas tank used in pre-compressed VB system design.



TUFFSHELL[®] H₂ Fuel Tanks

Product Information



The TUFFSHELL[®] gaseous fuel tank designed and produced by Lincoln Composites has all the performance characteristics desired of a vessel for hydrogen storage. TUFFSHELL[®] hydrogen tanks are the lightest weight tank on the market and offer superior fatigue life, excellent durability and low permeation at a competitive cost.

Over 55,000 TUFFSHELL[®] tanks are currently being used in different CNG and hydrogen storage applications throughout the world. Applications ranging from roof packs on transit buses to tanks mounted in automotive OEM vehicles and stationary hydrogen storage have benefited from the patented construction of the TUFFSHELL[®] Type 4 pressure vessel.

The all-composite construction of the vessel provides numerous advantages and design flexibility to adapt to a wide variety of application requirements. One of the most valuable assets of the tank is provided by the plastic liner. This liner allows for an almost unlimited fatigue life and resistance to many of the environmental elements that can affect metal-lined tanks. Further, the plastic liner is not susceptible to the hydrogen embrittlement that can affect metallic structures. The patented boss/liner interface allows versatility in the design of the bosses. Aluminum and stainless steel boss materials are both available.

The TUFFSHELL[®] hydrogen tanks listed below are available in volumes from 29 to 539 L and in service pressures up to 700 bar. Tanks can be purchased in lengths up to 3 meters and diameters up to 560 mm. Custom sizes and higher pressure tanks can be built to meet your specifications. TUFFSHELL[®] tanks meet the requirements of applicable and proposed standards for compressed hydrogen fuel cylinders such as ISO/DIS15869, EHP Draft, HGV2 Draft and METI-KHK hydrogen standard.

5,000 PSI (350 BAR)*											
Size (O.D. x Length)		Weight		Water Volume		Gas Mass		Gasoline Equivalent		Diesel Equivalent	
Inches	Millimeters	Lbs.	Kg.	Cu. In.	Liters	Lbs.	Kg.	Gallons	Liters	Gallons	Liters
11.8 x 45	300 x 1142	48.3	21.9	3402	55.7	2.9	1.3	1.3	5.0	1.2	4.4
12 x 36	306 x 914	49.0	22.2	2713	44.5	2.3	1.1	1.0	4.0	0.9	3.5
15.8 x 33	400 x 832	72.1	32.7	3986	65.3	3.4	1.6	1.6	5.9	1.4	5.2

7000 PSI (500 BAR)*											
Size (O.D. x Length)		Weight		Water Volume		Gas Mass		Gasoline Equivalent		Diesel Equivalent	
Inches	Millimeters	Lbs.	Kg.	Cu. In.	Liters	Lbs.	Kg.	Gallons	Liters	Gallons	Liters
22 x 50	558 x 1270	235.6	106.9	12292	201.4	13.7	6.2	6.1	23.3	5.5	20.8
22 x 129	558 x 3277	560.8	254.4	32880	536.8	36.7	16.6	16.4	62.3	14.7	55.8
16.7 x 40	425 x 1016	110.1	49.9	5758	94.3	6.4	2.9	2.9	10.9	2.6	9.8

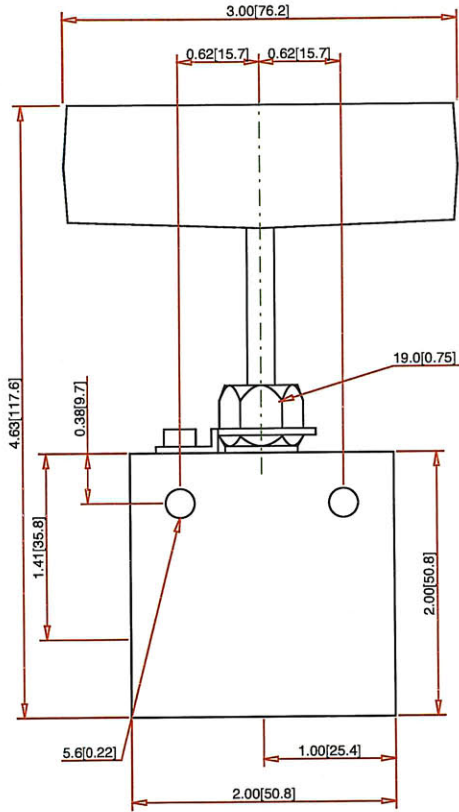
10,000 PSI (700 BAR)*											
Size (O.D. x Length)		Weight		Water Volume		Gas Mass		Gasoline Equivalent		Diesel Equivalent	
Inches	Millimeters	Lbs.	Kg.	Cu. In.	Liters	Lbs.	Kg.	Gallons	Liters	Gallons	Liters
11 x 32.6	279 x 827	64.8	29.4	1779	29.2	2.6	1.2	1.2	4.4	1.0	3.9
14.1 x 23	356 x 584	56.5	25.6	1888	30.9	2.7	1.3	1.2	4.7	1.1	4.2
17.6 x 49	447 x 1247	185.6	84.2	7225	118.4	10.5	4.8	4.7	17.8	4.2	16.0

*Pressure rating at 59 °F (15 °C)

Lincoln Composites, Inc.
 6801 Cornhusker Highway, Lincoln, NE 68507 USA
 Tel: 1-800-279-TANK or 402-464-6611 · Fax: 402-464-6777
 E-mail: tuffshell@lincolncomposites.com
 www.lincolncomposites.com

**LINCOLN
 COMPOSITES**
 A Member of Hexagon Composites Group

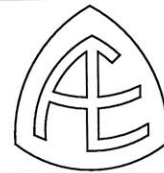
Figure D-2: Autoclave valve for Compressed Gas VB system



Note : - Drawing not to Scale.

Part No. :
15P4071

Description :
P Series Pipe Low Pressure Needle Valves



Autoclave Engineers

Address : 8325 Hessinger Drive
Erie, Pennsylvania 16509-4679 USA

Tel. : 814-860-5700

Email : ae_sales@snap-life.com

Web : www.autoclave.com

Appendix E

Modeling Code (MATLAB)

E.1 Code: Alvin HOV Pumped-Water VB System Model

```
1 % Harold F Jensen III
2 % Master's Thesis June 2009
3 % MIT/WHOI Joint Program
4
5 %% Alvin HOV VB System
6
7 clc, clear,
8 load vars.VBconstants.mat
9 load vars.AlvinSizeSpecs.mat
10
11 %% System Variables
12 P_charge = [3820 1910]; % psi - air precharge in spheres
13 % **The last P_charge value is used for the constant P_charge plots**
14 B_add = [25 50 100 200]; % kg - MAX buoyancy added (surface density)
15
16 %% System Specs
17 sphere_ID = 23; % in - inside diameter of sphere
18 N_sphere = 6; % number of spheres
19 gas_precharge = 78; % set the gas type used for precharge (78=air)
20 eff_motorC = 0.85; % Efficiency of motor controller
21 eff_motor = 0.85; % Efficiency of motor
22 eff_pump = 0.72; % Efficiency of pump
23 eff_alvin_VB = eff_motorC * eff_motor * eff_pump; % Eff. of VB system
24 rpm_pump = 1300; % RPM - pump rpm
25 displace_pump = 0.2124; % in^3 - pump displacement per rotation
26 capac_batt = 15; % kWh - battery capacity (note: 2 batts on Alvin)
27 m_batt = 2648; % lbs - battery weight
28 v_batt = 1206; % lbs seawater - 64.4 lbs/ft^3
29 d_max_alvin = 6500; % m - max depth of Alvin
30
31 %% Convert to Metric units
32 P_charge = P_charge * C_psi_Pa; % Pa - convert from psi
```

```

33     displace_pump = displace_pump*C_in_m^3; % m^3 - converted from in^3
34     sphere_ID = sphere_ID * C_in_m;      % m - converted from in
35     m_batt = m_batt * C_lbs_kg;          % kg - converted from lbs
36     v_batt = v_batt / 64.4 * C_ft3_m3;   % lbs seawater - 64.4 lbs/ft^3
37     % Precharge converted to depth of equivalent pressure
38     d_precharge = mSeaDepth(P_charge,T_water,Salinity);
39
40 %% Loop for creating plot of multiple PRECHARGE
41 for pc_index = 1:length(P_charge)
42     P_precharge = P_charge(pc_index);
43
44 %% Loop for creating plot of multiple BUOYANCY CHANGE
45 for index = 1:length(B_add)
46     B_change = B_add(index);
47     % **NOTE** buoyancy change is calculated by volume using the density
48     %           at the surface, thus, the actual buoyancy change is
49     %           slightly higher as depth increase.
50     v_change = B_change / rho_surface; % m^3 - vol of water added
51
52 %% Air in Spheres
53 % Air volume in spheres
54     v_sphere = ( 4/3*pi*(sphere_ID/2)^3 ); % m^3 - volume of 1 sphere
55     v_sphere_total = v_sphere * N_sphere; % m^3 - total volume
56
57 % Moles of air in spheres at T = 0C
58     N_air=v_sphere_total/C_L_m3*mVDW(gas_precharge,P_precharge,0);
59 % Mass of air in spheres at T = 0C
60     m_air = N_air * A_dense(78) / 1000; % kg
61
62 % Find Max pressure in spheres (when 400 lbs heavy at T = 0C for air)
63     v_air_min = v_sphere_total - v_change; % m^3 - volume minus water vol
64     P_air_max = mP_VDW(78,v_air_min,N_air,0); % Pa - max sphere pressure
65
66
67 %% Find the Power input to the pump system vs Depth head
68
69 % Determine volumetric flow rate
70     flow_rate = displace_pump*rpm_pump/60; % m^3/s
71
72 % Find the pressure difference the pump sees (head pressure)
73 % First find the average pre-charge for the buoyancy change, then use it
74 % to calculate the average head the pump sees.
75 % *Assumes the lower point is always the empty position.
76     P_precharge_avg = mean([P_precharge P_air_max]); % Pa - avg precharge
77     head_pump = abs(P_water*C_MPa_Pa-P_precharge_avg); % Pa - pump head
78
79 % Find the PV work done by the pump to the water
80     W_pump_out = head_pump * flow_rate; % Watts
81
82 % Find the work input to the pump
83     W_motor_out = W_pump_out / eff_pump; % Watts
84
85 % Find the work input to the motor from the motor controller
86     W_motorC_out = W_motor_out / eff_motor; % Watts

```

```

87
88 % Find the work input to the motor controller (actual energy used!!)
89   W_system_IN = W_motorC_out / eff_motorC; % Watts
90   W_system_IN_HP = W_system_IN/1000 / C_hp_kWh; % HP
91
92 %% Find the time & energy it takes to pump the max buoyancy change
93 % **NOTE ** it is assumed always pumping against the head
94   pump_time = v_change / flow_rate; % s - time to pump max B change
95   Energy_in = W_system_IN * pump_time; % J
96   Energy_in_kWh(:,index) = Energy_in * C_J_kWh; % kWh
97
98 % Find the efficiency of the system INCLUDING the precharge
99   eff_TOTAL(:,index)=(v_change*mSeaPressure(depth,T_water,Salinity))./...
100                                     Energy_in;
101 %% Find the Mass & Volume of Battery Used for VB system
102 % Mass of battery used for VB - kg
103   m_batt_VB = Energy_in_kWh(:,index)* m_batt/capac_batt; % kg - batt mass
104 % Volume of battery used for VB - kg
105   v_batt_VB = Energy_in_kWh(:,index) * v_batt/capac_batt; % m^3 - batt vol
106
107 %% Mass & Volume of the entire Alvin VB System with amount of Pb batt used
108 % Interesting note: using a B change of 400 lbs, incorporating battery
109 % mass in total buoyancy, the system is neutral at half depth (3250m).
110 % So no flotation is added to account for battery use a great depths
111
112 % Mass, Volume, & Buoyancy of ENTIRE Alvin VB System INCLUDING battery
113   m_alvin_total_wbatt = m_alvin_total + m_batt_VB; % kg
114   v_alvin_total_wbatt = v_alvin_total + v_batt_VB; % m^3
115   B_alvin_total_wbatt = v_alvin_total_wbatt*rho_surface...
116                                     - m_alvin_total_wbatt; % kg
117
118 %% Metric Calculation: **Alvin is a 2-way system**
119   VBm_metric_Alvin(:,index) = 2 * B_change ./ m_alvin_total_wbatt;
120   VBv_metric_Alvin(:,index) = 2 * v_change ./ v_alvin_total_wbatt;
121
122   VBm_metric_Alvin_NOBatt(:,index) = 2 * B_change ./ m_alvin_total;
123   VBv_metric_Alvin_NOBatt(:,index) = 2 * v_change ./ v_alvin_total;
124
125 %% Solve the system using Alvin II Lithium Batteries
126 % The Alvin II Lithium Batteries (May 2009) are calculated in mBattery.m
127 % The calculation include the mass and volume of the titanium housing
128 % The values labeled float use syntactic foam to make the system neutral B
129 % **NOTE** The battery portion designated to the VB system does not
130 % need flotation, as the VB system itself is buoyant enough
131   load vars_Battery_Alvin.mat; % load new battery data
132 % Alvin_batt_E = kWh per battery for the Alvin II (2 batts onboard)
133 % V_E_Alvin = L/kWh for Alvin II Lithium Batteries
134 % m_E_Alvin = kg/kWh for Alvin II Lithium Batteries
135 % V_E_Alvin_float = L/kWh for Alvin II Lithium Batteries w/ syntactic
136 % m_E_Alvin_float = kg/kWh for Alvin II Lithium Batteries w/syntactic
137
138 % Mass of Li battery used for VB - kg
139   m_batt_VB_Li = Energy_in_kWh(:,index) *m_E_Alvin; % kg - lith batt mass
140 % Volume of Li battery used for VB - kg

```

```

141     v_batt_VB_Li = Energy_in_kWh(:,index)*V_E_Alvin*C_L_m3; %m^3 - batt vol
142
143 % Mass, Volume, & Buoyancy of ENTIRE Alvin VB System INCLUDING Li battery
144     m_alvin_total_wbatt_Li = m_alvin_total + m_batt_VB_Li;      % kg
145     v_alvin_total_wbatt_Li = v_alvin_total + v_batt_VB_Li;      % m^3
146     B_alvin_total_wbatt_Li = v_alvin_total_wbatt_Li*rho_surface...
147                               - m_alvin_total_wbatt_Li; % kg
148
149 % Lithium Mass & Volume Metric Calculation: **Alvin is a 2-way system**
150     VBm_metric_Alvin_Li(:,index) = 2 * B_change ./ m_alvin_total_wbatt_Li;
151     VBv_metric_Alvin_Li(:,index) = 2 * v_change ./ v_alvin_total_wbatt_Li;
152
153 %% Create Plot Legend
154     legend_alvin(index) = {strcat('B^+ = ', (int2str(B_change)), ' kg')};
155
156     end, clear index
157
158
159 %% Remove values deeper than depth rating
160 % metric values without the battery are constant with depth
161     trigger = 0; % trigger used to keep the index of max depth for later
162     for d_index = 1:length(depth)
163         % metric values without the battery are constant with depth
164         VBm_metric_Alvin_NObatt(d_index,:) = VBm_metric_Alvin_NObatt(1,:);
165         VBv_metric_Alvin_NObatt(d_index,:) = VBv_metric_Alvin_NObatt(1,:);
166         % if depth is deeper than max depth, set metric to 0
167         if depth(d_index) > d_max_alvin
168             VBm_metric_Alvin(d_index,:) = 0;
169             VBv_metric_Alvin(d_index,:) = 0;
170             VBm_metric_Alvin_Li(d_index,:) = 0;
171             VBv_metric_Alvin_Li(d_index,:) = 0;
172             VBm_metric_Alvin_NObatt(d_index,:) = 0;
173             VBv_metric_Alvin_NObatt(d_index,:) = 0;
174             Energy_in_kWh(d_index,:) = 0;
175             eff_TOTAL(d_index,:) = 0;
176             trigger = 1;
177         end
178         if trigger == 0
179             max_depth_index = d_index; % Max depth index for later
180         end
181     end, clear d_index
182
183 %% Save data *****
184     depth_Alvin = depth;
185     save vars_Alvin.mat VBm_metric_Alvin VBv_metric_Alvin ...
186         VBm_metric_Alvin_NObatt VBv_metric_Alvin_NObatt ...
187         depth_Alvin legend_alvin
188
189 %% Store PRECHARGE Loop dataset
190 % Store the metric values for each precharge iteration in a 3rd dimension
191
192     VBm_metric_Alvin_PC(:,:,pc_index) = VBm_metric_Alvin;
193     VBv_metric_Alvin_PC(:,:,pc_index) = VBv_metric_Alvin;
194     VBm_metric_Alvin_Li_PC(:,:,pc_index) = VBm_metric_Alvin_Li;

```



```

195     VBv_metric_Alvin_Li_PC(:, :, pc_index) = VBv_metric_Alvin_Li;
196     Energy_in_kWh_PC(:, :, pc_index) = Energy_in_kWh;
197     eff_TOTAL_PC(:, :, pc_index) = eff_TOTAL;
198
199 end, clear pc_index
200
201 %% PLOTS
202 % Set plot axes
203     xmax = 8000;
204     xmin = 0;
205     ymax = 0.75;
206
207 % Plot Mass metric vs Added Buoyancy
208     figure(1);
209     set(gca, 'fontsize', pfs); % plot font size
210     plot(depth, VBm_metric_Alvin)
211     title('Alvin VB MASS Metric (\beta_m)', ...
212           'fontsize', pfs+1)
213     xlabel('Depth (m)', 'fontsize', pfs)
214     ylabel('\beta_m', 'fontsize', pfs+2)
215     legend(legend_alvin)
216     axis([xmin xmax 0 ymax])
217     print -depsc plot_metric_Alvin
218     print -dpdf plot_metric_Alvin
219
220 % Plot Volume metric vs Added Buoyancy
221     figure(2);
222     set(gca, 'fontsize', pfs); % plot font size
223     plot(depth, VBv_metric_Alvin)
224     title('Alvin VB VOLUME Metric (\beta_{vol})', ...
225           'fontsize', pfs+1)
226     xlabel('Depth (m)', 'fontsize', pfs)
227     ylabel('\beta_{vol}', 'fontsize', pfs+2)
228     legend(legend_alvin)
229     axis([xmin xmax 0 ymax])
230     print -depsc plot_Vmetric_Alvin
231     print -dpdf plot_Vmetric_Alvin
232
233 %% PLOT Mass metric WITHOUT accounting for the mass of the battery used
234     figure(3);
235     set(gca, 'fontsize', pfs); % plot font size
236     plot(depth, VBm_metric_Alvin_NObatt)
237     title('Alvin VB MASS Metric (\beta_m) WITHOUT Battery', ...
238           'fontsize', pfs+1)
239     xlabel('Depth (m)', 'fontsize', pfs)
240     ylabel('\beta_m', 'fontsize', pfs+2)
241     legend(legend_alvin)
242     axis([xmin xmax 0 ymax])
243     print -depsc plot_metric_Alvin_NObatt
244     print -dpdf plot_metric_Alvin_NObatt
245
246 % Plot Volume metric WITHOUT accounting for the mass of the battery used
247     figure(4);
248     set(gca, 'fontsize', pfs); % plot font size

```

```

249     plot(depth,VBv_metric_Alvin_NObatt)
250     title('Alvin VB VOLUME Metric (\beta_{vol}) WITHOUT Battery',...
251           'fontsize',pfs+1)
252     xlabel('Depth (m)', 'fontsize',pfs)
253     ylabel('\beta_{vol}', 'fontsize',pfs+2)
254     legend(legend_alvin)
255     axis([xmin xmax 0 ymax])
256     print -depsc plot_Vmetric_Alvin_NObatt
257     print -dpdf plot_Vmetric_Alvin_NObatt
258
259 %% PLOT Alvin II Lithium: Mass metric for Pb & Li battery system
260 % Choose the buoyancy change you wish to compare b/w batteries
261     BA = length(B_add);
262 % Create the legend for the battery compare plots
263     legend_alvin_Li = {strcat(...
264                       'Lead Acid Battery'),...
265                       strcat(...
266                       'Lithium Ion Battery')};
267
268 figure(5);
269     set(gca,'fontsize',pfs); % plot font size
270     plot(depth,[VBm_metric_Alvin(:,BA) VBm_metric_Alvin_Li(:,BA)] )
271     title_fig5 = {strcat(...
272                 'Alvin VB MASS Metric (\beta_m) (B^+ = ',...
273                 int2str(B_add(BA)), ' kg')};
274     title(title_fig5,'fontsize',pfs+1)
275     xlabel('Depth (m)', 'fontsize',pfs)
276     ylabel('\beta_m', 'fontsize',pfs+2)
277     legend(legend_alvin_Li)
278     axis([xmin xmax 0 ymax])
279     print -depsc plot_metric_Alvin_Li
280     print -dpdf plot_metric_Alvin_Li
281
282 % Alvin II Lithium: Plot Volume metric vs Added Buoyancy
283 figure(6);
284     set(gca,'fontsize',pfs); % plot font size
285     plot(depth,[VBv_metric_Alvin(:,BA) VBv_metric_Alvin_Li(:,BA)] )
286     title_fig6 = {strcat(...
287                 'Alvin VB VOLUME Metric (\beta_{vol}) (B^+ = ',...
288                 int2str(B_add(BA)), ' kg')};
289     title(title_fig6,'fontsize',pfs+1)
290     xlabel('Depth (m)', 'fontsize',pfs)
291     ylabel('\beta_{vol}', 'fontsize',pfs+2)
292     legend(legend_alvin_Li)
293     axis([xmin xmax 0 ymax])
294     print -depsc plot_Vmetric_Alvin_Li
295     print -dpdf plot_Vmetric_Alvin_Li
296
297 %% PLOT vs PRECHARGE: Alvin Mass metric for Pb & Li battery system
298
299 % Choose the buoyancy change you wish to compare b/w batteries
300 % **if the chart only plots 1 buoyancy change**
301 % the legend for that plot is last entry of BuoyAdd_toPlot
302     BuoyAdd_toPlot = [2 4];

```

```

303
304 % Extract 3D Matrix data to 2D for easy plotting
305 % Create legend for 3D matrix
306 col_index = 1; % column index
307 for BA = BuoyAdd_toPlot
308     for Pindex = 1:length(P_charge)
309         % LEAD Batts: Create plot values for Mass & Volume Metric
310             VBm_PRECHARGE(:,Pindex) = VBm_metric_Alvin_PC(:,BA,Pindex);
311             VBv_PRECHARGE(:,Pindex) = VBv_metric_Alvin_PC(:,BA,Pindex);
312         % LITHIUM Batts: Create plot values for Mass & Volume Metric
313             VBm_PRECHARGE_LI(:,Pindex)=VBm_metric_Alvin_Li_PC(:,BA,Pindex);
314             VBv_PRECHARGE_LI(:,Pindex)=VBv_metric_Alvin_Li_PC(:,BA,Pindex);
315         % Energy used for VB: Create plot values vs precharge and B added
316             Energy_in_kWh_Plot(:,col_index) = Energy_in_kWh_PC(:,BA,Pindex);
317         % TOTAL VB efficiency: Create plot values vs precharge and B added
318             eff_TOTAL_Plot(:,col_index) = eff_TOTAL_PC(:,BA,Pindex);
319         % Lead Batt Legend Titles
320             legend_Pb(Pindex) = {...
321                 strcat('Lead Acid: P =',...
322                     int2str(P_charge(Pindex)/C_MPa_Pa),...
323                     ' MPa')};
324         % Lithium Batt Legend Titles
325             legend_Li(Pindex) = {strcat(...
326                 'Lithium Ion: P = ',...
327                 int2str(P_charge(Pindex)/C_MPa_Pa),...
328                 ' MPa')};
329         % Energy Consumed Legend Titles
330             legend_Energy(:,col_index) = {strcat(...
331                 'P =',int2str(P_charge(Pindex)/C_MPa_Pa),...
332                 ' MPa, B^+ = ', ...
333                 int2str(B_add(BA)), ' kg')};
334         % Increase column index
335             col_index = col_index + 1;
336     end
337 end, clear col_index Pindex
338
339 figure(7);
340 set(gca,'fontsize',pfs); % plot font size
341 plot(depth,[VBm_PRECHARGE VBm_PRECHARGE_LI] )
342 title_fig7 = {strcat(...
343     'Alvin VB MASS Metric (\beta_m) (B^+ = ',...
344     ' ',int2str(B_add(BA)), ' kg')'};
345 title(title_fig7,'fontsize',pfs+1)
346 xlabel('Depth (m)','fontsize',pfs)
347 ylabel('\beta_m','fontsize',pfs+2)
348 legend([legend_Pb, legend_Li])
349 axis([xmin xmax 0 ymax])
350 print -depsc plot_metric_Alvin_Li_PC
351 print -dpdf plot_metric_Alvin_Li_PC
352
353 figure(8);
354 set(gca,'fontsize',pfs); % plot font size
355 plot(depth,[VBv_PRECHARGE VBv_PRECHARGE_LI] )
356 title_fig8 = {strcat(...

```

```

357         'Alvin VB VOLUME Metric (\beta_{vol}) (B^+ = ',...
358         ' ',int2str(B.add(BA)), ' kg')});
359     title(title_fig8,'fontsize',pfs+1)
360     xlabel('Depth (m)','fontsize',pfs)
361     ylabel('\beta_{vol}','fontsize',pfs+2)
362     legend([legend_Pb, legend_Li])
363     axis([xmin xmax 0 ymax])
364     print -depsc plot_Vmetric_Alvin_Li_PC
365     print -dpdf plot_Vmetric_Alvin_Li_PC
366
367 %% PLOT Energy used for VB vs. Buoyancy Added and vs. Precharge
368
369 figure(9);
370     set(gca,'fontsize',pfs); % plot font size
371     plot(depth,Energy_in_kWh)
372     title_fig9 = {strcat(...
373         'Alvin Battery Energy consumed by VB System (P =',...
374         int2str(P_charge(length(P_charge))/C.MPa_Pa),...
375         ' MPa)')});
376     title(title_fig9,'fontsize',pfs+1)
377     xlabel('Depth (m)','fontsize',pfs)
378     ylabel('kWh','fontsize',pfs+2)
379     legend(legend_alvin,'Location','NorthWest')
380     axis([xmin xmax 0 6])
381     print -depsc plot_Alvin_Energy
382     print -dpdf plot_Alvin_Energy
383
384
385 figure(10);
386     set(gca,'fontsize',pfs); % plot font size
387     plot(depth,Energy_in_kWh_Plot)
388     title('Alvin Battery Energy consumed for VB System vs. Precharge (P)',...
389         'fontsize',pfs+1)
390     xlabel('Depth (m)','fontsize',pfs)
391     ylabel('kWh','fontsize',pfs+2)
392     legend(legend_Energy,'Location','NorthWest')
393     axis([xmin xmax 0 8])
394     print -depsc plot_Alvin_Energy_PC
395     print -dpdf plot_Alvin_Energy_PC
396
397 %%
398
399 figure(11);
400     set(gca,'fontsize',pfs); % plot font size
401     plot(depth,eff_TOTAL_Plot)
402     title('Alvin VB Energy Efficiency (\eta = ideal/actual)',...
403         'fontsize',pfs+1)
404     xlabel('Depth (m)','fontsize',pfs)
405     ylabel('\eta','fontsize',pfs+2)
406     grid on
407     legend(legend_Energy,'Location','NorthEast')
408     axis([xmin xmax 0 5])
409     print -depsc plot_Alvin_Energy_effic
410     print -dpdf plot_Alvin_Energy_effic

```

```

411
412
413 %% Plot fraction of Battery energy used on VB
414
415 % Fraction of Lithium Ion Battery used for VB (** 2 batts onboard **)
416     frac_batt_used_Li = Energy_in_kWh_PC ./ (2 * Alvin_batt_E);
417 % Energy Consumed by VB System as fraction of total onboard (2 batts)
418     frac_batt_used_Pb = Energy_in_kWh_PC ./ (2 * capac_batt);
419
420 %% Export Spec Table to LaTeX
421
422 % Col and row titles for the table
423     columnLabels = {...
424         'No Battery',...
425         'Lead Acid',...
426         'Lithium Ion',...
427     };
428
429     rowLabels = {...
430         'Depth (m)',...
431         'Mass (kg)',...
432         'Volume (L)',...
433         'Static B (kg)',...
434         'B+ (added kg)',...
435         'Energy Used (kWh)',...
436         'Battery Mass (kg)',...
437         'Efficiency',...
438         '\betaM',...
439         '\betaV',...
440     };
441
442 % Make the matrix to export
443
444     MD = max_depth_index; % index of max depth
445     BA = find(B_add == B_change);
446     table_E = Energy_in_kWh(MD, BA);
447
448
449     specs_alvin = [...
450         d_max_alvin      d_max_alvin      d_max_alvin;
451         m_alvin_total    m_alvin_total_wbatt(MD) m_alvin_total_wbatt_Li(MD);
452         v_alvin_total/C_L_m3...
453         v_alvin_total_wbatt(MD)/C_L_m3...
454         v_alvin_total_wbatt_Li(MD)/C_L_m3;
455         B_alvin_total    B_alvin_total_wbatt(MD) B_alvin_total_wbatt_Li(MD);
456         B_change         B_change         B_change;
457         table_E         table_E         table_E;
458         0                m_batt_VB(MD)     m_batt_VB_Li(MD);
459         eff_alvin_VB     eff_alvin_VB     eff_alvin_VB;
460         VBm_metric_Alvin_NObatt(MD, BA)...
461         VBm_metric_Alvin(MD, BA) VBm_metric_Alvin_Li(MD, BA);
462         VBv_metric_Alvin_NObatt(MD, BA)...
463         VBv_metric_Alvin(MD, BA) VBv_metric_Alvin_Li(MD, BA);
464     ];

```

```
465
466 % Output to table to Latex format (.tex file)
467     matrix2latex(specs.alvin, 'table_specs.alvin.tex',...
468         'rowLabels', rowLabels, 'columnLabels', columnLabels,...
469         'alignment', 'c', 'format', '%.2f')
```

E.2 Code: Pre-compressed Gas Tank VB System

```
1 % Harold F Jensen III
2 % Master's Thesis June 2009
3 % MIT/WHOI Joint Program
4
5 %% Pressure tank VB buoyancy capabilities
6 % given a pressure of a tank and the tank volume
7 % calculate the buoyancy change capabilities of the VB system
8
9 % Future refinement:
10 % - the static system buoyancy decreases slightly as gas mass is lost to
11 % the bladder
12 % - the bladder buoyancy does not factor in mass of the gas
13 % - the density change in seawater with depth not factored - use sw_dens
14 % plugin from 12.808
15
16
17 clear;clc;
18
19 % Load Constants and fixed variables
20 load vars_VBconstants.mat;
21
22 % Tank Specs *****
23
24 % Auxiliary system specs
25 % tubing, attachment mechanisms, battery, protective casings
26 rho_316ss = 8.027; % kg/L (0.29lb/in^3) OE mat'l handbook, Dexter
27 % Valve Specs - Autoclave 15P4071
28 V_valve = 0.0492; % L - (3 in^3) volume of one valve
29 M_valve = V_valve*rho_316ss; % kg - mass of one valve
30 % Auxiliary Estimate
31 M_estimate = 2; % **ESTIMATED 2 kg of 316 SS
32 V_estimate = M_estimate/rho_316ss; % volume *ESTIMATED auxiliary
33 % Final Auxiliary system specs
34 M_aux = M_estimate + 2*M_valve; % kg - mass aux parts, tank system
35 V_aux = V_estimate + 2*V_valve; % L - vol aux parts of tank system
36
37 % Tank 1 *****
38 tank = 1; % tank index
39 % Lincoln TuffShell (LT)
40 name_tank(tank) = {'1: LT 35 MPa'};
41 V_tank(tank) = 44.5; % L - high pressure tank interior vol
42 M_tank(tank) = 22.2; % kg - tank mass
43 P_tank(tank) = 35; % MPa - max tank pressure
44 T_tank(tank) = 15; % Celcius - Temp of tank at fillup
45 Dia_tank(tank) = 0.306; % m - tank diameter
46 L_tank(tank) = 0.914; % m - tank length
47
48 % Tank 2 *****
49 tank = tank + 1; % tank index
50 % Lincoln TuffShell (LT)
```

```

51     name_tank(tank) = {'2: LT 50 MPa'};
52     V_tank(tank) = 94.3;    % L - high pressure tank interior vol
53     M_tank(tank) = 49.9;    % kg - tank mass
54     P_tank(tank) = 50;     % MPa - max tank pressure
55     T_tank(tank) = 15;     % Celcius - Temp of tank at fillup
56     Dia_tank(tank) = 0.425; % m - tank diameter
57     L_tank(tank) = 1.016;  % m - tank length
58
59 % Tank 3      *****
60     tank = tank + 1;      % tank index
61     % Lincoln TuffShell (LT)
62     name_tank(tank) = {'3: LT 70 MPa'};
63     V_tank(tank) = 30.9;  % L - high pressure tank interior vol
64     M_tank(tank) = 25.6;  % kg - tank mass
65     P_tank(tank) = 70;    % MPa - max tank pressure
66     T_tank(tank) = 15;    % Celcius - Temp of tank at fillup
67     Dia_tank(tank) = 0.356; % m - tank diameter
68     L_tank(tank) = 0.584; % m - tank length
69
70 % Tank 4      *****
71     tank = tank + 1;      % tank index
72     % Lincoln TuffShell (LT)
73     name_tank(tank) = {'4: LT 70 MPa'};
74     V_tank(tank) = 118.4; % L - high pressure tank interior vol
75     M_tank(tank) = 84.2;  % kg - tank mass
76     P_tank(tank) = 70;    % MPa - max tank pressure
77     T_tank(tank) = 15;    % Celcius - Temp of tank at fillup
78     Dia_tank(tank) = 0.447; % m - tank diameter
79     L_tank(tank) = 1.247; % m - tank length
80
81 % Tank 5      *****
82     % Future 15,000 psi tank - (based off of LT 70 MPa, 118L tank)
83     % The tank was estimate to have %50 more mass than the 70 MPa tank
84     % of same interior volume. To match the shell density, 1.5 cm was
85     % addented to the shell thickness, increasing dia and length by 3cm
86
87     tank = tank + 1;      % tank index
88     name_tank(tank) = {'5: Future 100 MPa'};
89     % estimate tank exterior to be 50% larger in volume and weight
90     V_tank(tank) = V_tank(4); % L - high press tank interior vol
91     M_tank(tank) = M_tank(4)*1.25; % kg - mass, 125% of 70MPa tank
92     P_tank(tank) = 100;     % MPa - max tank pressure
93     T_tank(tank) = 15;     % Celcius - Temp of tank, fillup
94     Dia_tank(tank) = Dia_tank(4)+0.03; % m - tank diameter (+3cm)
95     L_tank(tank) = L_tank(4)+0.03;    % m - tank length (+3cm)
96
97 % Convert inputs *****
98     T_water = T_water + C_C_Kelvin; % convert C to K
99     P_water = P_water * C_MPa_Pa;  % convert MPa to Pa
100    P_tank = P_tank * C_MPa_Pa;    % convert MPa to Pa
101    T_tank = T_tank + C_C_Kelvin;  % convert C to K
102    V_tank = V_tank * C_L_m3;      % convert L to m^3
103    V_aux = V_aux * C_L_m3;       % convert L to m^3
104

```



```

105 % Loop through each tank model *****
106 for tank = 1:5
107
108     % Tank Specs found from input specs above
109     V_tank_ext(tank) = ((4/3*pi()* (Dia_tank(tank)/2)^3) +...
110         (pi()* (Dia_tank(tank)/2)^2*(L_tank(tank)-Dia_tank(tank))));
111         % m3 - exterior volume of tank
112     M_apparatus(tank) = M_tank(tank)+M_aux; % kg - mass entire system
113     V_apparatus(tank) = V_tank_ext(tank)+V_aux; % m^3-total system vol
114
115     % use to figure out wall density of the tank
116     % density_tank(tank) = M_tank(tank)/(V_tank_ext(tank)-V_tank(tank))
117
118 % Loop through each gas type *****
119     % Solve moles of gas in tank at original pressure
120     % Set gas type: H2=1, He=2, N2=7, O2=8, Ne=10, CO2=68
121     for gas = [1,2,7,8,10,68]
122
123         % Initialize variables
124         a = a_gas(gas);
125         b = b_gas(gas);
126         P = P_tank(tank);
127         V = V_tank(tank);
128         T = T_tank(tank);
129
130         % Van der Waals - solve for moles of gas in pressurized tank
131         complex = solve('(P+(a/V^2)*x^2)*(V-b*x)-x*R*T');
132         n = subs(complex);
133
134         % Sort real answer from imaginary
135         if (abs(imag(n(1))) < abs(imag(n(2))))...
136             && abs((imag(n(1))) < abs(imag(n(3))))
137             mol_tank(tank,gas) = real(n(1));
138         elseif (abs(imag(n(2))) < abs(imag(n(1))))...
139             && abs((imag(n(2))) < abs(imag(n(3))))
140             mol_tank(tank,gas) = real(n(2));
141         else
142             mol_tank(tank,gas) = real(n(3));
143         end
144
145         % Add the mass of the gas to the total system mass
146         M_gas(tank, gas) = mol_tank(tank,gas)*A_dense(gas)/1000;
147         % kg - mass of gas in tank originally
148
149         M_tank_sys(tank,gas) = M_apparatus(tank) +...
150             M_gas(tank,gas);
151         % kg - mas of tank aparatus including gas mass
152
153         % Determine the static buoyancy of the tank system
154         Buoy_apparatus(tank,gas) = V_apparatus(tank)*rho_Swater(1)...
155             - M_tank_sys(tank,gas); % kg buoyancy
156
157     % Loop through each water depth *****
158     % Van der Waals - solve moles in tank at given water pressure

```

```

159     for index = 1:length(P_water)
160         P = P_water(index);
161         T = T_water;
162         V = V_tank(tank);
163         n = subs(complex);
164
165         % Sort real answer from imaginary
166         if (abs(imag(n(1))) < abs(imag(n(2))))...
167             && abs((imag(n(1))) < abs(imag(n(3))))
168             mol_pres(index, gas) = real(n(1));
169             index = index + 1;
170         elseif (abs(imag(n(2))) < abs(imag(n(1))))...
171             && abs((imag(n(2))) < abs(imag(n(3))))
172             mol_pres(index, gas) = real(n(2));
173             index = index + 1;
174         else
175             mol_pres(index, gas) = real(n(3));
176             index = index + 1;
177         end
178     end, clear index
179     % moles of gas in tank for water pressure
180     mol_pres;
181     % moles pushed to bladder
182     % (moles in tank originally - moles at depth)
183     mol_bladder(:, gas) = mol_tank(tank, gas) - mol_pres(:, gas);
184
185     % Determine bladder volume from bladder moles vs. tank volume
186     V_bladder(:, gas) = (mol_bladder(:, gas) ./ mol_pres(:, gas)) *...
187         V_tank(tank); % m^3 - volume of added buoyancy
188
189     % The one-way added buoyancy for the tank
190     % (actual increase, not scaled)
191     Buoy_added(:, gas, tank) = V_bladder(:, gas) .* rho_Swater; %kg buoy added
192
193
194     % VB mass metric = 2*added buoyancy / mass of VB system
195     VBm_metric_PPress(:, gas, tank) = (2*V_bladder(:, gas) .* rho_Swater) /...
196         M_tank_sys(tank, gas); % kg/kg - VB metric
197
198     % VB volume metric = 2*volume of displacement / volume of VB system
199     % the displacement is multiplied by 2 because it is a two way system:
200     % it creates the displacement, then it can remove the displacement
201
202     VBv_metric_PPress(:, gas, tank) = 2*V_bladder(:, gas) ./ V_apparatus(tank);
203
204     end
205 end
206
207 % Save *****
208     depth_PPress = depth; % save depth for combined plots
209
210     % Save entire workspace
211     save vars_PPress.mat
212

```

```

213 %% Plot results *****
214 load vars_PPress.mat
215 load vars_VBconstants.mat
216 % Designated the GAS to plot
217     single_tank = 4; % Tank to plot multiple gases on
218     gas = [1,2,7,8,10]; % set gas range to plot
219     % Setup Legend Names
220     clear gas_legend_names
221     for index = 1:length(gas)
222         gas_legend_names(index) = name_gas(gas(index));
223     end, clear index
224
225 % Designated the TANKS to plot
226     tank = [1,2,4,5];
227     % Setup Legend Names
228     clear tank_legend_names
229     for index = 1:length(tank)
230         tank_legend_names(index) = name_tank(tank(index));
231     end, clear index
232
233 % For plotting a single gas vs various tanks, change data from 3D to 2D
234     single_gas = 2; % set single gas to plot vs tanks
235     clear VBm_2D VBv_2D
236     for index = 1:length(tank)
237         VBm_2D(:,index) = VBm_metric_PPress(:,single_gas,tank(index));
238         VBv_2D(:,index) = VBv_metric_PPress(:,single_gas,tank(index));
239     end, clear index
240
241
242
243 % Plot MASS Metric for all tanks
244
245     figure(1);
246     set(gca,'fontsize',pfs); % plot font size
247     plot(depth, VBm_2D)
248     title('Compressed Gas VB System (Helium): VB MASS Metric ( \beta_m )',...
249         'fontsize',pfs+1)
250     xlabel('Depth (m)', 'fontsize',pfs)
251     ylabel('\beta_m', 'fontsize',pfs+2)
252     legend(tank_legend_names)
253     axis([1000 10000 0 10])
254     print -depsc plot_metric_PPress_He
255     print -dpdf plot_metric_PPress_He
256
257 % Plot VOLUME Metric for all tanks
258
259     figure(2);
260     set(gca,'fontsize',pfs); % plot font size
261     plot(depth, VBv_2D)
262     title('Compressed Gas VB System (Helium): VB VOLUME Metric ( \beta_{vol} )',...
263         'fontsize',pfs+1)
264     xlabel('Depth (m)', 'fontsize',pfs)
265     ylabel('\beta_{vol}', 'fontsize',pfs+2)
266     legend(tank_legend_names)

```

```

267     axis([1000 10000 0 5])
268     print -depsc plot_Vmetric_PPress_He
269     print -dpdf plot_Vmetric_PPress_He
270
271 % Plot All gases on one tank
272
273     figure(3);
274     set(gca,'fontsize',pfs); % plot font size
275     plot(depth, VBm_metric_PPress(:,gas,single_tank))
276     title('Compressed Gas VB System (Tank #4): VB MASS Metric ( \beta_m )',...
277           'fontsize',pfs+1)
278     xlabel('Depth (m)','fontsize',pfs)
279     ylabel('\beta_m','fontsize',pfs+2)
280     legend(gas_legend_names)
281     axis([1000 7000 0 10])
282     print -depsc plot_metric_PPress_T4
283     print -dpdf plot_metric_PPress_T4
284
285 % Plot All gases on one tank
286
287     figure(4);
288     set(gca,'fontsize',pfs); % plot font size
289     plot(depth, VBv_metric_PPress(:,gas,single_tank))
290     title('Compressed Gas VB System (Tank #4): VB VOLUME Metric ( \beta_{vol} )',...
291           'fontsize',pfs+1)
292     xlabel('Depth (m)','fontsize',pfs)
293     ylabel('\beta_{vol}','fontsize',pfs+2)
294     legend(gas_legend_names)
295     axis([1000 7000 0 6])
296     print -depsc plot_Vmetric_PPress_T4
297     print -dpdf plot_Vmetric_PPress_T4
298
299     figure(5);
300     set(gca,'fontsize',pfs); % plot font size
301     plot(depth, Buoy_added(:,[gas 68],single_tank))
302     title('Compressed Gas VB System (Tank #4): Positive Buoyancy Created',...
303           'fontsize',pfs+1)
304     xlabel('Depth (m)','fontsize',pfs)
305     ylabel('kg','fontsize',pfs+2)
306     legend(gas_legend_names)
307     axis([1000 7000 0 500])
308     print -depsc plot_BuoyAdded_PPress_T4
309     print -dpdf plot_BuoyAdded_PPress_T4
310
311
312 %% Export to LaTeX Tank Specs *****
313 % Make a Table showing characteristics of each tank system
314
315 % Set depth to display properties
316     depth_display = 3000; % m in depth
317     Dindex = find(depth == depth_display); % find index of desired depth
318 % Set the tanks to display
319     tanks = 1:5;
320 % Col and row headings for the table

```

```

321     columnLabels = {'$\nabla$\{\footnotesize\ (L)\}',...
322     '$m $\{\footnotesize\ (kg)\}$',...
323     '$B$\{\footnotesize\ (kg)\}',...
324     '$SG$',...
325     '$B^+\{\footnotesize\ (kg)\}',...
326     '$\beta_{\text{m}}$', '$\beta_{\text{vol}}$'};
327     rowLabels = name_tank;
328
329     rowLabels(5) = {'5: 100 MPa*'};
330
331 % Create SG matrix for tanks
332     % (vol metric/mass metric) * (rho sea / rho fresh)
333     SG_tanks = (VBv_metric_PPress(Dindex, single_gas, tanks) ./...
334     VBm_metric_PPress(Dindex, single_gas, tanks)) *...
335     (rho_Swater(1)/rho_Fwater);
336
337 % Make the matrix to export
338     % tank name - vol - mass - B - SG - B+ - Beta_m - Beta_vol
339     tankspecs = [(V_apparatus(tanks)/C_L.m3)', M_tank_sys(tanks, single_gas), ...
340     Buoy_apparatus(tanks, single_gas)];
341     tankspecs(:,4) = SG_tanks;
342     tankspecs(:,5) = Buoy_added(Dindex, single_gas, tanks);
343     tankspecs(:,6) = VBm_metric_PPress(Dindex, single_gas, tanks);
344     tankspecs(:,7) = VBv_metric_PPress(Dindex, single_gas, tanks);
345
346 % Output to table to Latex format (.tex file)
347     matrix2latex(tankspecs, 'tableLTspecs.tex', 'rowLabels', rowLabels, ...
348     'columnLabels', columnLabels, 'alignment', 'c', 'format', '%.2f')
349
350 %% Export to LaTeX Tank PERFORMANCE *****
351 % Make a Table showing performance of each system for design use
352
353 % Set depth to display properties
354     gas = 2; % Set gas to use
355     depth_display = [3000 4000 5000 6000]; % m in depth
356     for index = 1:length(depth_display)
357         Dindex(index) = find(depth == depth_display(index));
358         % find index of desired depth
359     end, clear index
360
361 % Set the tanks to display
362     tanks = [2,3,4,5];
363 % Col and row headings for the table
364     columnLabels = {...
365     '$m$\{\footnotesize\ (kg)\}',...
366     '$\nabla$\{\footnotesize\ (L)\}',...
367     '$B$\{\footnotesize\ (kg)\}',...
368     '$B^+\}_{\text{ 3 km}}$',...
369     '$B^+\}_{\text{ 4 km}}$',...
370     '$B^+\}_{\text{ 5 km}}$',...
371     '$B^+\}_{\text{ 6 km}}$',...
372     };
373     rowLabels = {'2: 50 MPa', '3: 70 MPa', '4: 70 MPa', '5: 100 MPa*'};
% create row header

```

```

374
375 % Make the matrix to export
376 % tank | m | V | static B | added B 3km | added B 4km |added B 5km |
377
378 for index = 1:length(tanks)
379     tankspecs_detailed(index,:) = [...
380         M_tank_sys(tanks(index),gas),...
381         V_apparatus(tanks(index))/C_Lm3,...
382         Buoy_apparatus(tanks(index),gas),...
383         Buoy_added(Dindex(1),gas,tanks(index)),...
384         Buoy_added(Dindex(2),gas,tanks(index)),...
385         Buoy_added(Dindex(3),gas,tanks(index)),...
386         Buoy_added(Dindex(4),gas,tanks(index)),...
387     ];
388 end, clear index
389
390 % Get rid of negative values
391 for index = 1:numel(tankspecs_detailed)
392     if tankspecs_detailed(index)<0
393         tankspecs_detailed(index)=0;
394     end
395 end, clear index
396
397 % Output to table to Latex format (.tex file)
398 matrix2latex(tankspecs_detailed, 'table_LTsparams_detailed.tex',...
399     'rowLabels', rowLabels, 'columnLabels', columnLabels,...
400     'alignment', 'c','format', '%.1f')
401
402 %% Export to LaTeX: Buoyant materials SG COMparison *****
403 % Make a Table comparing SG for various buoyant materials
404 load vars_MD.mat
405
406 % Col and row titles for the table
407 columnLabels = {...
408     '5 km',...
409     '7 km',...
410     '10 km',...
411 };
412 rowLabels= {'Alumina SeaSphere',...
413     'Glass Sphere',...
414     'Syntactic Foam',...
415     'Gas Tank (2,4,5)',...
416 };
417
418
419 % Make the matrix to export
420 % 5 km | 7 km | 10 km |
421
422 SG_compare = [...
423     SG(10), SG(11), SG(11);...
424     SG(20), SG(20), SG(22);...
425     SG(15), SG(17), SG(18);...
426     SG_tanks(2), SG_tanks(4), SG_tanks(5),...
427 ];

```

```

428
429 % Output to table to Latex format (.tex file)
430     matrix2latex(SG_compare, 'table_SG_compare.tex',...
431         'rowLabels', rowLabels, 'columnLabels', columnLabels,...
432         'alignment', 'c','format', '%.2f')
433
434 %% The structure of the variables
435 %{
436 tank properties =   tank1 tank2 tank3
437
438 M_gas(tank, gas) =  tank1 gas1 gas2 gas3
439                   tank2 gas1 gas2 gas3
440
441 M_tank_sys(tank,gas)=  tank1 gas1 gas2 gas3
442                      tank2 gas1 gas2 gas3
443
444 Buoy_apparatus(tank,gas)=  tank1 gas1 gas2 gas3
445                           tank2 gas1 gas2 gas3
446
447 mol_bladder(press,gas) = press1 gas1 gas2 gas3
448                       press2 gas1 gas2 gas3
449
450 V_bladder(press,gas) =  press1 gas1 gas2 gas3
451                       press2 gas1 gas2 gas3
452
453
454 Buoy_added(:,gas,tank) =      tank1                tank2
455                             press1 gas1 gas2 gas3  press1 gas1 gas2 gas3
456                             press2 gas1 gas2 gas3  press2 gas1 gas2 gas3
457
458 VBm_metric_PP(:,gas,tank) =  tank1                tank2
459                             press1 gas1 gas2 gas3  press1 gas1 gas2 gas3
460                             press2 gas1 gas2 gas3  press2 gas1 gas2 gas3
461 %}

```

E.3 Code: Spray Glider Pumped Oil VB System

```
1 % Harold F Jensen III
2 % Master's Thesis June 2009
3 % MIT/WHOI Joint Program
4
5 %% SPRAY GLIDER
6 % The Spray Glider is a sea glider developed at Scrips (bought by Bluefin
7 % Robotics). It uses a pump to transfer oil from a pressure housing to an
8 % external bladder to add buoyancy.
9
10 % Sources: WHOI Engineer, John Ahern
11 %           Bluefin Robotics Engineer, Jake Maysmith
12
13 clear,clc
14
15 %% Load Constants
16     load vars_VBconstants.mat
17
18 %% System Specs
19
20 % Buoyance - this system pumps mineral oil from an internal housing to
21 % and external bladder.
22     dive_depth = 1500;           % m - dive depth for buoyancy change
23     time_cycle = 9;             % hours - dive cycle duration
24     N = 350;%floor(4*30 * 24/time_cycle); % 4 months of operation
25     N_max = 600;               % Bluefin claims 600 cycles at 1500 m
26
27     D_cycle = 700 * C_cc_m3;    % m^3 - buoyancy added per cycle
28     D_total = D_cycle * N;     % m^3 - total displacement per deployment
29
30     B_cycle = D_cycle * sw_dens(Salinity,T_water,dive_depth); % kg- B/cycle
31     B_total = B_cycle * N;     % kg - total added buoyancy per deployment
32
33 % Mass & Volume
34     n=1;
35     name_spray_parts(n,1) = {'VB Pressure Housing - Al6061'};
36     v_spray_parts(n,1)   = 12 * pi*(8/2)^2 * C_in_m^3; % m^3
37     m_spray_parts(n,1)   = 12*pi*((8/2)^2-(7.25/2)^2)*C_in_m^3*rho_Al_6061;
38
39     n=n+1;
40     name_spray_parts(n,1) = {'Bladders'};
41     v_spray_parts(n,1)   = 2*(6 * 10 * 0.375 * C_in_m^3); % Empty bladder
42     m_spray_parts(n,1)   = 0.5;
43
44     n=n+1;
45     name_spray_parts(n,1) = {'Hydraulic Oil Penreco Drakeol #9'};
46     m_spray_parts(n,1)   = 800 * C_cc_m3 * 850 ; % kg - oil mass SG=0.85
47     v_spray_parts(n,1)   = 0; % m^3 - inside housing
48
49     n=n+1;
50     name_spray_parts(n,1) = {'Pump Assembly & Aux parts'};
```



```

51     m_spray_parts(n,1)    = 1.6;           % kg - **currently estimated
52     v_spray_parts(n,1)    = 0;           % m^3 - inside housing, no volume
53
54
55 % Mass & Volume TOTALS
56     m_spray_total = sum(m_spray_parts); % kg - TOTAL system mass
57     v_spray_total = sum(v_spray_parts); % m^3 - TOTAL system volume
58
59 %% Energy
60 % Battery power on board
61 % There are 52 DD cells arranged in sticks of 4 (same as SOLO floats)
62 % A battery stick has 4 DD cells - 3.9 V and 30 Ah rating
63 % WHOI derates to 25 Ah for operating T of 6 C
64 % I derate voltage by 10% for T and error margin as well
65 % So each stick has 25 Ah at 14.04 V, and there are 13 sticks on
66 % board, one of which is dedicated to communications. The other 12
67 % are for VB, sensors, and computing
68
69     volt_batt = 15;% 3.9*4*0.90; % V - pump voltage (de-rate voltage for T)
70     E_batt_total = 12 * 25 * volt_batt; % Wh on board
71
72 % Energy Consumption - info from Jake Mayfield email
73 % The motors draw 50mA @ 15V, are only active for about 60s per cycle.
74 % The card writer draws 30mA @ 15V and is active only on the ascent.
75 % The iridium modem draws 300mA @ 7V and is active ~60s per dive cycle.
76 % The GPS draws about 70mA @ 7V and is active ~60 seconds per cycle.
77 % The pumped CTD draws 175mA @12V only on the ascent.
78
79     E_motor_cycle = 0.050 * volt_batt *1/60; % Wh per cycle
80     E_log_cycle = 0.030 * volt_batt * time_cycle/2; % Wh per cycle
81     E_modem_cycle = 0.300 * volt_batt/2 *1/60; % Wh per cycle
82     E_GPS_cycle = 0.070 * volt_batt/2 *1/60; % Wh per cycle
83     E_CTD_cycle = 0.175 * volt_batt/2 * time_cycle/2; % Wh per cycle
84 % Total energy use by the 'rest' of the glider (Wh)
85     E_other_cycle = E_motor_cycle +E_log_cycle +E_modem_cycle ...
86                   +E_GPS_cycle +E_CTD_cycle;
87
88 % VB Energy
89 % 2.3 Amps for 450 seconds at 15 Volts at 2000 psi (1370 m)
90     E_VB_cycle = 2.3 *450/60/60 *volt_batt; % Wh - Energy used per cycle
91
92 % Cycle Energy Subtotals
93     E_spray_cycle = E_other_cycle + E_VB_cycle; % Wh used per cycle
94
95 % Fraction of the battery for VB (auxiliary VB parts energy use neglected)
96     frac_batt_VB = E_VB_cycle / E_spray_cycle;
97
98 % Battery Mass & Volume (213g, 11.1cm length, 3.35cm dia per DD cell)
99     m_batt_total = 52 * 0.213; % kg - batt mass (213 g per DD cell)
100 % %     v_batt_total = 52*(pi*(3.35/2)^2*11.1)*C_cc_m3; % m^3 - batt V
101
102 % Pressure housing for batteries
103 % Since the VB system uses 40-50% of the battery power, I must add the
104 % mass and volume of a pressure house for the batteries used by VB

```

```

105 % 24 cm long, and 8in (20.32 cm) in dia
106 v_batt_house = 24*pi*(20.32/2)^2 * C_cc.m3; % m^3
107 % Mass of battery housing, neglecting endcaps
108 m_batt_house = 24*pi*( (20.32/2)^2-(18.415/2)^2 )*C_cc.m3*rho_Al_6061;
109 % Mass of bateries for VB
110 m_batt_VB = m_batt_total * frac_batt_VB; % kg
111
112 %% System Summary
113
114 % TOTAL Mass of VB system
115 m_spray_VB = m_spray_total + m_batt_VB + m_batt_house ; % kg
116 % TOTAL Volume of VB system
117 v_spray_VB = v_spray_total + v_batt_house ; % kg - total VB system mass
118
119 % Static Buoyancy of system
120 B_spray_static = v_spray_VB * rho_surface - m_spray_VB;
121
122 % Specific Gravity of System
123 SG_spray_VB = (m_spray_VB/v_spray_VB) / rho_Fwater;
124
125 % Efficiency pf Oil Pump VB system at 1370 m (ideal / actual)
126 effic_spray= (D_cycle * mSeaPressure(1370,0,Salinity) /60^2) / ...
127 ( E_VB_cycle );
128
129 %% Metrics - ** 2-WAY SYSTEM **
130
131 VBm_metric_spray = (2 * B_total) / m_spray_VB;
132 VBv_metric_spray = (2 * D_total) / v_spray_VB;
133
134 %% PLOT Results
135
136
137 figure(1);
138 set(gca,'fontsize',pfs); % plot font size
139 plot( [ 0; dive_depth; dive_depth ], ...
140 [ [ VBm_metric_spray; VBm_metric_spray; 0 ] ...
141 [ VBv_metric_spray; VBv_metric_spray; 0 ] ] );
142 title_fig1 = {'Spray Glider Oil Pump VB System Metrics'};
143 title(title_fig1,'fontsize',pfs+1)
144 xlabel('Depth (m)','fontsize',pfs)
145 ylabel('\beta_m','fontsize',pfs+2)
146 legend('Mass Metric (\beta_m)','Volume Metric (\beta_{vol})')
147 axis([0 5000 0 50])
148 print -depsc plot_metric_spray
149 print -dpdf plot_metric_spray
150
151
152 %% Export Spec Table to LaTeX
153
154 % Col and row titles for the table
155 columnLabels = {...
156 'Spray Glider',...
157 'SOLO float',...
158 };

```

```

159
160     rowLabels=     {...
161                   'Depth Rating (m)',...
162                   'VB System Mass (kg)',...
163                   'VB System Volume (L)',...
164                   'VB Batteries Mass (kg)',...
165                   'VB System SG',...
166                   'B $\hat{+}$ $ (kg/cycle)',...
167                   'Total Cycles (Max depth)',...
168                   'VB System efficiency',...
169                   '\betaM'...
170                   '\betaV'...
171                 };
172
173 % Make the spray matrix to export
174     specs_spray = [...
175                   dive_depth; m_spray_VB; v_spray_VB/C_L_m3;m_batt_VB;...
176                   SG_spray_VB; B_cycle; N; effic_spray;...
177                   VBm_metric_spray; VBv_metric_spray...
178                   ];
179 % Load SOLO float data
180     load vars_specs_SOLO.mat
181
182 % Make the matrix to export
183     specs_SOLO_spray = [specs_spray specs_SOLO];
184
185 % Output to table to Latex format (.tex file)
186     matrix2latex(specs_SOLO_spray, 'table_specs_SOLO_spray.tex',...
187                 'rowLabels', rowLabels, 'columnLabels', columnLabels,...
188                 'alignment', 'c','format', '%.2f')

```

E.4 Code: SOLO Float Piston-Driven Oil VB System

```
1 % Harold F Jensen III
2 % Master's Thesis June 2009
3 % MIT/WHOI Joint Program
4
5 %% SOLO floats - Piston VB system
6 % The SOLO floats are a profiling float that cycles to the surface once
7 % every 10 days. The buoyancy is increased at depth by inflating an
8 % external oil bladder. The oil is displaced using a piston
9
10 % The air buoyancy system is not incorporated into the metric. It would
11 % skew the results of the oil system because it operates at such a shallow
12 % depth. It only uses 2.4% of the system energy, vs 33.3% by oil system.
13
14 % Sources: WHOI Engineer, John Ahern
15 %           WHOI Engineer, Robert Tavares
16
17 clear,clc
18 % Load Constants
19     load vars_VBconstants.mat
20
21 %% System Specs
22
23 % Battery power on board
24 % A battery stick has 4 DD cells - 3.9 V and 30 Ah rating
25 % WHOI derates to 25 Ah for operating T of 6 C
26 % I derate voltage by 10% for T and error margin as well
27 % So each stick has 25 Ah at 14.04 V, and there are 4 sticks on board
28     volt_batt = 3.9 * 4 * 0.90; % V
29     E_batt_total = 4 * 25 * volt_batt; % Wh
30
31
32 % Cycles per dive
33     N = 200; % cycles at minimum
34     N_high = 230; % cycles at best
35
36 % Mass
37     m_batt = 2*1.785; % kg - battery
38     m_house = 13.0; % kg - aluminum pressure housing
39     m_parts = 5.950; % kg - all other parts (pump, oil, tubing, etc)
40
41 % Volume: 6.5" diameter, 41" long
42     v_SOLO_VB = 41 * pi*(6.5/2)^2 * (C_in_m)^3; % m^3 - total system vol
43
44 % Depth Rating
45     d_max = 1800; % m - max depth of OIL bladder inflation
46     d_air = 10; % m - max depth of AIR bladder inflation
47
48 % Buoyancy Specs
```

```

49     % Piston inflate oil bladder by 280 cc at depth (1800m)
50     D_cycle = 280 * C_cc.m3;           % m^3 - OIL displacement per cycle
51     B_add_cycle = D_cycle * sw_dens(Salinity,T_water,d_max); %kg
52     B_add_total = N * B_add_cycle; %kg
53
54     % Air pump inflates bladder by 800 cc at 10 m
55     D_cycle_air = 800 * C_cc.m3;      % m^3 - AIR displacement per cycle
56     B_add_cycle_air = D_cycle_air * sw_dens(Salinity,T_water,d_air);
57     B_add_total_air = N * B_add_cycle_air; % kg
58
59 %% Energy use for each system per cycle
60 % Energy to fill oil bladder - 400 mA for 17 min
61     E_oil_out = (0.400 * 17/60) * volt_batt; % Wh per cycle
62 % Energy to shrink oil bladder (piston return) - 100 mA for 17 min
63     E_oil_in = (0.100 * 17/60) * volt_batt; % Wh per cycle
64 % Energy to pump air to inflate air bladder - 300 mA for 2 min
65     E_air = (0.300 * 2/60) * volt_batt; % Wh per cycle
66 % Energy to CTD: 7 hr rise, 20.13 mA, 3.6 x 2 mA chnl for 5 min data log
67     E_CTD = (0.02013*7 + 0.0036*2*5/60) * volt_batt; % Wh per cycle
68 % Energy for ARGOS (wireless) transmit: 350 mA for 1.65 s/min for 12 hrs
69     E_ARGOS = (0.350*(1.65*60/60^2)*12) * volt_batt; % Wh per cycle
70 % Energy used during sleep delay at depth: 0.07 mA for 10 days
71     E_sleep = (0.00007 * 10*24) * volt_batt; % Wh per cycle
72
73 % PER CYCLE Energy used for entire system (Wh)
74     E_total_cycle = E_oil_out +E_oil_in +E_air +E_CTD +E_ARGOS +E_sleep;
75
76 % PER CYCLE Energy used on VB system (Wh)
77     E_VB_cycle = E_oil_out +E_oil_in;
78
79 % TOTAL Energy used on the VB system (Wh)
80     E_VB_total = N * E_VB_cycle;
81
82 % Fraction of energy used for VB system
83     E_frac_VB = E_VB_cycle/E_total_cycle;
84
85 % Figure the mass of the battery for VB
86     m_batt_VB = E_frac_VB * m_batt; % kg
87
88 %% System summary
89 % ** the air pump buoyancy system is not incorporated into the results **
90
91 % Mass of VB system
92     m_SOLO_VB = m_house + m_parts + m_batt_VB; % kg - total VB system mass
93
94 % Static Buoyancy of system
95     B_SOLO_static = v_SOLO_VB * rho_surface - m_SOLO_VB;
96
97 % Specific Gravity of System
98     SG_SOLO_VB = (m_SOLO_VB/v_SOLO_VB) / rho_Fwater;
99
100 % Efficiency of Piston System at 1800 m (ideal / actual)
101     effic_SOLO = (D_cycle * mSeaPressure(d_max,0,Salinity) /60^2) / ...
102                 ( E_VB_cycle );

```

```

103
104 %% Metrics - ** 2-WAY SYSTEM **
105
106     VBm_metric_SOLO = (2 * B_add_total) / m_SOLO_VB;
107     VBv_metric_SOLO = (2 * D_cycle * N) / v_SOLO_VB;
108
109 %% Save metrics
110     depth_SOLO = [0 d_max d_max]; % save depth for plot comparison
111     VBm_metric_SOLO_plot = [VBm_metric_SOLO VBm_metric_SOLO 0];
112     VBv_metric_SOLO_plot = [VBv_metric_SOLO VBv_metric_SOLO 0];
113     save vars_SOLO.mat VBm_metric_SOLO_plot VBv_metric_SOLO_plot depth_SOLO
114
115 %% PLOT Results
116 % Since I do not know the pump characteristics, the metric results at
117 % full depth (1800m) will be extended to surface.
118
119 figure(1);
120     set(gca,'fontsize',pfs); % plot font size
121     plot(depth_SOLO, VBm_metric_SOLO_plot, ...
122          depth_SOLO, VBv_metric_SOLO_plot)
123     title_fig1 = {'SOLO Float Piston-driven Oil VB System Metrics'};
124     title(title_fig1,'fontsize',pfs+1)
125     xlabel('Depth (m)','fontsize',pfs)
126     ylabel('\beta_m','fontsize',pfs+2)
127     legend('Mass Metric (\beta_m)','Volume Metric (\beta_{vol})')
128     axis([0 5000 0 8])
129     print -depsc plot_metric_SOLO
130     print -dpdf plot_metric_SOLO
131
132
133
134 %% Export Spec Table to LaTeX
135
136
137     specs_SOLO =     [...
138                    d_max; m_SOLO_VB; v_SOLO_VB/C_L_m3; m_batt_VB;...
139                    SG_SOLO_VB; B_add_cycle; N; effic_SOLO;...
140                    VBm_metric_SOLO; VBv_metric_SOLO...
141                    ];
142
143 % The table is exported in mSprayGlider.m file (compared to spray glider)
144     save vars_specs_SOLO.mat specs_SOLO

```

E.5 Code: Discharge VB System

```
1 % Harold F Jensen III
2 % Master's Thesis June 2009
3 % MIT/WHOI Joint Program
4
5 %% Mass Discharge VB System
6 %
7 clear;clc;
8
9 % Constants and fixed variables
10     load vars_VBconstants.mat; % load VB constants and fixed variables
11
12     M_dis = 1; % kg - solve system per 1 kg of discharge material
13
14 % Change SG to density
15
16     rho_dis = SG*rho_Fwater; % kg/m^3 - density of discharge material
17     V_dis = M_dis./rho_dis; % m^3 - Vol of 1 kg discharge material
18
19 %% Iterate depth and density to find insitu values for Forces & Metric
20
21 % Determine the net force (Fnet) acting on the discharge material
22 % Fnet is equal to the buoyant force minus the gravitational force
23
24 % N - Gravitational force DOWNWARD (weight1)
25     F_G = M_dis*g;
26
27 for index = 1:length(rho_Swater) % loop through depth
28     % N - Buoyant force UPWARD
29     F_B(index,:) = V_dis*rho_Swater(index)*g;
30     % N - Total NET force on material, positive UPWARD
31     F_net(index,:) = F_B(index,:) - F_G;
32
33 % Remove F_net values deeper than rated depth of material
34     for index2 = 1:length(SG) % loop through materials
35         if D_max(index2) < depth(index) % if depth > max depth
36             F_net(index,index2) = 0; % set F_net to 0
37         end
38     end
39
40 % VB metric
41     % VB mass metric
42     VBm_metric_MD(index,:) = abs(F_net(index,:)) / F_G;
43     % VB volume metric
44     VBv_metric_MD(index,:) = abs(F_net(index,:))./...
45         (rho_Swater(index)*g*V_dis);
46 end
47 clear index index2
48
49 depth_MD = depth; % save depth for all plot
50
```

```

51 % Save Data *****
52
53     save 'vars_MD.mat'
54
55 %% Plot Results
56
57 % Designated the Materials to plot
58     material = [3,5,10,11,13,17,18,22,25,26];
59     % Setup Legend Names
60     for index = 1:length(material)
61         MD_legend_names(index) = mat_name(material(index));
62     end
63     figure(1)
64     set(gca,'fontsize',pfs); % plot font size
65     plot(depth, VBm_metric_MD(:,material))
66     legend(MD_legend_names,'fontsize',pfs-1),'Location','NorthWest')
67     title('Discharge VB System - VB Mass Metric ( \beta_{m} )',...
68           'fontsize',pfs+1)
69
70     xlabel('Depth (m)','fontsize',pfs)
71     ylabel('\beta_{m}','fontsize',pfs+2)
72     axis([1000 10000 0 3.5])
73     print -depsc plot_metric_MD
74     print -dpdf plot_metric_MD
75
76     figure(2)
77     set(gca,'fontsize',pfs); % plot font size
78     plot(depth, VBv_metric_MD(:,material))
79     legend(MD_legend_names,'fontsize',pfs-1),'Location','NorthWest')
80     title('Discharge VB System - VB Volume Metric ( \beta_{vol} )',...
81           'fontsize',pfs+1)
82
83     xlabel('Depth (m)','fontsize',pfs)
84     ylabel('\beta_{vol}','fontsize',pfs+2)
85     axis([1000 10000 0 18])
86     set(gca,'YTick',0:2:18,'YMinorTick','on'); % set tick marks
87     print -depsc plot_Vmetric_MD
88     print -dpdf plot_Vmetric_MD
89
90 % Plot zoomed in on y axis less than 1.25
91     figure(3)
92     material = material(3:length(material));
93     MD_legend_names = MD_legend_names(3:length(MD_legend_names));
94     set(gca,'fontsize',pfs); % plot font size
95     plot(depth, VBv_metric_MD(:,material))
96     legend(MD_legend_names,'fontsize',pfs-1),'Location','NorthWest')
97     title('Discharge VB System - VB Volume Metric ( \beta_{vol} )',...
98           'fontsize',pfs+1)
99
100    xlabel('Depth (m)','fontsize',pfs)
101    ylabel('\beta_{vol}','fontsize',pfs+2)
102    axis([1000 10000 0 1.1])
103    print -depsc plot_Vmetric_MD_zoom
104    print -dpdf plot_Vmetric_MD_zoom

```


E.6 Code: Floodable Volume Model

```
1 % Harold F Jensen III
2 % Master's Thesis June 2009
3 % MIT/WHOI Joint Program
4
5 %% Flood a volume buoyancy change
6 % determine buoyancy metrics for flooding a sphere to decrease buoyancy
7 % (cylinder not yet investigated, not as efficient as sphere)
8 % (assumes no precharge, as sphere is designed to be flooded only)
9 clear,clc
10 % Load Constants
11     load vars.VBconstants.mat
12
13 % Set size of sphere (*note, I later found metrics are independent of size)
14     R_out = 1;           % m - radius of sphere exterior
15 % Set Safety Factor
16     SF = 1.25;           % Safety factor for max stress vs. rated stress
17 % Set material
18     % Titanium/cite{MATLWEB: Titanium Ti-6Al-4V (Grade 5),
19     % Annealed
20     rho_sphere = 4430; % kg/m^3
21     nu_cy = 970 * C_MPa_Pa; % Pa - Compression Yield Strength
22 % Set depth maximum
23 % Set Sphere depth rating (**make sure depth matches a depth in
24 % VB constants depth variable
25     D_sphere_max = [4000,6500,10000];
26     names_flood={'Flood Ti sphere 4 km','Flood Ti sphere 6.5km',...
27                 'Flood Ti sphere 10 km'};
28 % Iterate through the different sphere ratings
29     for sphere = 1:length(D_sphere_max)
30         % Pressure at rated depth (MPa)
31         P_sphere_max = P_water(find(depth==D_sphere_max(sphere)))*C_MPa_Pa;
32 % Get Sphere Values
33 % [mass of sphere (kg), thickness of sphere wall (m),...
34 % exterior sphere volume, or displacement (m^3), interior volume (m^3)
35     [m_sphere,t_sphere,V_sphere,Vi_sphere] = ...
36         mRoarkSphere(P_sphere_max,R_out,rho_sphere,nu_cy,SF);
37 % Solve for sphere buoyancy vs depth (kg)
38     B_sphere = V_sphere * rho_Swater - m_sphere;
39 % Get added buoyancy by flooding the sphere
40     B_sphere_added = - Vi_sphere * rho_Swater;
41 % Set added buoyancy to 0 if deeper than reated depth
42     for index = 1:length(depth)
43         if depth(index) > D_sphere_max(sphere)
44             B_sphere_added(index) = 0;
45         end
46     end, clear index
47
48 % Solve for metrics
49     VBm_metric_flood(:,sphere) = abs(B_sphere_added) ./ m_sphere;
50     VBv_metric_flood(:,sphere) = (abs(B_sphere_added)./rho_Swater)/V_sphere;
```

```

51     % the numerator is not simply V becuase this way sets the depth max
52     % without iteration
53
54     end, clear sphere
55
56     % Save metrics
57     depth.Flood = depth;      % save depth for plot comparison
58     save vars_flood.mat VBm_metric_flood VBv_metric_flood names_flood ...
59         depth.Flood
60
61     %% Plot Metrics
62
63     figure(1)
64         set(gca,'fontsize',pfs); % plot font size
65         plot(depth, VBm_metric_flood)
66         legend(names_flood)
67         title('Floodable Sphere (Ti-Al6-V4) - VB Mass Metric ( \beta_{m} )',...
68             'fontsize',pfs+1)
69         xlabel('Depth (m)','fontsize',pfs)
70         ylabel('\beta_{m}','fontsize',pfs+2)
71         axis([1000 11000 0 3])
72         print -depsc plot_metric_flood
73         print -dpdf plot_metric_flood
74
75     figure(2)
76         set(gca,'fontsize',pfs); % plot font size
77         plot(depth, VBv_metric_flood)
78         legend(names_flood)
79         title('Floodable Sphere (Ti-Al6-V4) - VB Volume Metric ( \beta_{vol} )',...
80             'fontsize',pfs+1)
81         xlabel('Depth (m)','fontsize',pfs)
82         ylabel('\beta_{vol}','fontsize',pfs+2)
83         axis([1000 11000 0 1.25])
84         print -depsc plot_Vmetric_flood
85         print -dpdf plot_Vmetric_flood

```

E.7 Code: Roark's Stress on Thin-walled Spheres Model

```

1 % Harold F Jensen III
2 % Master's Thesis June 2009
3 % MIT/WHOI Joint Program
4 %
5 % [m,t,V,Vi] = mRoarkSphere(P,a,rho,nu_cy,SF)
6 %
7 %% Roark's Stress Equation for a sphere under uniform external pressure
8 % Determines the thickness needed for the sphere and outputs specs \
9 %
10 % INPUTS
11 %   P      exterior pressure          (P or psi)
12 %   a      exterior sphere radius     (m or in)
13 %   rho    sphere material density    (kg/m^3 or lb/in^3)
14 %   nu_cy  Compression Yield (max stress) (Pa or psi)
15 %   SF     Safety Factor
16 %
17 % OUTPUTS
18 %   t      thickness of tank wall      (m or in)
19 %   V      volume of tank exterior     (m^3 or in^3)
20 %   Vi     volume of tank interior     (m^3 or in^3)
21 %   m      mass of sphere              (kg or lbs)
22 %
23
24 function [m,t,V,Vi] = mRoarkSphere(P,a,rho,nu_cy,SF)
25
26 % Determine the maximum inner radius
27   b = a * ( 1 - (3/2)*P*SF/nu_cy)^(1/3);
28 % Determine the minimum wall thickness
29   t = a-b;
30 % Determine the exterior volume (submerged displacement)
31   V = 4/3 * pi*a^3;
32 % Determine the interior volume (floodable volume)
33   Vi = 4/3 * pi*b^3;
34 % Determine the mass of the sphere
35   m = (V-Vi)*rho;

```

E.8 Code: Modeling Constants

```
1 % Harold F Jensen III
2 % Master's Thesis June 2009
3 % MIT/WHOI Joint Program
4
5 %% VB Constants
6
7 clear;clc;
8
9 % Constants *****
10 g = 9.80665; % m/s^2 - standard gravity
11 R = 8.314; % J/(K mol) Gas constant
12 pfs = 12; % plot font size
13
14 % Conversions *****
15 C_C_Kelvin = 273.15; % convert C to Kelvin
16 C_bar_Pa = 100000; % convert bar to Pa
17 C_MPa_Pa = 1000000; % convert MPa to Pa
18 C_atm_Pa = 101325; % convert atm to Pa
19 C_psi_Pa = 6894.75729; % convert psi to Pa
20 C_in_m = 0.0254; % convert inches to meters
21 C_lbs_kg = 0.45359237; % convert lbs to kg
22 C_L_m3 = 1/1000; % convert L to m^3
23 C_ft3_m3 = 0.0283168466; % convert cubic ft to m^3
24 C_cc_m3 = 1.0E-6; % convert cubic cm to m^3
25 C_gpm_m3s = 6.30901964E-5; % convert GPM to m^3/s
26 C_hp_kW = 0.745699872; % convert horsepower to kW
27 C_J_kWh = (1/60^2)/1000; % convert Joules to kWh
28
29 % Inputs Variables *****
30
31 % Flood Volume depths
32 % depth = [1 100 1000 4000 4001 6500 6501 10000 10001 11000];
33 % Solo, spray, Alvin depths
34 % depth = [1,200:200:1000, 1010:10:1990 2000:200:4000 4010:10:4190 ...
35 % 4200:200:6400 6500 6501 6600:200:11000]; % m - water depth
36 % Mass Discharge depths
37 depth = [1000,2000,3000,3001,4000,4001,5000,5001,6000,6001,7000,7001,...
38 8000,8001,9000,9001,10000];
39 % PPress Tanks depths
40 % depth = [1 200:200:10000];
41 % Quick depths
42 % depth = [1 100 1000:1000:10000];
43
44
45 Salinity = 34.75; % Average salinity of Oceans ~3,000m
46 T_water = 2; % Celcius - Temperature
47 rho_fw = 1000; % kg/m^3 - freshwater density
48 rho_surface = sw_dens(Salinity,17,0); % Mean SS density T=17C
49
50 rho_Al6061 = 0.098 * C_lbs_kg / (C_in_m^3); % kg/m^3 - Al6061 density
```

```

51
52 % Determine insitu seawater Pressure (MPa) & Density (kg/m^3)
53 % sw_dens function, average salinity, and average temperature
54 % from Jim Price's course 12.808, Fall 2007
55 for index = 1:length(depth)
56     P_water(index,1)=mSeaPressure(depth(index),T_water,Salinity); % Pa
57     rho_Swater(index,1)=sw_dens(Salinity,T_water,depth(index)); %kg/m^3
58 end, clear index
59
60 P_water = P_water/C_MPa_Pa; % MPa - convert to MPa from Pa
61
62 % GAS SPECS - van der Waals constants and atomic mass *****
63 % \cite{CRC:2008} - CRC Chem & Phys Handbook 89th edition
64 % a { L^2 bar/mol^2 } = van der Waals constant
65 % b { L/mol } = van der Waals constant
66 % A_dense {g/mol} = atomic density
67
68 % Hydrogen
69     a_gas(1) =0.2452; b_gas(1)=0.0265; A_dense(1) = 2.016;
70     name_gas(1)={'H_2'}; name_gas_long(1)={'Hydrogen'};
71 % Helium
72     a_gas(2) =0.0346; b_gas(2)=0.0238; A_dense(2) = 4.003;
73     name_gas(2)={'He'}; name_gas_long(2)={'Helium'};
74 % Nitrogen
75     a_gas(7) =1.370; b_gas(7)=0.0387; A_dense(7) = 28.013;
76     name_gas(7)={'N_2'}; name_gas_long(7)={'Nitrogen'};
77 % Oxygen
78     a_gas(8) =1.382; b_gas(8)=0.0319; A_dense(8) = 31.999;
79     name_gas(8)={'O_2'}; name_gas_long(8)={'Oxygen'};
80 % Neon
81     a_gas(10)=0.208; b_gas(10)=0.0167; A_dense(10)= 20.180;
82     name_gas(10)={'Ne'}; name_gas_long(10)={'Neon'};
83 % Argon
84     a_gas(18)=1.355; b_gas(18)=0.0320; A_dense(18)= 39.948;
85     name_gas(18)={'Ar'}; name_gas_long(18)={'Argon'};
86 % Carbon Dioxide
87     a_gas(68)=3.658; b_gas(68)=0.0429; A_dense(68)= 44.010;
88     name_gas(68)={'CO_2'}; name_gas_long(68)={'Carbon Dioxide'};
89 % Air
90     a_gas(78)=0.79*a_gas(7) + 0.21*a_gas(8);
91     b_gas(78)=0.79*b_gas(7) + 0.21*b_gas(8);
92     A_dense(78)=0.79*A_dense(7) + 0.21*A_dense(8);
93     name_gas(78)={'AIR'};
94     name_gas_long(78)={'AIR'};
95
96 % CONVERT GAS CONSTANTS to metric units
97     a_gas = a_gas*C_bar_Pa*C_L_m3^2;
98     % convert from {L^2 bar/mol^2} to {m^3 Pa/mol^2}
99     b_gas = b_gas*C_L_m3;
100    % convert from {L/mol} to {m^3/mol}
101
102
103 % Material Density (Specific Gravity = SG) & Maximum Depth rating (D_max)
104 % Specific Gravity - \cite{Dexter:1979}

```

```

105     SG(1) = 21.47;      mat_name(1) = {'platinum'};
106     SG(2) = 19.34;      mat_name(2) = {'gold'};
107     SG(3) = 11.36;      mat_name(3) = {'lead'};
108     SG(4) = 8.03;       mat_name(4) = {'300s Stainless'};
109     SG(5) = 7.87;       mat_name(5) = {'carbon steel'};
110     SG(6) = 7.15;       mat_name(6) = {'zinc'};
111     SG(7) = 2.66;       mat_name(7) = {'aluminum'};
112     %SG(8) = 3.96;      mat_name(8) = {'Alumina'};
113     SG(9) = 4.52;       mat_name(9) = {'titanium'};
114
115     D_max(1:10) = inf; % Set max depth for material
116
117     % Deep Sea Power & Light Alumina SeaSpheres - \cite{SeaSphere:2009}
118     SG(10) = 0.24;      % 6000m Alumina SeaSphere
119     D_max(10) = 6000;   mat_name(10) = {'6km Alumina Sphere'};
120     SG(11) = 0.35;     % 11000m Alumina SeaSphere
121     D_max(11) = 11000; mat_name(11) = {'11km Alumina Sphere'};
122
123     % Trelleborg Emerson & Cuming Inc Syntactic Foam - cite{Trelleborg:2009}
124     SG(12) = 0.40;     % 2000m syntactic epoxy foam
125     D_max(12) = 2000;   mat_name(12) = {'2km Syntactic TG-24'};
126     SG(13) = 0.42;     % 3000m syntactic epoxy foam
127     D_max(13) = 3000;   mat_name(13) = {'3km Syntactic TG-26'};
128     SG(14) = 0.45;     % 4000m syntactic epoxy foam
129     D_max(14) = 4000;   mat_name(14) = {'4km Syntactic TG-28'};
130     SG(15) = 0.48;     % 5000m syntactic epoxy foam
131     D_max(15) = 5000;   mat_name(15) = {'5km Syntactic DS-30'};
132     SG(16) = 0.52;     % 6000m syntactic epoxy foam
133     D_max(16) = 6000;   mat_name(16) = {'6km Syntactic DS-33'};
134     SG(17) = 0.56;     % 8000m syntactic epoxy foam - DS35
135     D_max(17) = 8000;   mat_name(17) = {'8km Syntactic DS-35'};
136     SG(18) = 0.61;     % 11500m syntactic epoxy foam - DS38
137     D_max(18) = 11500; mat_name(18) = {'11.5km Syntactic DS-38'};
138
139     % Teledyne Benthos Deep Sea Glass Spheres - cite{SeaSphere:2009}
140     % SG = weight in air / (weight in air + net buoyancy)
141     SG(20) = 0.4767;    %4.1/(4.1+4.5); % 6700m Benthos Sphere
142     D_max(20) = 6700;   mat_name(20) = {'6.7km Glass Sphere'};
143     SG(21) = 0.4746;    %9.07/(9.07+10.04); % 9000m Benthos Sphere
144     D_max(21) = 9000;   mat_name(21) = {'9km Glass Sphere'};
145     SG(22) = 0.41067;   %17.7/(17.7+25.4); % 9000m Benthos Sphere
146     D_max(22) = 9000;   mat_name(22) = {'9km Glass Sphere'};
147
148     % Liquids - \cite{CRC:2008}
149     SG(25) = 3.38;      % Calcium Bromide
150     D_max(25) = inf;    mat_name(25) = {'Calcium Bromide'};
151     SG(26) = 0.7914;    % Methanol
152     D_max(26) = inf;    mat_name(26) = {'Methanol'};
153
154     % Save Constants and fixed variables
155     save vars_VBconstants.mat;

```

Bibliography

- [1] Teledyne Benthos. *Benthos Deep Sea Glass Spheres*. Teledyne Benthos, 49 Edgerton Drive, North Falmouth, MA 02556 USA, August 2007.
- [2] A Bowen, D Yoerger, C Taylor, and R McCabe. The Nereus Hybrid Underwater Robotic Vehicle for Global Ocean Science Operations to 11,000 m Depth. *Wood Hole Oceanographic Institution*, 2009.
- [3] A. Bradley, M. Feezor, H. Singh, and F. Sorrell. Power Systems for Autonomous Underwater Vehicles. *IEEE Journal of Oceanic Engineering*, 26(4), 2001.
- [4] E. Desa, R. Madhan, and P. Maurya. Potential of Autonomous Underwater Vehicles as New Generation Ocean Data Platforms. *Current Science*, 90(9):1202–1209, 2006.
- [5] Stephen C Dexter. *Handbook of Oceanographic Engineering Materials*. Ocean Engineering, a Wiley Series. Wiley, New York, 1979.
- [6] J.A Dowdeswell, J Evans, R Mugford, G Griffiths, S McPhail, N Millard, P Stevenson, M.A Brandon, C Banks, K.J Heywood, M.R Price, P.A Dood, A Jenkins, K.W Nicholls, and D Hayes. Instruments and Methods: Autonomous underwater vehicles (AUVs) and investigations of the ice–ocean interface in Antarctic and Arctic waters. *Journal of Glaciology*, Jan 2008.
- [7] Paul Fernandes, Pete Stevenson, Andrew Brierley, Frederick Armstrong, and E Simmonds. Autonomous Underwater Vehicles: Future Platforms for Fisheries Acoustics. *ICES Journal of Marine Science: Journal du Conseil*, 60(3):684, Jan 2003.
- [8] Thomas Charles Gillmer and Bruce Johnson. *Introduction to Naval Architecture*. Naval Institute Press, Annapolis, MD, 1982.
- [9] J Kinsey, M Tivey, and D Yoerger. Toward High-Spatial Resolution Gravity Surveying of the Mid-Ocean Ridges with Autonomous Underwater Vehicles. *WHOI*, 2009.
- [10] John Koehr. ASME Codes and Standards for Hydrogen Infrastructure. Technical report, DOE Hydrogen and Fuel Cell Summit VIII, June 2004.

- [11] C. Kunz, C. Murphy, R. Camilli, H. Singh, and J. Bailey. Deep Sea Underwater Robotic Exploration in the Ice-Covered Arctic Ocean with AUVs. *IEEE/RSJ International Conference on Intelligent Robots and . . .*, Jan 2008.
- [12] David R Lide. *CRC Handbook of Chemistry and Physics*. CRC; Taylor & Francis, Boca Raton, FL, 2008.
- [13] Lincoln Composites. *TUFFSHELL H₂ Fuel Tanks Product Information*, viewed March 2009.
- [14] R Muller. *Physics for Future Presidents: The Science Behind the Headlines*. W.W. Norton & Co., New York, 1st ed edition, 2008.
- [15] Norman L. Newhouse. ASME Standards Development for High Pressure Composite Hydrogen Pressure Vessels in Section X. Technical report, ASME/USCG Workshop on Marine Technology and Standards, June 2008.
- [16] Scripps Institution of Oceanography. *Spray Autonomous Underwater Vehicle Operations Manual Version 2.0*. University of California, San Diego, 2007.
- [17] Michael E. Q. Pilson. *An Introduction to the Chemistry of the Sea*. Prentice Hall, Upper Saddle River, N.J., 1998.
- [18] Raymond Jefferson. Roark and Warren C. Young. *Roark's Formulas for Stress and Strain*. McGraw-Hill, New York, 1989.
- [19] DL Rudnick, RE Davis, CC Eriksen, DM Fratantoni, and MJ Perry. Underwater Gliders for Ocean Research. *Marine Technology Society Journal*, 38:73–84, 2004.
- [20] SeaSphere. *DeepSea SeaSphere Spec.* Deep Sea Power and Light, 4033 Ruffin Rd. San Diego, CA 92123, April 2009.
- [21] J.D Stachiw, D Peters, and G McDonald. Ceramic External Pressure Housings for Deep Sea Vehicles. *OCEANS 2006*, pages 1–7, 2006.
- [22] S Tangirala and J Dzielski. A Variable Buoyancy Control System for a Large AUV. *IEEE JOURNAL OF OCEANIC ENGINEERING*, 32(4):762–771, 2007.
- [23] Trelleborg - Emerson & Comming Inc. *Microballoon Based Syntactic Foams Specifications*, April 2009.
- [24] S Tripp. Autonomous Underwater Vehicles (AUVs): A Look at Coast Guard Needs to Close Performance Gaps and Enhance Current Mission Performance. *Storming Media*, Jan 2006.
- [25] Andrew Weisberg, Blake Myers, and Gene Berry. Hydrogen Storage Using Lightweight Tanks. Technical report, Lawrence Livermore National Laboratory, 2002.
- [26] Andreas Zuttel. Hydrogen storage methods. *Die Naturwissenschaften*, 91(4):157–72, Mar 2004.